Copy 2

APR 10 1933

THE PHYSICAL REVIEW

VOLUME 43 *Second Series* NUMBER 7

APRIL 1, 1933

Published for the

AMERICAN PHYSICAL SOCIETY

by the

AMERICAN INSTITUTE OF PHYSICS
Incorporated

LANCASTER, PA., AND NEW YORK, N. Y.

THE AMERICAN PHYSICAL SOCIETY

OFFICERS OF THE SOCIETY

PAUL D. FOOTE, *President*
The Gulf Companies
Pittsburgh, Pennsylvania

ARTHUR H. COMPTON, *Vice-President*
University of Chicago
Chicago, Illinois

W. L. SEVERINGHAUS, *Secretary*
Columbia University
New York, New York

G. B. PEGRAM, *Treasurer*
Columbia University
New York, New York

JOHN T. TATE, *Editor*
University of Minnesota
Minneapolis, Minnesota

L. B. LOEB, *Local Secretary for the Pacific Coast*
University of California
Berkeley, California

THE PHYSICAL REVIEW

BOARD OF EDITORS

JOHN T. TATE, *Editor*

J. W. BUCHTA, *Assistant Editor*

Associate Editors

A. J. DEMPSTER
DAVID M. DENNISON
J. C. SLATER
R. C. GIBBS
E. O. LAWRENCE
J. H. VAN VLECK
K. K. DARROW
J. C. HUBBARD
A. E. RUARK

THE PHYSICAL REVIEW, which was established in 1893, is a journal of experimental and theoretical physics. It is published for the American Physical Society by the American Institute of Physics Incorporated. There are two volumes annually with twelve issues in each volume.

Manuscripts for publication should be submitted to John T. Tate, University of Minnesota, Minneapolis, Minnesota.

Proof and all correspondence concerning papers in the process of publication, should be addressed to the Editorial Secretary, American Institute of Physics, 11 East 38th Street, New York, New York.

Subscription price $15.00 per year. Single copies $1.50 each for issues prior to July 1, 1929 (Vols. 1–33); $.75 each for issues subsequent thereto. Subscriptions and orders for back numbers should be addressed to Prince and Lemon Streets, Lancaster, Pennsylvania, or to the American Institute of Physics, 11 East 38th Street, New York, New York.

Advertising is not accepted for the *Physical Review* but attention is called to the *Review of Scientific Instruments with Physics News and Views*, a companion publication of the Institute, and a medium through which the field of physics can be reached most effectively. Rates and other information will be furnished on request to the Editorial Secretary.

Changes of address and complaints of failure to receive the *Physical Review*, in the case of members of the American Physical Society, should be addressed to the Treasurer; in the case of other subscribers, to the Editorial Secretary. New copies can be sent free in response to complaints of non-delivery only if notice of non-delivery is received within three months of date of issue.

The Physical Review is published semi-monthly at Prince and Lemon Streets, Lancaster, Pennsylvania.

Entered at the Post Office at Lancaster, Pennsylvania, as second class matter.

Acceptance for mailing at special rate of postage provided for in section 1103, Act of October 3, 1917, authorized September 6, 1926.

THE
PHYSICAL REVIEW
A Journal of Experimental and Theoretical Physics
VOL. 43, NO. 7 APRIL 1, 1933 SECOND SERIES

Scattering of X-Rays from Powdered Crystals

G. E. M. JAUNCEY* AND FORD PENNELL, *Department of Physics, Washington University*
(Received February 9, 1933)

When monochromatic x-rays are scattered by a powdered crystal, the scattered rays consist partly of those rays which are scattered in special directions and which give rise to the Debye-Scherrer circles in a photograph and partly of those rays which are diffusely scattered and which give rise to the background between the circles. If the scattered rays from a powdered crystal enter a *wide* window of an ionization chamber, the intensity of the rays per unit solid angle is an average for several Debye-Scherrer circles and the diffuse background between the circles. Coven has experimentally examined this "average scattering" for the case of monochromatic x-rays, but his results are inconclusive. In our experiments we have used not only a wide window (the extreme angular width of the rays entering the window was 6°) but also a wide band of wave-lengths obtained by passing the x-rays from a tungsten target x-ray tube operated at 54.9 kv through 3.25 mm of aluminum or its equivalent. The spectral distribution of the intensity of these rays was obtained by reflection from rocksalt. The scattered intensities at average angles varying from 5° to 90° from powdered crystal brickettes of KCl, CaS, NaF and MgO were compared with the scattered intensity at 90° from paraffin. From Jauncey and Harvey's theory of the diffuse scattering from crystals together with the theory of the intensity of the Debye-Scherrer circles, a formula has been obtained for the ionization current produced by the rays entering a narrow window and consisting of a wide band of wave-lengths of known intensity distribution. This formula was then integrated graphically so as to obtain theoretical values for the case of a wide window. The calculation of the theoretical values involves f and f'' values. James and Brindley's f values as obtained from wave mechanics were used. Values of f'' were calculated from data given in James and Brindley's paper and are tabulated for F^-, Na^+, Cl^-, K^+, neon and argon. Excellent agreement between the theoretical and experimental values of the scattered intensity is shown over the whole range of average angles of scattering for each of the crystals. It is shown that, in experiments on the diffuse scattering of x-rays by crystals, an average wave-length as determined by absorption in aluminum may to a fairly close approximation be treated as if it were a single wave-length and so the S curves obtained for KCl by Harvey and for NaF by Jauncey and Williams are reasonably accurate.

I. INTRODUCTION

ACCORDING to the theory as it has been developed by Jauncey, Harvey and Woo[1, 2, 3, 4, 5] the intensity of the x-rays diffusely scattered from a crystal consisting of atoms of one kind is given by

$$S = S_1 + S_2/(1+\alpha \text{ vers } \phi)^3, \quad (1)$$

where

$$S_1 = (f^2 - F^2)/Z \quad (2)$$

and

$$S_2 = 1 - f''^2/Z^2. \quad (3)$$

Furthermore, the intensity of the x-rays scattered from a monatomic gas is given by Eqs. (1) and (3) together with

$$S_1 = f^2/Z. \quad (4)$$

* The senior author was aided in part by a grant from the Rockefeller Foundation to Washington University for research in science.

[1] G. E. M. Jauncey, Phys. Rev. **37**, 1193 (1931).
[2] G. E. M. Jauncey and G. G. Harvey, Phys. Rev. **37**, 1203 (1931).
[3] G. E. M. Jauncey, Phys. Rev. **42**, 453 (1932).
[4] Y. H. Woo, Phys. Rev. **38**, 6 (1931).
[5] Y. H. Woo, Phys. Rev. **41**, 21 (1932).

For the definitions of the various quantities in Eqs. (1) to (4) the reader is referred to Jauncey's paper.[3] Jauncey and Harvey[6] have further shown that the intensity of the x-rays scattered by an inert gas is related to the intensities of the x-rays diffusely scattered and regularly reflected from the corresponding crystal by the formula

$$S_{\text{gas}}=(S+F^2/Z)_{\text{crystal}}. \tag{5}$$

The experimental S and F values for the right side of Eq. (5) have been obtained in different experiments and in different laboratories. It would be an advantage to devise an experiment in which at one and the same time the values of the sum of S and F^2/Z could be obtained. In a private discussion with A. H. Compton it developed that this might be accomplished by scattering the x-rays from a powdered crystal and by using a wide window in front of the ionization chamber so as to collect arcs of several Debye-Scherrer circles together with the diffuse scattering in between the circles. Following Compton's suggestion Coven[7] has scattered monochromatic x-rays of wave-length 0.71A from powdered crystals of KCl, NaF and MgO. Using Coven's notation we shall represent the sum of the intensities of the diffuse scattering and of the Debye-Scherrer diffraction circles by S_t and shall call this the total scattering. Coven found that the relation

$$S_t=S_{\text{gas}} \tag{6}$$

holds very well for KCl and argon but does not hold nearly so well for NaF or MgO and neon, the S_{gas} values for argon and neon being those obtained by Wollan.[8]

Since the conclusions to be drawn from Coven's experimental findings are uncertain and since the theory given in his paper is somewhat inadequate, we have again attacked the problem of the total scattering from powdered crystals from both the experimental and theoretical sides. Furthermore, the essential point of Compton's suggestion is that x-rays for a band of values of $(\sin \frac{1}{2}\phi)/\lambda$ enter the window of the ionization chamber for a given setting of the spectrometer. This may be accomplished by using (1) a wide chamber window with a single wave-length, (2) a narrow window with a wide band of wave-lengths, or (3) a wide window together with a wide band of wave-lengths. Coven used the first method, while in the research to be described we have used the third method. We have measured the total scattering from powdered crystals of CaS, KCl, MgO and NaF.

II. Experimental Method

A specimen of the substance to be examined was finely powdered and pressed into a brickette in the hollow of a brass ring. The ring containing the brickette was then mounted on the axis of an x-ray spectrometer. In the case of both CaS and MgO, waterproof celophane was sealed over the two faces of the brass ring to prevent CO_2 and moisture from coming in contact with the sample and decomposing it. The general radiation from a tungsten tube was used to illuminate the brickette. The scattered rays were then measured by means of an ionization chamber and electrometer.

An oil immersed x-ray outfit employing the balanced circuit as described by Bennett[9] was used to give a constant source of radiation. For reasons of convenience, the x-ray tube was mounted directly in front of the oil tank in a lead box. The maximum excitation potential as determined experimentally by the Duane-Hunt[10] relation was 54,900 volts and the current through the tube was 8.1 milliamperes. The ionization chamber was 35.2 cm long and was filled with methyl bromide at 74 cm pressure at a temperature of 22°C. The diameter of the chamber was such that the x-rays travelled the whole length of the chamber without hitting the sides. The window was made of thin glass.

The readings at an angle ϕ were made as follows: The paraffin was set at an angle of 45° to the main beam between the x-ray tube and the powdered crystal brickette which was mounted on the spectrometer axis in the Crowther[11] position. The scattered intensity was measured at an angle ϕ. The brickette and the paraffin were

[6] G. E. M. Jauncey and G. G. Harvey, Phys. Rev. **38**, 1071 (1931).

[7] A. W. Coven, Phys. Rev. **41**, 422 (1932).

[8] E. O. Wollan, Phys. Rev. **37**, 862 (1931).

[9] R. D. Bennett, N. S. Singrich and W. C. Pierce, Rev. Sci. Inst. **2**, 226 (1931).

[10] W. Duane and F. L. Hunt, Phys. Rev. **6**, 166 (1915).

[11] J. A. Crowther, Proc. Roy. Soc. **A86**, 478 (1912).

then interchanged. The ionization chamber was moved to 90° and the scattered intensity from the paraffin measured. The reason for this procedure is that the intensity of the primary beam penetrating the substance in the scattering position is the same irrespective of whether the paraffin or the crystal brickette is in that position.

In a preliminary experiment, the crystal brickette was removed and the paraffin slab set so as to scatter x-rays into the ionization chamber at an angle of 30°. Sheets of aluminum were placed between the paraffin and the x-ray tube and the logarithm of the intensity of the x-rays entering the chamber was plotted against the thickness of the aluminum. For thicknesses of aluminum greater than 3.25 mm the graph as shown in Fig. 1 becomes a straight line. In the

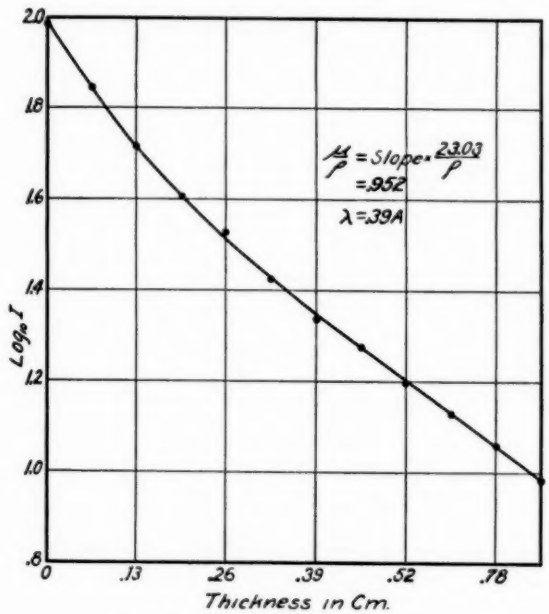

FIG. 1. Absorption in aluminum.

actual scattering experiments, a thickness of aluminum was placed in the main beam such that the absorption in the aluminum plus that in the crystal brickette and that in the paraffin slab was equal to the absorption in 3.25 mm of aluminum. The mass absorption coefficient in aluminum for the straight portion of the graph in Fig. 1 is 0.952 per g/cm². Using Compton's tables,[12] this corresponds to a wave-length of 0.39A. However, we have not used this average wave-length in the way described by Harvey[13] and by Jauncey and Williams[14] but have instead obtained the distribution of the energy in the spectrum of the x-rays which have passed through 3.25 mm of aluminum.

The energy distribution with respect to wave-length was obtained in a separate experiment. We reflected the x-rays from a (1, 0, 0) face of a single crystal of rocksalt into the same ionization chamber as was used in the scattering experiment. The integrated intensity[15] of x-rays of wave-length λ as reflected by a mosaic crystal is given by

$$\frac{W\omega}{I}=n^2\frac{A\lambda^3F^2}{4\mu}\frac{e^4}{m^2c^4}\frac{1+\cos^2 2\theta}{\sin 2\theta}, \qquad (7)$$

where θ is the glancing angle for the reflected rays. Eq. (7) holds for monochromatic rays when the crystal is rotated at an angular speed ω. W is the total energy reflected into the ionization chamber while the crystal is being turned through a reflection position for the wave-length λ. The purpose of the rotation of the crystal is to bring all the minute crystals of the mosaic crystal into the reflection position. However, when the continuous spectrum is being analyzed the difference in the orientations of the minute crystals of the mosaic causes wave-lengths of a range λ to $\lambda+d\lambda$ to be reflected and consequently each minute crystal is able to find some wave-length to reflect when the face of the large crystal is set at a glancing angle θ with the primary beam. Hence, at least approximately,

$$W=\text{const.}\times(I\lambda^3F^2/\mu)(1+\cos^2 2\theta)/\sin 2\theta, \quad (7a)$$

where W is the intensity of the x-rays in the wave-length range λ to $\lambda+d\lambda$ reflected into the ionization chamber, μ is the absorption coefficient of rays of wave-length λ in the crystal and F is the atomic structure factor for the crystal. F is a function of $(\sin\theta)/\lambda$. We have used the F values for rocksalt as given by James and Firth.[16] The

[12] A. H. Compton, *X-Rays and Electrons*, p. 184.

[13] G. G. Harvey, Phys. Rev. **38**, 593 (1931).

[14] G. E. M. Jauncey and P. S. Williams, Phys. Rev. **41**, 127 (1932).

[15] See reference 12, p. 128.

[16] R. W. James and E. M. Firth, Proc. Roy. Soc. **A117**, 62 (1928).

values of μ used were those for the ordinary absorption coefficient in rocksalt. We made no attempt to correct for extinction. After obtaining values of W, Eq. (7a) was solved for I, the intensity of the x-rays in the range λ to $\lambda+d\lambda$ existing in the primary beam. Values of I were then plotted against λ. Next, it was necessary to correct for second and third order reflection of

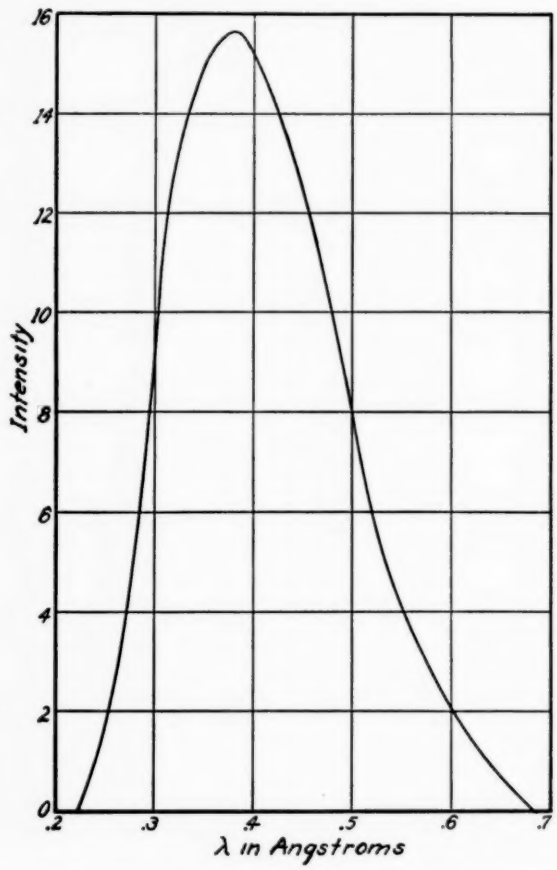

FIG. 2. Distribution of the intensity in the continuous spectrum. For ease in calculation the curve is drawn to meet the wave-length axis at $\lambda=0.68$A.

x-rays. The shortest wave-length present was 0.225A, so that second order reflection began at an apparent wave-length of 0.450A. For reflection from a given set of planes in a given crystal—for instance, the (1, 0, 0) planes—F is a function of the order of reflection. Hence, knowing the value of I as calculated from the first order reflection of, say, $\lambda=0.30$A, the values of W for the second order reflection of $\lambda=0.30$A can be obtained from Eq. (7a). This value is subtracted from the experimental value of W found for a value of θ corresponding to first order reflection of $\lambda=0.60$A. The remaining value of W is the true value of W for $\lambda=0.60$A. Also at $\lambda=3\times0.225=0.675$A third order reflection begins and a further correction must be made. The final corrected curve for the spectral distribution is shown in Fig. 2. It should be noted that this curve is for the spectral distribution of the x-rays as absorbed in the ionization chamber. The mass of the methyl bromide in the chamber is not sufficient to absorb completely x-rays of all the wave-lengths in the spectrum. However, the same ionization chamber was used as in the scattering experiments. The scattered rays of various wave-lengths are absorbed to the same extent in the methyl bromide as the reflected rays of the same wave-lengths in the spectral distribution experiment. We shall see later that the spectral distribution as measured by absorption in the chamber is all we need to know.

As previously mentioned, Harvey[13] and Jauncey and Williams[14] in their experiments measured the absorption coefficient of the x-rays in aluminum and from this coefficient determined the average wave-length and then used this average wave-length as if it were the wave-length of monochromatic x-rays. From the spectral distribution curve of Fig. 2, the average wave-length was found to be 0.41A, while the absorption coefficient obtained from the straight portion of the curve of Fig. 1 leads to an average wave-length of 0.39A. We submit that the agreement of these two average wave-lengths is reasonably good. We shall return later to the question of the use of an average wave-length as if it were a monochromatic wave-length.

III. Formulas for Calculation

Referring to the paper by Jauncey and Williams,[14] we see that the energy of ionization produced per second is not equal to the rate of flow of x-ray energy into the ionization chamber unless all of the x-rays are absorbed in the gas of the chamber. When the absorption is incomplete, the situation is expressed by Eq. (20) of the above

paper. Then, eliminating s_1 and s_2 by means of Eqs. (21) and (22) of that paper, we obtain

$$C_\phi = \frac{ACt}{R^2 \cos \frac{1}{2}\phi} \cdot \frac{NZ\rho}{W} \cdot \frac{e^4}{m^2c^4} \cdot \frac{1+\cos^2 \phi}{2} \cdot \left\{ S_1 + \frac{S_2 K_\phi T_\phi}{K_0(1+\alpha \text{ vers } \phi)^3} \right\}, \tag{8}$$

where C_ϕ and C are the ionization currents produced respectively by the scattered and the transmitted rays, S_1 and S_2 are respectively the coherent and incoherent scattering factors, K_0 and K_ϕ are respectively the fractions of the coherent and incoherent rays absorbed in the chamber, T_ϕ is a quantity introduced by Jauncey and DeFoe[17] into the Crowther[11] formula for scattering by a slab in order to take account of the extra absorption of the incoherent scattered rays in the slab itself, A is the area of the ionization chamber window, and R the distance of the window from the scattering slab.

Eq. (8) is for a given wave-length. However, in our experiments we used the band of wave-lengths shown in Fig. 2. The intensity in the range $d\lambda$ at λ is $I(\lambda)d\lambda$ where $I(\lambda)$ is proportional to the ordinate of the graph and hence we replace C in the right side of Eq. (8) by $I(\lambda)d\lambda$. Also we shall write the left side in the form $C_\phi d\lambda$ because $C_\phi d\lambda$ is the ionization current produced by the scattered rays which are due to the primary rays in the range $d\lambda$ at λ. To obtain the ionization current D_ϕ when the whole spectrum of wave-lengths is scattered, we integrate over all wave-lengths present in the primary beam. Several of the quantities on the right side of Eq. (8) are not functions of λ and so we obtain

$$D_\phi = \frac{A}{R^2} \cdot \frac{NZ\rho t}{W} \cdot \frac{1+\cos^2 \phi}{2 \cos \frac{1}{2}\phi} \cdot \frac{e^4}{m^2c^4} \cdot \int \left\{ S_1 + \frac{S_2 K_\phi T_\phi}{K_0(1+\alpha \text{ vers } \phi)^3} \right\} I d\lambda. \tag{9}$$

For the wave-lengths used the x-rays scattered by paraffin at 90° were almost entirely incoherent, as pointed out by Harvey[13] and Coven.[7] Consequently for scattering from paraffin at 90° we obtain an equation similar to Eq. (9), but with $S_1=0$ and $S_2=1$. We shall prime (′) those quantities in this equation which specifically refer to paraffin. Then, dividing Eq. (9) for the crystal by the similar equation for paraffin, we obtain

$$\frac{D_\phi}{D'_{90^\circ}} = \frac{Z\rho t W'}{Z'\rho' t' W} \cdot \frac{(1+\cos^2 \phi) \cos 45^\circ}{\cos \frac{1}{2}\phi} \cdot \frac{B}{B'}, \tag{10}$$

where B is an integral for the crystal and B' is the corresponding integral for the paraffin.

We shall now consider B', where

$$B' = \int \frac{K'_{90^\circ} T'_{90^\circ}}{K_0(1+\alpha)^3} I d\lambda. \tag{11}$$

According to Jauncey and Williams,[14]

$$T = (1-e^{-g})/g, \tag{12}$$

where

$$g = (\mu_2 - \mu_1)t/\cos \tfrac{1}{2}\phi \tag{13}$$

and μ_2 and μ_1 are the linear absorption coefficients of the incoherent and coherent scattered rays, respectively, in the scattering slab. The value of $\rho' t'$ for the paraffin slab was 0.439 g/cm². From Compton's absorption tables[12] we have calculated the absorption coefficient of paraffin for various wave-lengths. Putting values in Eqs. (12) and (13) we find that T'_{90° varies from 0.990 to 1.000 over the range of wave-lengths 0.7A to 0.2A and so may be regarded as practically a constant whose value is 0.995. If μ_1 is the absorption coefficient of wave-length λ and μ_2 that of wave-length $\lambda+\delta\lambda$ in methyl bromide, the fractions absorbed are

$$K_0 = 1-e^{-\mu_1 t} \tag{14}$$

and

$$K_{90^\circ} = 1-e^{-\mu_2 t}, \tag{15}$$

where t is the length of the gas in the ionization chamber. The change of wave-length $\delta\lambda$ is

[17] G. E. M. Jauncey and O. K. DeFoe, Phil. Mag. 1, 711 (1926).

0.0242A, the Compton change at 90°. Consider the quantity

$$y = K_{90°}/K_0(1+\alpha)^3. \tag{16}$$

The graph of y plotted against λ is shown in Fig. 3 and it is seen that y has the practically constant value of 0.884 over the range $\lambda = 0.25$A to $\lambda = 0.65$A, which is the range of the wave-lengths of appreciable intensity in the spectrum, as shown in Fig. 2. Hence the factor of I in the integrand of the right side of Eq. (11) is constant with respect to the wave-length and so may be taken outside of the integral sign and we have $B' = 0.880 \int I d\lambda$. Solving Eq. (10) for $B/\int I d\lambda$, we obtain

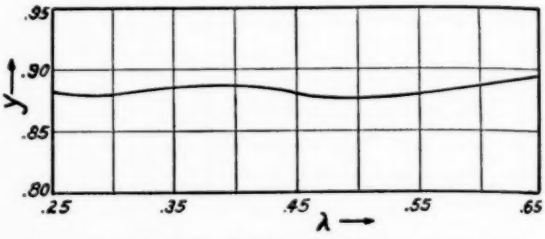

FIG. 3. Graph of $K_\phi/K_0(1+\alpha)^3$ against wave-length.

$$\int \left\{ S_1 + \frac{S_2 K_\phi T_\phi}{K_0(1+\alpha \text{ vers } \phi)^3} \right\} I d\lambda \Big/ \int I d\lambda = 0.314 \times \frac{D_\phi}{D'_{90°}} \cdot \frac{\cos \tfrac{1}{2}\phi}{1+\cos^2 \phi} \cdot \frac{W}{Z\rho t} \tag{17}$$

after putting in numerical values. For convenience we shall denote the value of the right side of Eq. (17) when experimental values are inserted by S_{exp}. It is interesting to note that this same numerical formula for S_{exp} is obtained if either of the average wave-lengths mentioned in the last paragraph of §2 had been used.

IV. Experimental Results

Values of the experimental ratio $D_\phi/D'_{90°}$ for the respective powdered crystals were obtained and substituted in the right side of Eq. (17) and the corresponding values of S_{exp} calculated. These values of S_{exp} are shown in Tables I and II. The values of the mass per unit area of the

TABLE I. *Total scattering from powdered crystals of KCl and CaS. Values of $D_\phi/D'_{90°}$ and S_{exp}.*

		KCl		CaS				KCl		CaS	
ϕ	$\sin \frac{\phi}{2}$	$\frac{D_\phi}{D'_{90°}}$	S_{exp}	$\frac{D_\phi}{D'_{90°}}$	S_{exp}	ϕ	$\sin \frac{\phi}{2}$	$\frac{D_\phi}{D'_{90°}}$	S_{exp}	$\frac{D_\phi}{D'_{90°}}$	S_{exp}
5.0°	0.044	2.64	3.97			18°	0.156	3.27	5.10	3.22	4.36
6.0°	.052	5.02	7.59			20°	.174			2.87	3.92
7.0°	.061	6.51	9.85			22°	.191			2.78	3.83
7.5°	.065			6.00	7.95	24°	.208	2.29	3.67	2.41	3.36
8.0°	.070	6.72	10.19	6.36	8.39	30°	.259	1.80	2.99	1.99	2.87
8.5°	.074	6.89	10.46	6.60	8.70	36°	.309	1.44	2.50	1.59	2.39
9.0°	.078	6.67	10.15	6.80	8.96	42°	.358	1.13	2.05	1.32	2.07
9.5°	.083	6.56	9.96	6.60	8.70	48°	.407	0.948	1.80		
10.0°	.087	6.05	9.20	6.49	8.57	54°	.454	0.773	1.54	0.876	1.52
10.5°	.092	5.71	8.71			60°	.500	0.656	1.37		
11.0°	.096	5.75	8.77	5.95	7.88	66°	.545	0.632	1.31	0.707	1.33
12.0°	.105	5.15	7.85	5.37	7.13	72°	.588	0.505	1.12		
14.0°	.122			4.45	5.94	78°	.629	0.510	1.14	0.599	1.16
15.0°	.131	3.94	6.09			84°	.669	0.500	1.12		
16.0°	.139			3.68	4.95	90°	.707	0.470	1.00	0.597	1.10

TABLE II. *Total scattering from powdered crystals of NaF and MgO. Values of $D_\phi/D'_{90°}$ and S_{exp}.*

		NaF		MgO				NaF		MgO	
ϕ	$\sin \frac{\phi}{2}$	$\frac{D_\phi}{D'_{90°}}$	S_{exp}	$\frac{D_\phi}{D'_{90°}}$	S_{exp}	ϕ	$\sin \frac{\phi}{2}$	$\frac{D_\phi}{D'_{90°}}$	S_{exp}	$\frac{D_\phi}{D'_{90°}}$	S_{exp}
9°	0.078	9.21	4.55			30°	0.259	2.63	1.42	1.06	1.63
10°	.087	10.17	5.04	2.71	3.81	36°	.309	2.19	1.25	0.837	1.34
11°	.096	10.25	5.08	2.96	4.17	42°	.358	1.98	1.17	.738	1.23
12°	.104	9.84	4.90	3.14	4.44	54°	.454	1.54	1.11	.608	1.12
15°	.130	6.97	3.50	2.58	3.67	66°	.545	1.49	1.05	.529	1.06
18°	.156	5.34	2.71	1.90	2.75	78°	.629	1.37	1.00	.497	1.02
24°	.208	3.54	1.85	1.32	1.95	90°	.707	1.40	0.97	.486	0.96

various powdered crystal brickettes were as follows: NaF, 0.678; MgO, 0.229; KCl, 0.218; CaS, 0.242 g/cm². The width of the window of the ionization chamber subtended an angle of 4° at the axis of the spectrometer. The widths of the defining slits in the primary beam were such that the total variation in ϕ for a given setting of the ionization chamber was about 6° so long as the average angle was less than 30°. In addition to the defining slits, screening slits were added so as to prevent rays scattered by the defining slits from entering the ionization chamber. These screening slits are very important at small angles.

V. Comparison with Theory

The left side of Eq. (17) contains S_1 and S_2 and these quantities[3] are dependent upon f and f'' as well as upon F. The atom form factors f and f'' can be calculated from wave mechanics. Tables of f values so calculated have been published by James and Brindley.[18] Furthermore, James and Brindley give tables of f_0 values. The symbol f_0 refers to the same quantity as does the symbol E used by Jauncey[1, 3] and Woo,[5] and hence values of f'' have been calculated from James and Brindley's tables by means of the formula[3]

$$f''^2 = Z\sum_r E_r^2. \tag{18}$$

Because calculated values of f'' may be of use to others working in this field, these values are given in Table III. The values for neon and for argon in Table III are the averages of the corresponding values for F^- and Na^+ and for Cl^- and K^+, respectively. We have used Froman's method[19] for extrapolating the f values beyond $(\sin\frac{1}{2}\phi)/\lambda = 1.0$. For the extrapolation of the f'' values we have applied Froman's method to James and Brindley's E (or f_0) values for each type of electron and have then used Eq. (18).

Table III. *Atom form factors. Values of f and f''.*

$\frac{\sin\frac{1}{2}\phi}{\lambda}$	F^-		Na^+		Neon		Cl^-		K^+		Argon	
	f	f''	f	f''	f	f''	f	f''	f	f''	f	f''
0.00	10.00	10.00	10.00	10.00	10.00	10.00	18.00	18.00	18.00	18.00	18.00	18.00
.1	8.73	8.76	9.55	9.58	9.14	9.17	15.20	15.50	16.40	16.50	15.80	16.00
.2	6.69	6.89	8.18	8.23	7.44	7.56	11.50	13.10	13.36	14.05	12.43	13.57
.3	4.77	5.38	6.62	6.82	5.70	6.10	9.34	12.00	10.78	12.53	10.06	12.26
.4	3.52	4.63	5.26	5.71	4.39	5.17	7.98	10.92	8.80	11.50	8.39	11.21
.5	2.74	4.29	4.08	4.88	3.41	4.59	7.16	9.97	7.74	10.67	7.45	10.32
.6	2.23	4.10	3.22	4.43	2.73	4.27	6.47	9.01	7.04	9.82	6.75	9.42
.7	1.82	3.92	2.62	4.15	2.22	4.04	5.86	8.13	6.44	8.95	6.15	8.54
.8	1.60	3.76	2.22	4.00	1.91	3.88	5.12	7.36	5.91	8.18	5.51	7.77
.9	1.53	3.59	1.94	3.84	1.73	3.72	4.41	6.75	5.32	7.56	4.86	7.16
1.0	1.53	3.42	1.73	3.68	1.63	3.55	3.77	6.25	4.72	6.88	4.25	6.56
1.5					0.96	2.14					2.23	3.86
2.0					0.59	1.32					1.32	2.35
3.0					0.28	0.62					0.60	1.14

For a given value of ϕ, S_1 and S_2 are functions of λ alone. Since in the case of the diffuse scattering from a single crystal S_1 and S_2 are given by Eqs. (2) and (3), respectively, it is seen that S_1 and S_2 may be calculated from wave mechanics. In our experiments we have not used single large crystals but have scattered x-rays from brickettes of powdered crystals and so it is necessary to find formulas for S_1 and S_2 for our experimental case. The formula for S_2 remains as given in Eq. (3), but the formula for S_1 is changed. We now proceed to the derivation of the formula for S_1 for the case of a powdered crystal.

Referring to Eq. (5.23) on p. 131 of A. H. Compton's *X-Rays and Electrons*, we see that for a powdered crystal brickette placed in the Crowther position

$$\frac{P_s}{P} = \frac{N^2\rho^2\lambda^3F^2}{W^2}\cdot\frac{e^4}{m^2c^4}\cdot\frac{1+\cos^2\phi}{2\sin^2\phi}\cdot\frac{plt\rho'}{4\pi R\rho}, \tag{19}$$

where P_s is the intensity of the Debye-Sherrer

[18] R. W. James and G. W. Brindley, Phil. Mag. **12**, 81 (1931).

[19] D. K. Froman, Phys. Rev. **36**, 1339 (1930).

circle diffracted into an ionization chamber window whose height is l, P is the intensity of the primary beam penetrating the brickette, ρ is the density of a little crystal in the brickette and ρ' the overall density of the brickette. Now the intensity I_ϕ of the coherent part of diffusely scattered x-rays entering the chamber window is given by

$$\frac{I_\phi}{P}=\frac{A}{R^2}\cdot\frac{NZ}{W}\cdot\frac{e^4}{m^2c^4}\cdot\frac{1+\cos^2\phi}{2}\cdot\frac{\rho' t S_1}{\cos\frac{1}{2}\phi}, \tag{20}$$

where S_1 is given by Eq. (2). If both a Debye-Scherrer circle and the coherent part of the diffuse scattering on either side of the circle enter the ionization chamber window, Eqs. (19) and (20) combine to give

$$\frac{I_\phi+P_s}{P}=\frac{A}{R^2}\cdot\frac{NZ}{W}\cdot\frac{e^4}{m^2c^4}\cdot\frac{1+\cos^2\phi}{2}\cdot\frac{\rho' t}{\cos\theta}\times\left\{S_1+\frac{N\rho\lambda^3}{W}\cdot\frac{F^2}{Z}\cdot\frac{plR}{16\pi A\sin^2\theta\cos\theta}\right\}, \tag{21}$$

where $\theta=\frac{1}{2}\phi$. Hence, if we represent the coherent scattering factor for a powdered crystal by S_1', we have

$$S_1'=S_1+\frac{N\rho\lambda_r^3}{W}\cdot\frac{F_r^2}{Z}\cdot\frac{p_r lR}{16\pi A\sin^2\theta_r\cos\theta_r}. \tag{22}$$

Because the second member of Eq. (22) depends upon the particular Debye-Scherrer circle which enters the chamber, various quantities are subscripted with r. For the r^{th} circle we have

$$\lambda_r=2d_r\sin\theta_r \tag{23}$$

where, for a simple cubic crystal,

$$d_r=d_1/(r)^{\frac{1}{2}}. \tag{24}$$

The counter r is given by

$$r=\alpha^2+\beta^2+\gamma^2, \tag{25}$$

where α, β and γ are integers or zero but not more than two of them may be zero. The counter r according to Eq. (25) may be any integer excepting 7, 15, 23, 28, 31 and so on. But for a simple cubic crystal the principle grating space is given by

$$d_1=(W/N\rho)^{\frac{1}{3}}. \tag{26}$$

Now the area A of the ionization chamber window may be replaced by lw where w is the width of the window. Furthermore, the width w may be replaced by $R\delta\phi$, where R is the distance of the window from the axis of the spectrometer and $\delta\phi$ is the angle subtended by the width of the window. Hence, after eliminating λ_r from Eq. (22) by means of Eqs. (23), (24) and (26), we obtain

$$S_1'=S_1+\frac{F_r^2}{Z}\cdot\frac{p_r}{(r)^{\frac{1}{2}}}\cdot\frac{\tan\theta_r}{2\pi\delta\phi}. \tag{27}$$

This quantity S_1' replaces S_1 in the integrand in the numerator of the left side of Eq. (17). However, since, for a given angle ϕ, F_r only has values for particular values of λ, the integral as applied to the second term on the right of Eq. (27) becomes a summation. In this summation the $I(\lambda)d\lambda$ which appears under the integral is replaced by $I(\lambda_r)\delta\lambda_r$. The quantity $\delta\lambda_r$ is due to the angular width $\delta\phi$ of the window. Differentiating Eq. (23) and then dividing the equation so obtained by Eq. (23), we obtain after rearrangement

$$\delta\lambda_r=\tfrac{1}{2}\lambda_r\cot\theta_r\delta\phi. \tag{28}$$

The left side of Eq. (17) in virtue of Eqs. (2), (3) and (28) becomes

$$S_{\text{th}}=G-H+L, \tag{29}$$

where

$$G=\int\left\{\frac{f^2}{Z}+\frac{(1-f''/Z^2)K_\phi T_\phi}{K_0(1+\alpha\ \text{vers}\ \phi)^3}\right\}Id\lambda\Big/\int Id\lambda \tag{30}$$

and

$$H=\int(F^2/Z)Id\lambda\Big/\int Id\lambda \tag{31}$$

and

$$L=\left\{\frac{1}{4\pi}\sum_r\frac{F_r^2}{Z}\cdot\frac{p_r\lambda_r I(\lambda_r)}{(r)^{\frac{1}{2}}}\right\}\Big/\int^{*}Id\lambda. \tag{32}$$

The numerical value of the right side of Eq. (29) is determined by the wave-mechanics values of f and f'' and hence we shall designate this numerical value by S_{th}. If our theory is correct, S_{exp} as given by the right side of Eq. (17) should equal S_{th}. We have not used the theoretical values of F in the calculation of S_{th} because of the uncertainty of the Debye-Waller temperature factor, but have used the values of F as experi-

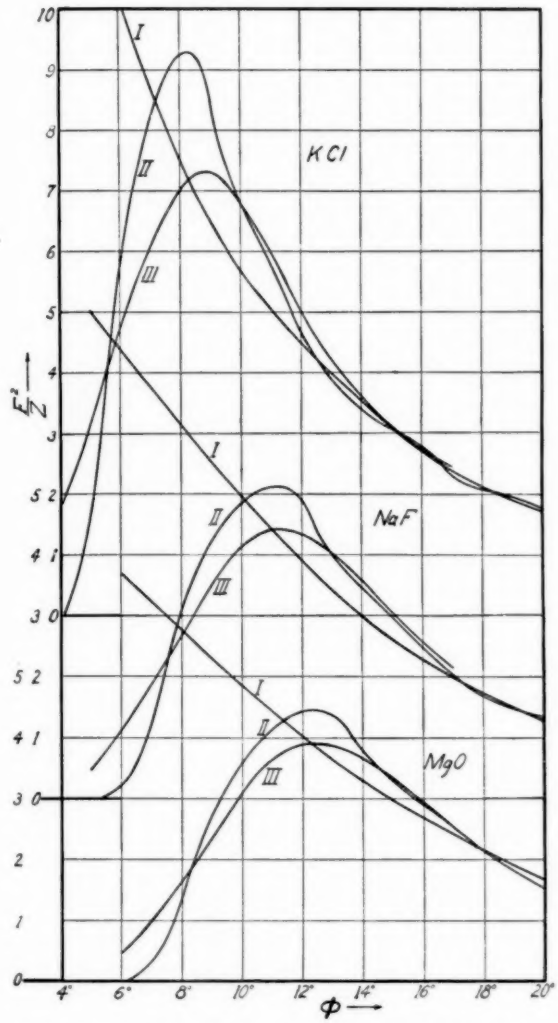

FIG. 4. Curves I, F^2/Z averaged over the wave-length band shown in Fig. 2 and an ionization chamber window width of 6°; curves II, L (see Eq. (32)) averaged over the wave-length band; curves III, L averaged over the wave-length band and the window width.

mentally obtained for KCl by James and Brindley,[20] for NaF by Havighurst,[21] and for MgO by Froman.[22]

Values of H as defined by Eq. (31) have been calculated for a given crystal for various values of ϕ and have been plotted against ϕ. Each of these values of H is for a small range of angles about ϕ. However, in our experiments, the range of angles was intentionally large, being about 6° for a given setting of the ionization chamber. We have therefore obtained the value of H as averaged over a range of 6° for each average value of the angle. The graphs for these average values of H are designated by the Roman numeral I in Fig. 4. Likewise, L as defined by Eq. (32) was plotted against ϕ (curve II) and from this curve average values of L were obtained. The graphs for these average values of L are designated by the Roman numeral III in Fig. 4. It is seen that for a given crystal there is an angle above which $(L-H)$ is nearly zero. For angles above this particular value, therefore. $S_{th}=G$ approximately. But G, in virtue of Eq. (30), is the value of S_{th} for the corresponding inert gas. Hence the relation as expressed by Eq. (6) should approximately hold for angles greater than the particular angle for each crystal. As the angles are made smaller than the par-

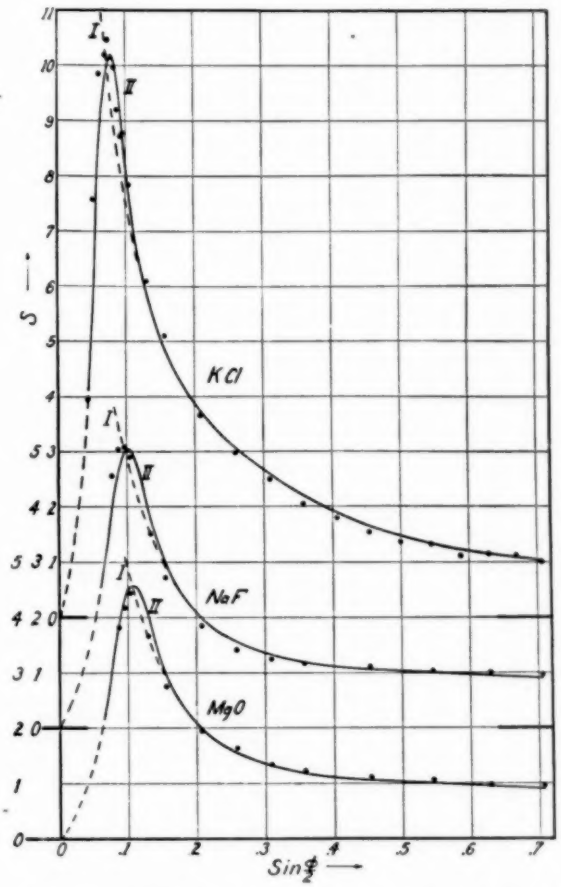

FIG. 5. Scattering of x-rays by powdered crystals. Curves I, theoretical S values for argon or neon; curves II, theoretical S values for powdered crystals (see Eq. (29)); black circles, experimental points.

[20] R. W. James and G. W. Brindley, Proc. Roy. Soc. **A121**, 155 (1928).

[21] R. J. Havighurst, Phys. Rev. **29**, 1 (1927).

[22] D. K. Froman, Phys. Rev. **36**, 1330 (1930).

ticular angle, the value of $(L-H)$ first increases, then decreases, and finally becomes a large negative number. At zero angle, $(L-H)$ very nearly equals $-Z$.

Using the values of f and f'' for neon and argon shown in Table III, we have calculated the values of G as defined by Eq. (30). As for the graphs of the average values of H and L, the values of G were averaged over an angular width of 6°. These average values of G are plotted against $\sin\frac{1}{2}\phi$ and the resulting graphs are designated by the Roman numeral I in Fig. 5. Graphs of S_{th} averaged over an angular width of 6° are now obtained and are designated by the Roman numeral II in Fig. 5. Since G very nearly equals $+Z$ at zero angle, S_{th} in virtue of Eq. (29) becomes $Z-Z$ or zero at zero angle.

Values of S_{exp} are shown as black circles in Fig. 5. It is seen how closely these circles fall upon the respective S_{th} curves. Particularly is this the case for KCl where the experimental points were taken down to angles as low as 5°. The experimental points follow the theoretical curve up to the maximum and then follow it by rapidly dropping as the angle approaches zero. An S_{th} curve for CaS is not shown because F values for this crystal were not available.

VI. Concluding Remarks

We feel that the agreement between our theory and the experimental results as shown by the curves and experimental points in Fig. 5 is excellent. Such discrepancy as appears is probably due to numerical approximations in the theory and to experimental errors.

With regard to Coven's experiment[7] with monochromatic rays, we believe that the relation expressed by Eq. (6) is only approximately true for particular angles of scattering, but is not generally true. The argument as developed in Eqs. (19) to (27) leads to an equation similar to Eq. (27), but with a summation sign in front of the second term on the right side of this equation. For monochromatic rays and a wide window, we arrive at

$$S_t = S_{\text{gas}} - \frac{F^2}{Z} + \sum_r \frac{F_r^2}{Z}\cdot\frac{p_r}{(r)^{\frac{1}{2}}}\cdot\frac{\tan\theta_r}{2\pi\delta\phi}. \qquad (33)$$

It is seen that the discrepancy between S_t and S_{gas} is equal to the algebraic sum of the second and third terms on the right side of Eq. (33). Values of the second term with a positive sign have been plotted against the angle for the case of KCl and $\lambda=0.71$A as shown by the curve in Fig. 6. Values of the third or summation term in Eq. (33) have been calculated for particular angles and are shown in Fig. 6 as black dots and white circles. The black dots refer to the case for a 10° window and the white dots to that for a 7° window. The curve in Fig. 6 depends also upon the

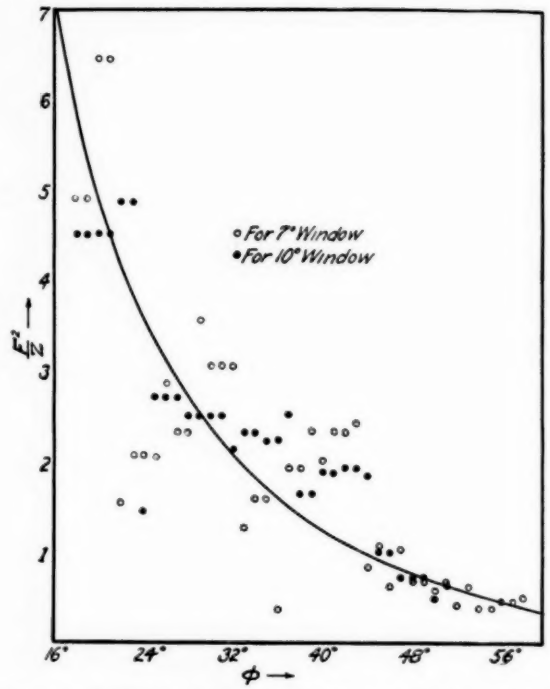

Fig. 6. Scattering of $\lambda=0.71$A from a powdered crystal of KCl. Curve, values of F^2/Z averaged over a window width of 6°; circles, values of third term on right side of Eq. (33) for different window widths.

width of the window but only slightly. The curve shown is for a 6° window. If a 7° window is used, the discrepancy between S_t and S_{gas} for a given angular setting of the ionization chamber is equal to the difference between the ordinate of a white circle and that of the curve for this setting. For a 10° window, the discrepancy is equal to the difference between the ordinate of a black circle and that of the curve. It is seen that, generally speaking S_t is not equal to S_{gas}.

In previous experiments performed in this laboratory on the diffuse scattering of x-rays from crystals an average wave-length has been

determined from an absorption curve such as shown in Fig. 1. This average wave-length has then been treated as a single wave-length and values of S plotted against $(\sin \frac{1}{2}\phi)/\lambda$. There has been some objection to this procedure. However, we have pointed out at the end of the last paragraph of §2 that the average wave-length as obtained from the spectral distribution is very nearly that obtained from absorption measurements. Also, at the end of §3 it is pointed out that the numerical formula for S_{exp} is very nearly independent of the precise wave-length assumed if the x-rays are supposed to consist of a single wave-length. Hence, in experiments such as those of Harvey[13] and of Jauncey and Williams,[14] the values of S are reasonably accurate. The trouble, however, arises in the values of $(\sin \frac{1}{2}\phi)/\lambda$ to which the respective values of S should be assigned. As a result of our present investigation it seems that, excepting in those portions of the graphs of S *versus* $(\sin \frac{1}{2}\phi)/\lambda$ where the slope is large, the values of $(\sin \frac{1}{2}\phi)/\lambda$ may be calculated from the angle and that value of λ which is found from the absorption curve. It seems, then, that a beam of x-rays which has passed through a sufficient thickness of aluminum acts for scattering purposes very nearly as if it were made up of monochromatic rays. The homogeneity of x-rays which had passed through a sufficient thickness of aluminum was noted several years ago by C. G. Barkla. The S curves shown in the papers by Harvey and by Jauncey and Williams are therefore reasonably accurate, excepting at small angles. As a result of this present investigation, we now believe that the proper procedure is to obtain the distribution of energy in the spectrum of the x-rays used and to calculate from theory the scattering to be expected at each angle. These theoretical values are then compared with the experimental values. For convenience the curve of the theoretical values and the points representing the experimental values are plotted against $(\sin \frac{1}{2}\phi)$.

In conclusion, we wish to thank Dr. J. A. Van den Akker for much help and advice in regard to the assembling of the all-in-oil x-ray outfit.

Diffraction of Low-Speed Electrons by a Tungsten Single Crystal

WAYNE T. SPROULL, *Department of Physics, University of Wisconsin*

(Received February 14, 1933)

The (1–1–2) and (1–0–0) planes of a tungsten crystal were bombarded at normal incidence with primary electrons and the intensity of the full-velocity secondary beams measured as a function of azimuth, co-latitude (θ), and primary voltage. A new magnetic deflection method of analyzing the secondaries permitted observations at co-latitudes down to zero. The crystal was outgassed 1550 hours at temperatures up to 1600°C at pressures of 10^{-7} mm of Hg or less. Strong sharp beams were observed in the AA' azimuth (Fig. 1) of the (1–1–2) plane at all wave-lengths which were used, and were found to be governed in every case by the volume equation $n_2\lambda = d/6^{\frac{1}{2}} + 2(d/6^{\frac{1}{2}})\sin(30° - \theta)$ and in no case by the surface equation. This is the first time that such a pronounced deviation from the usual theory has been observed. The final average experimental value for W_a was 5.52 volts which, combined with photoelectric and thermionic data yields a value for W_i of about 1 volt. The values obtained for W_a were unusually consistent. A few beams of the usual type obeying both interference equations were observed in the B and C azimuths of the (1–1–2) plane and also in an azimuth 30° from B. They were all quite broad, however, and consequently no attempt was made to estimate W_a from them. Beams were found in the case of the (1–0–0) plane which could be detected for various wave-lengths within the immediate neighborhood of their predicted location and which showed a tendency to vary in latitude in obedience with the volume equation, but became too weak to observe if the wave-length chosen was very far from the predicted value. Slight variations in the angle of incidence were found to have a very great effect on the observations. Some of those portions of the observations which differ from typical results obtained in similar investigations with other metals can be correlated qualitatively with the peculiarities of the tungsten crystal lattice. It seems likely that the explanation of the peculiarly governed beams observed in the AA' azimuth of the (1–1–2) plane and of Kikuchi's "N-pattern" for mica is somehow contained in the relation of atomic plane population to interplanar distance.

I. INTRODUCTION

THE present work was undertaken partly for the purpose of trying out a new type of apparatus[1] to see how it would perform in actual service, and partly to see whether a change from the low melting point face-centered cubic crystals which have so far been the usual subject of low-speed single crystal work to a high melting point body-centered cubic crystal would produce any noteworthy difference in the results. Having decided upon a new type of apparatus and a different type of crystal, conventional procedure was further violated by selecting as the first plane for study the (1–1–2) plane which has several unique characteristics as pointed out in section IV. The (1–0–0) plane was studied subsequently. The apparatus is unusual in two respects. (1) It enables one to analyze diffracted electron beams emitted at angles with the normal as small as one pleases, down to zero, even though the primaries are incident normally. (2) It eliminates the necessity of allowing for contact potentials between the filament and other parts of the electron gun when determining the velocity of the incident primary electrons.

[1] Sproull, R. S. I. **4**, 193 (1933).

II. THE CRYSTAL

The crystal was cut from a bar of tungsten about 20 mm long by 7 mm wide by 5 mm thick for which we are indebted to Professor P. I. Wold of Union College. The material reached Professor Wold rather indirectly from Germany, and formed part of a larger bar with which he proposes to carry out Hall-effect measurements.

The bar contained perhaps a dozen crystals ranging in size from about $1\times3\times1$ mm up to a large one which was approximately $7\times7\times4$ mm. A section of the bar containing this crystal along with two or three other much smaller ones was carefully sawed out using a thin sheet of copper armored with carborundum powder. The bar was moved back and forth along the edge and held in the fingers so as not to damage it by clamps.

The positions of the various atomic planes

were determined before the crystal was sawed from the bar, taking advantage of the well-known fact that chemicals which attack a metal crystal dissolve away the surface in such a way as to expose facets which coincide with various of the more prominent atomic planes. The bar was dropped into a boiling 3 percent solution of H_2O_2 and etched for about five minutes and then mounted on a goniometer. The angular positions of the reflected beams of light from an incident beam of parallel rays were determined with respect to one edge of the bar and the normal to the surface. By locating a dozen or so of these beams, it is possible to determine from which plane each individual beam is reflected, and thus to determine accurately the orientation of the unit atomic cubes in the bar. It was found that the large 7×7 mm face of the bar lacked only 6° 40′ of coinciding with the (1–1–2) plane. The (1–1–2) plane is an important one in a body-centered cubic, and is the plane which tends to develop most prominently in tungsten when it is etched, according to Smithels.[2] From this, we suspected that it might also tend to become more prominent under the action of outgassing in a vacuum.

Next, the crystal was sawed from the bar. A steel wedge about an inch square with its faces at an angle of 6° 40′ with each other was machined, and a hole about 1 cm in diameter was bored through it. The wedge was then bolted to a steel plate an inch square, the bolt heads being countersunk so as to leave the upper face of the wedge clear. The upper and lower faces of the tungsten segment containing the crystal were parallel. Consequently, when it was placed in the hole in the wedge with its bottom face resting on the steel plate, and then turned to the proper azimuth, the part which protruded above the upper face of the wedge was just the part which should be removed in order to expose a (1–1–2) plane. Wood's metal was poured around the crystal, and when it froze, the crystal was ready for grinding. It was ground with fine carborundum powder and water on plate glass until flush with the upper face of the wedge. It was then polished to mirror brilliance on a high-speed linen wheel with emery flour. After removal from the wedge, the crystal was re-etched and mounted in an x-ray camera, and from the positions of the Bragg x-ray lines it was determined that the (1–1–2) plane really coincided with the geometrical surface within less than a degree.

For the electron diffraction experiments, the crystal was inserted in a molybdenum socket having jaws which were too small to be struck by any appreciable number of primary electrons, the socket being rigidly fastened to a long heavy quartz tube mounted in bearings so that the azimuth could be varied by rotating the quartz tube. The tube was rotated and the molybdenum socket bent until no perceptible wobble of the (1–1–2) face remained. In this manner the (1–1–2) face was aligned with its normal within 10 or 20 minutes of the axis of the quartz tube, for when the error was 1°, the wobble was very noticeable. The quartz tube was then aligned with its axis parallel to the direction of motion of the primary electrons striking the crystal, this adjustment being made by heating and bending the outer Pyrex walls of the experimental tube, and being accurate to $\frac{1}{2}$°.

III. Outgassing Treatment and Reproducibility of Results

A vacuum of 10^{-7} mm of mercury or better was maintained throughout the work, and the crystal was outgassed continuously except when a set of readings was being taken, the temperature at the start being about 1000°C, and being increased gradually to about 1600°C after 1550 hours at the close of the experiments. After the first 100 hours of outgassing, the contact potential between the tungsten crystal and the surrounding molybdenum chamber became constant and remained 2 volts during the rest of the work. This early attainment of stability is in agreement with the observations of Dowling[3] and Glasoe.[4] After the first 300 hours of outgassing, it was found that diffraction data could be duplicated almost exactly if a given set of observations were repeated, even after a lapse of several weeks.

Langmuir has found that a monatomic layer of oxygen clings to tungsten surfaces even at very high temperatures, half of it being driven off in 15

[2] See Smithels' book *Tungsten*, Chapman and Hall, London.

[3] Dowling, Phys. Rev. **25**, 812 (1925).

[4] Glasoe, Phys. Rev. **38**, 1490 (1931).

seconds at 1800°C. Boas and Rupp[5] in their work with polycrystalline tungsten found "additional beams" fitting the usual diffraction theory if one postulates a lattice spacing of 4.46A which they attributed to this oxygen layer. Such beams were not found in the present work, which might indicate that the oxygen layer and other impurities were drawn off as positive ions by the electric field while the crystal was being bombarded at 2000 volts although they might not have been removed by simply heating the crystal to the same, or even a higher temperature.

IV. Peculiarities of the (1–1–2) Plane

According to Davey,[6] the length of an edge of the unit cube in tungsten is $d=3.155$A. Fig. 1 is a plan of the (1–1–2) plane. If the circles be taken as atoms at the corners of the unit cubes, the squares will represent "body-centered atoms," and *vice versa*. Those numbered 1 are in the surface layer; those numbered 2 are in the first layer beneath the surface, those numbered 3 in the second, etc. It is to be noted that there is line symmetry about the line BC in Fig. 1, but not

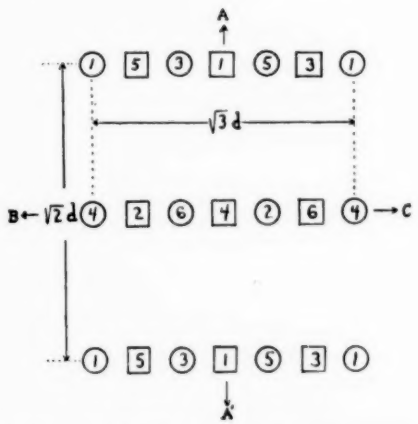

Fig. 1. The tungsten lattice viewed along the perpendicular to the (1–1–2) planes.

about the line AA'. Hence electron beams in the azimuths marked A and A' should be alike, but beams in the B azimuth should be different from those in the C azimuth. Atoms in the sixth layer beneath the surface lie directly beneath surface atoms, contrasting with the situation in the (1–0–0) plane, where atoms directly beneath the surface atoms are found in the second layer beneath the surface, and in the case of the (1–1–1) plane, the third, these planes being cited for comparison because they are the ones other experimenters have chosen for study. The atoms in the (1–1–2) planes are staggered to an unusual extent with respect to the normal to the planes, and the perpendicular distance between the (1–1–2) planes is only $d/6^{\frac{1}{2}}$ or 1.29A, very much shorter than the corresponding distance for the crystal faces usually bombarded by other experimenters with single crystals. Another unusual feature of the (1–1–2) plane is that the distance measured in the AA' azimuth between rows of atoms parallel to the BC azimuth is $4\frac{1}{2}$A, much longer than the "grating spacings" that have been used in most of the single crystal electron diffraction experiments. Consequently, the ratio of the grating spacing to the interplanar distance is extraordinarily high in this azimuth. Another fact possibly of significance is that the rows of atoms parallel to the BC azimuth happen to be the most densely packed rows in the crystal. That is, the atoms in these rows (which are the diagonals of the lattice cubes) are $3^{\frac{1}{2}}d/2$ apart, and this is the distance of closest approach for tungsten. These peculiarities are described at length because they may help to account for the unusual behavior of the secondary beams diffracted in the AA' azimuth.

V. Theory

Throughout the paper, we are dealing exclusively with the "full velocity secondaries," that is, those electrons which have undergone elastic collision with atoms of the crystal and have recoiled with a velocity equal to that of the incident primary electrons.

In Fig. 1, imagine a plane perpendicular to the paper (i.e., perpendicular to the (1–1–2) plane) and lying in the azimuth marked AA'. The arrangement of the atoms in this section is represented in the inset of Fig. 2. By examining this inset it is easy to see that phase waves of length λ incident normally upon the crystal and diffracted by the atoms Z and X at a co-latitude θ as shown will be in phase after diffraction provided

$$n_1\lambda = 2^{\frac{1}{2}}d \sin\theta, \qquad (1)$$

[5] Boas and Rupp, Ann. d. Physik [5], **7**, 983 (1930).
[6] Davey, Phys. Rev. **26**, 736 (1925).

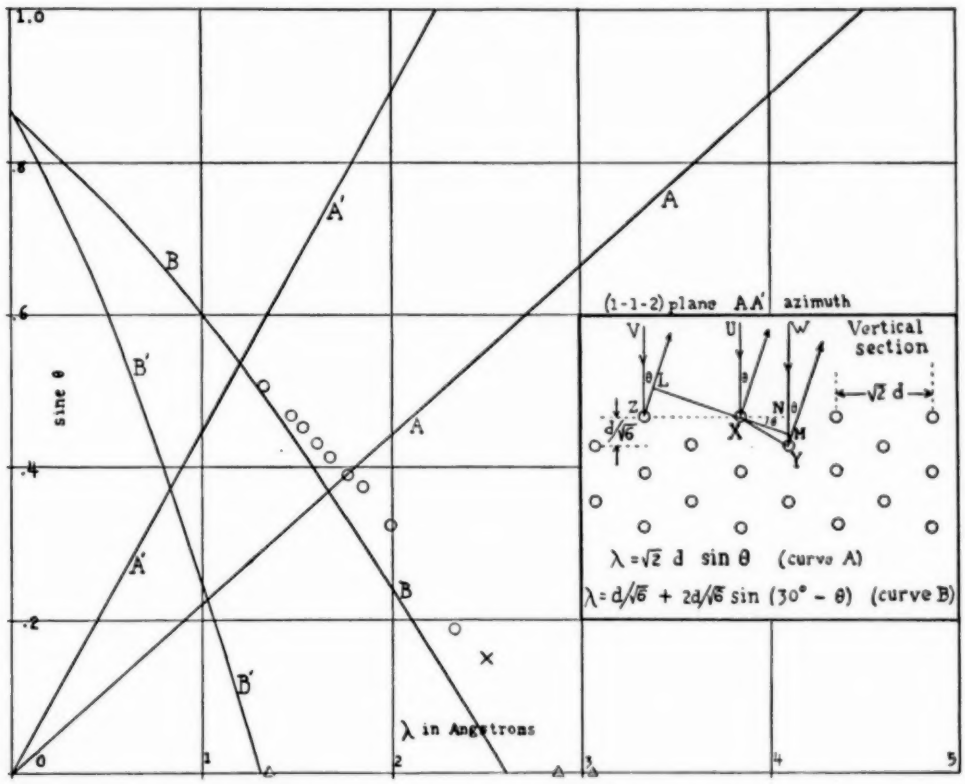

FIG. 2. Graphs of the interference equations for the (1–1–2) plane in the azimuths A or A' of Fig. 1. Inset is a vertical section of the (1–1–2) planes in the AA' azimuth.

where n_1 is any integer and d is the edge of a unit cube = 3.155A. This is the condition for constructive interference between all the atoms of any one layer, by an obvious generalization.

If, in addition, we are to have constructive interference between the rays diffracted from all the layers, the waves diffracted from such atoms as X and Y must be in phase. That is, $NY + YM$ must be an integral number of wave-lengths, n_2, whence we have

$$n_2\lambda = d/6^{\frac{1}{2}} + 2(d/6^{\frac{1}{2}}) \sin (30° - \theta) \qquad (2)$$

as the second interference condition. Beams are usually expected only when λ and θ have such values as to satisfy both (1) and (2) simultaneously. Eq. (1) is often called the "surface condition" and (2) the "volume condition" of interference. Following usual practice, these two equations are graphed (main part of Fig. 2) with sin θ as ordinates and λ as abscissae, the intersections of the two sets of curves predicting the co-latitude θ and the wave-length λ (and hence the primary voltage V, since $\lambda = h/mv = (150/V)^{\frac{1}{2}}$) at which the beams should occur. The straight lines represent the surface condition for $n_1 = 1, 2,$ etc., and the curved lines represent the volume condition for $n_2 = 1, 2,$ etc.

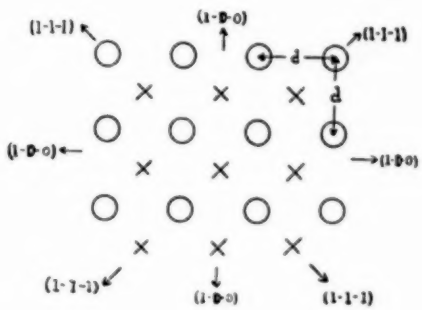

FIG. 3. The tungsten lattice viewed along the perpendicular to the (1–0–0) planes.

If we do the same thing for the (1–0–0) plane in the azimuths marked (1–0–0) (Fig. 3), we obtain the surface condition

$$n_1\lambda = d \sin \theta$$

and the volume condition

$$n_2\lambda = \tfrac{1}{2}d + d/2^{\frac{1}{2}} \sin(45° - \theta)$$

illustrated and plotted in Fig. 4.

Corresponding equations for some of the other cases studied are: (1–1–2) plane, B azimuth

$$n_1\lambda = 3^{\frac{1}{2}}d/2 \sin\theta, \quad \text{(surface)}$$

$$n_2 = (2/3)^{\frac{1}{2}}d + 3^{\frac{1}{2}}d/2 \sin(70°\ 30' - \theta); \quad \text{(volume)}$$

(1–1–2) plane, C azimuth

$$n_1\lambda = 3^{\frac{1}{2}}d/2 \sin\theta, \quad \text{(surface)}$$

$$n_2\lambda = d/6^{\frac{1}{2}} + \tfrac{1}{2}d \sin(54°\ 45' - \theta). \quad \text{(volume)}$$

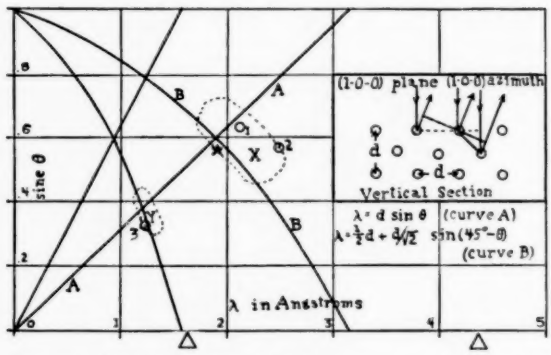

FIG. 4. Graphs of the interference equations for the (1–0–0) plane in the (1–0–0) azimuths of Fig. 3. Inset is a vertical section of the (1–0–0) planes in the (1–0–0) azimuth.

These sets of equations differ because there is not line symmetry about the line AA' (see Section IV). For the case of diffraction in the azimuths marked X due to the rows of atoms indicated by the dotted lines in Fig. 5, one obtains

$$n_1\lambda = (6/11)^{\frac{1}{2}}d \sin\theta \quad \text{(surface)}$$

and

$$n_2\lambda = d/6^{\frac{1}{2}} + (2/11)^{\frac{1}{2}}d \sin(73°\ 10' - \theta); \quad \text{(volume)}$$

(1–0–0) plane, (1–1–1) azimuths (see Fig. 3)

$$n_1\lambda = 2^{\frac{1}{2}}d \sin\theta, \quad \text{(surface)}$$

$$n_2\lambda = \tfrac{1}{2}d + 3^{\frac{1}{2}}d/2 \sin(35°\ 16' - \theta). \quad \text{(volume)}$$

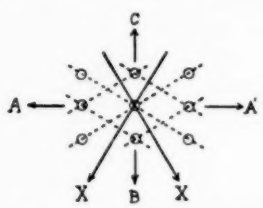

FIG. 5. Plan of the (1–1–2) plane similar to Fig. 1, but showing only one layer.

In the present apparatus, the collector can be moved into such a position as to catch secondary electrons leaving the crystal at normal exodence, so that the case $\theta = 0$ can be studied. One should note that this represents the zeroth order of surface interference, that is, $n_1 = 0$ for all the surface equations, which degenerate to $0 = 0$. In Figs. 2 and 4 this means that the surface equation is represented merely by the λ axis which should therefore be regarded as one of the system of straight lines in the graphs. At $\theta = 0$, therefore, one should expect to find maxima in the collector current at certain specific values of λ (and hence V) determined by the intersections of the curved lines with the λ axis. When $\theta = 0$, all of the volume equations for the various azimuths of any one plane become identical, as one would expect.

VI. The Observed Beams

Each set of observed beams will be described upon the basis of the following aspects:

A, *Intensity* of the beams compared to the background of random scattering upon which they are superimposed.

B, *Sharpness in co-latitude.* That is, maintaining the bombarding potential constant at the value at which a typical beam of the set is fully developed, does the electron current at various colatitudes in the neighborhood of the maximum decrease rapidly or slowly for a given azimuth?

C, *Sharpness in azimuth.* Maintaining the bombarding potential constant at the value at which a typical beam of the set is fully developed, does the electron current at various azimuths in the neighborhood of the one being studied decrease rapidly or slowly for a given co-latitude?

D, *Rate of growth and decay.* If one explores a typical beam of the set by varying the co-latitude with constant azimuth, not only at the critical bombarding potential at which the beam is fully developed, but also at various other values of V in the neighborhood, does the beam fade out or "decay" rapidly as V recedes from this critical value?

E, *Mode of growth and decay.* If one maintains the bombarding potential at a constant value differing slightly from the critical value at which a typical beam of the set is fully developed, is the location of the beam in co-latitude such as to

agree closely with the *surface* interference condition or with the *volume* interference condition, or with neither? (A beam should be fully developed in a given azimuth only when both θ and V are chosen so as to simultaneously satisfy both conditions; when V is varied slightly, *both* conditions can not be satisfied.)

1. Sets of beams in the B and C azimuths of the (1-1-2) plane. (Fig. 1)

A, Very weak and difficult to detect. B, Moderately sharp in co-latitude. C, Moderately sharp in azimuth. D, Very rapid decay. E, Mode of decay indeterminate, because decay is too rapid.

2. The sets of beams in the azimuths of the (1-1-2) plane marked X in Fig. 5

Exactly similar to the sets just described.

3. Beams in the (1-1-1) azimuths of the (1-0-0) plane (Fig. 3)

A, Weak. B, Very broad in co-latitude. C, Broad in azimuth. D, Fairly rapid decay. E, Tendency to satisfy the volume condition rather than the surface condition.

4. Beams in the (1-0-0) azimuths of the (1-0-0) plane (Fig. 3)

A, Rather weak. B, Very broad in co-latitude. The $n_1=1=n_2$ beam is shown plotted in co-latitude (θ) in Fig. 6A where the radii represent collector current for the various values of θ. The arrow indicates the peak which is approximately at its maximum development at this voltage. The $n_1=1$; $n_2=2$ beam is shown similarly in Fig. 6C. C, Broad in azimuth. The $n_1=1=n_2$ beam is shown plotted in azimuth in Fig. 7, the radii again representing collector current. D, Unusually slow growth and decay. The $n_1=1=n_2$ beam could be detected at any value of V between 25 and 50 volts. Fig. 6B shows co-latitude curves taken at a value of V ten volts less than that at which the beam is fully developed, the peaks being indicated by the arrows. These curves were both taken in (1–0–0) azimuths, but are 90° apart in azimuth (see Fig. 3) and were taken about two weeks apart. The curves of Figs. 6A, B, C were all corrected for change of solid angle subtended by the collector opening as discussed in the article in R. S. I.[1] E, Close agreement with the volume condition.

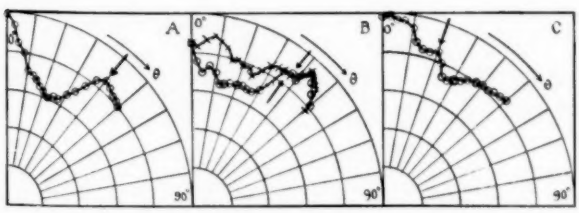

FIG. 6. Co-latitude curves for the (1–0–0) plane. A, The $n_1=1=n_2$ beam at full development. B, Two curves showing the same beam at a bombarding potential 10 volts less than A.C. The $n_1=1$; $n_2=2$ beam.

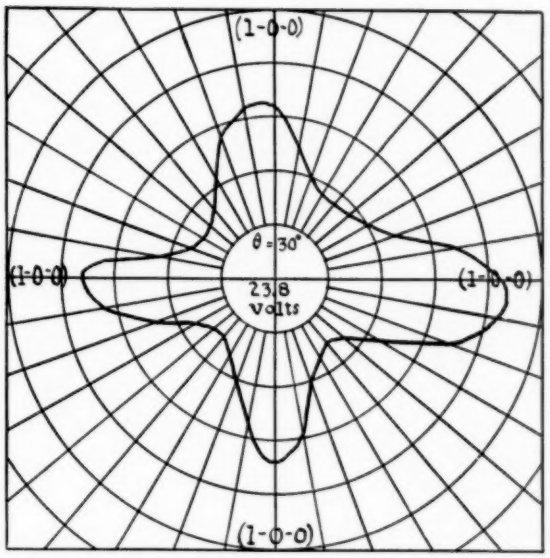

FIG. 7. An azimuth curve of the $n_1=1=n_2$ beam for the (1–0–0) plane taken at a co-latitude of 30°; bombarding potential $V=23.8$ volts.

5. Beams in the *A* and *A′* azimuths of the (1-1-2) plane (Fig. 1)

A, Very strong. B, Exceedingly sharp in co-latitude; see Fig. 8. C, Very sharp in azimuth; see Fig. 9, note curve marked 22° (co-latitude). D, No decay whatever; the various co-latitude curves of Fig. 8 were taken at the various voltages indicated, and it is seen that the beam is equally well developed at every voltage which was tried. Only the central portion of each peak was plotted because it was desired to record the whole set in one afternoon under exactly the same conditions. These peaks are so narrow that it was not necessary to make correction for change of solid angle subtended by the collector opening. E, After allowance for refraction (to be

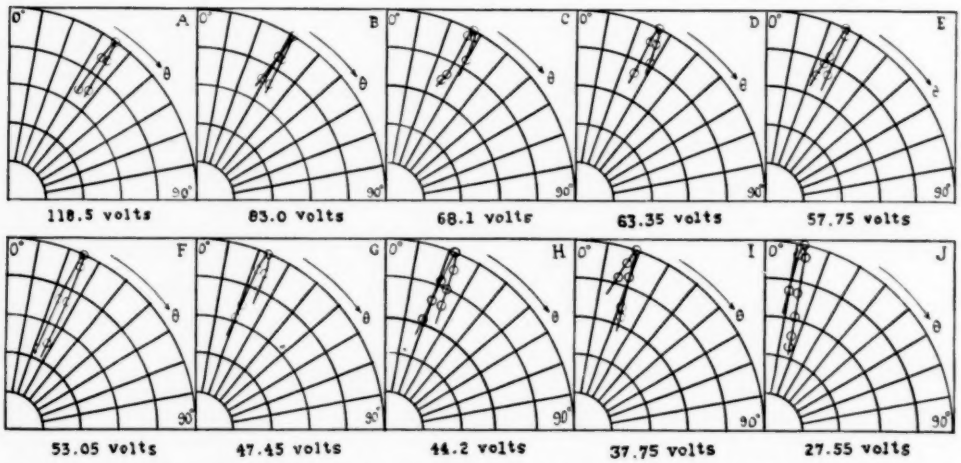

FIG. 8. Co-latitude curves showing the unusual series of $n_2=1$ maxima found in the AA' azimuth of the (1–1–2) plane at ten different values of V as indicated.

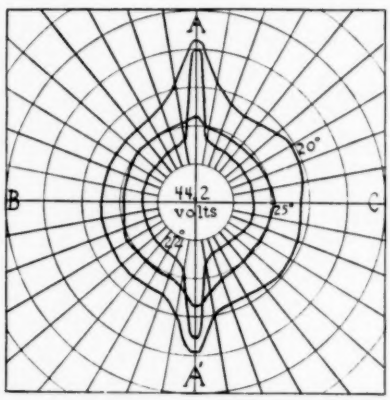

FIG. 9. Azimuth curves of the $n_2=1$ maxima in the AA' azimuth of the (1–1–2) plane at a bombarding potential of 44.2 volts at co-latitudes of 20, 22 and 25 degrees as indicated

discussed in Section VIII), the positions of the beams agree almost perfectly with the volume condition (2), and since there is no voltage of maximum development, it seems that these beams are governed exclusively by Eq. (2) and not at all by Eq. (1).

VII. Correlation of the Observed Beams with the Theory

The sets of beams described in the preceding section were enumerated in order of their agreement with the theory of Section V. The first beams described behaved most nearly in accord with the theory, while the ones described last departed markedly from it. The behavior of the beams observed in the (1–0–0) azimuth of the (1–0–0) plane at voltages in the vicinity of the critical value of full development can be illustrated graphically in Fig. 4 by saying that they could be observed throughout the regions X and Y indicated by the dotted lines near the intersections of the curves. The tendency to obey the volume condition rather than the surface condition is indicated by the fact that these regions lie along the curved (volume) graphs and not along the straight (surface) graphs. Other experimenters[7] studying the process of growth and decay of the electron beams have found a tendency to obey the surface condition more closely than the volume condition. The circles numbered 1, 2 and 3 in Fig. 4 mark the values of θ and λ at which the curves of Fig. 6A, B and C were taken respectively.

The beams found in the AA' azimuth of the (1–1–2) plane and shown in Figs. 8, A–J are located at values of θ and λ indicated by the circles in Fig 2, where one sees immediately that they are falling along the $n_2=1$ volume curve.[8] They do not fall exactly on the curve because we have so far neglected to correct for refraction. This correction will be made in the next section.

[7] See Davisson and Germer, Phys. Rev. **30**, last paragraph, p. 734 (1927) or Farnsworth, Phys. Rev. **34**, top of p. 693 (1929).

[8] The striking behavior of these beams as regards growth and decay can be illustrated graphically by comparing Fig. 2 with Fig. 3 obtained by Farnsworth for copper, Phys. Rev. **34**, p. 685 (1929), or comparing Fig. 8 with Fig. 10 obtained by Davisson and Germer for nickel, Phys. Rev. **30**, 716 (1927).

The cross in Fig. 2 indicates a beam found after only 28 hours of outgassing which evidently falls in line with the circled beams which were discovered later after 440 hours of outgassing at about 1200°C. The beams were followed right up to $\theta=0$.

VIII. Correction for Refraction and Calculation of the Surface Work Functions W_a and W_i

A. Normal exodence

In the case of the experiments at $\theta=0$, one does not need to make any correction for bending at the surface. The only effect of refraction is to make the length of the phase waves within the crystal less than it is outside. Therefore one can merely subtract the experimental value of the bombarding potential V at which a maximum occurs from that at which it is predicted and say that the difference represents the surface work function W_a. If one sets $\theta=0$ in Eq. (2) and solves for λ and then for V using $\lambda=(150/V)^{\frac{1}{2}}$, it turns out that maxima in the collector current should be expected at $\theta=0$ for the (1–1–2) plane for the values of V given in the second column of Table I, corresponding to the choices of n_2 in the first column. Proceeding similarly for the (1–0–0) plane, we obtain Table II. The average of the six values of W_a in Tables I and II is 5.19 volts. The variation in the six values may be due to small variations in the angle of incidence as pointed out by Farnsworth.[9] The 7.9 volt maximum of Table II is shown plotted[10] in Fig. 10 which shows some indication of an accompanying satellite of the type found for copper and silver by Farnsworth.[9] The positions of these $\theta=0$ maxima are indicated in Figs. 2 and 4 by triangles.

Table I. (1–1–2) *plane.*

n_2	$V_{calc.}$ (volts)	$V_{obs.}$ (volts)	$W_a(=V_{calc.}-V_{obs.})$ (volts)
1	22.5	16.0 (218 hrs. outgassing)	6.5
2	90.0	84.6 (259 hrs. outgassing)	5.4
1	22.5	19.25 (383 hrs. outgassing)	3.25
2	90.0	84.6 (383 hrs. outgassing)	5.4

Table II. (1–0–0) *plane.*

n_2	$V_{calc.}$ (volts)	$V_{obs.}$ (volts)	$W_a(=V_{calc.}-V_{obs.})$ (volts)
1	15.1	7.9	7.2
2	60.2	56.8	3.4

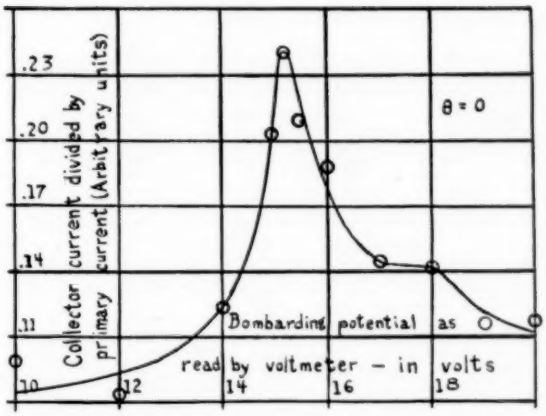

Fig. 10. The $n_1=0$; $n_2=1$ (normal exodence) maximum in the (1–0–0) azimuth of the (1–0–0) plane.[10]

B. Oblique exodence

The extreme sharpness and great intensity of the beams found in the A and A' azimuths of the (1–1–2) plane made it seem advisable to base the estimates of W_a exclusively on these beams, for all of the other beams were so broad in comparison that estimates of comparable accuracy would be impossible. In Fig. 2, it is supposed that the points lie near the volume curves instead of on them because no correction has been made for refraction. If the curves are now corrected for refraction until they are shifted over to coincide with the points, one can estimate from the amount of the correction necessary what must have been the value of the surface work function W_a to which the refraction is due. We now proceed to do this.

[9] Farnsworth, Phys. Rev. **40**, 684 (1932).

[10] In Fig. 10, the abscissae give the apparent bombarding potential as read by a voltmeter (connected from filament to grid) and it is seen that the voltage of the maximum read in this way is about 15¼, although the true bombarding potential was 7.9 volts as marked, the discrepancy being due to contact potentials in the electron gun. These contact potentials which are not only large, but quite variable from day to day are of no importance in the present work, but Fig. 10 was plotted so as to emphasize them because they must be considered in using apparatus of the usual type, and their wide fluctuation may account for the irregular variations of W_a reported by some observers.

It must be remembered that due to refraction, the length of the phase waves within the crystal is not λ, but λ', and that the angle θ at which the beams are observed is not identical with the angle θ' at which the diffraction is really occurring. Consequently, Eq. (2) should be corrected by replacing λ by λ' and θ by θ' using the relation

$$\lambda/\lambda' = \mu = \sin\theta/\sin\theta' \tag{3}$$

μ being the index of refraction given by $\mu = (1+W_a/V)^{\frac{1}{2}}$ where W_a is the surface work function. If Eq. (2) is thus corrected, and if at the same time one substitutes for d its value (3.155A), one obtains for the first order equation ($n_2=1$)

$$\lambda' = 1.29(1+2\sin(30°-\theta')) \tag{4}$$

or substituting for λ' and θ' their values in terms of λ, θ, and μ from Eq. (3), one obtains

$$\frac{\lambda}{\mu} = 1.29\left(1+\left(1-\frac{\sin^2\theta}{\mu^2}\right)^{\frac{1}{2}} - 1.732\frac{\sin\theta}{\mu}\right). \tag{5}$$

Solving this equation for μ, one obtains

$$\mu = \frac{(\lambda/1.29)^2 + 2.685\lambda\sin\theta + 4\sin^2\theta}{2(\lambda/1.29 + 1.732\sin\theta)}. \tag{6}$$

In Table III, the first column gives the co-latitude at which the beam occurred as read from Fig. 8. The second column gives the primary voltage V at which the beam was actually observed, this being computed from the magnetic field as explained in the article in R. S. I.[1] The wave-length λ corresponding to this primary voltage as computed from the equation $\lambda = (150/V)^{\frac{1}{2}}$ is given in the third column. Substituting the values of θ and λ from columns 1 and 3 into Eq. (6), one computes the values of μ given in the fourth column. Then using the equation $\mu = (1+W_a/V)^{\frac{1}{2}}$ one computes the values of W_a recorded in the fifth column. These values are seen to be fairly consistent and their average is 5.65 volts. If one includes in the average the values for W_a given in Tables I and II, one obtains a final average for W_a of 5.52 volts, which the writer regards as his best experimental value.

TABLE III. *A–A' azimuth* (1–1–2) *plane.*

θ (degrees)	V (volts)	λ (Angstroms)	μ	W_a (volts)
0	17.62	2.918	1.1324	5.0
12	27.55	2.334	1.0949	5.5
19	37.75	1.994	1.0773	6.1
22	44.2	1.843	1.0743	6.8
23	47.45	1.779	1.0659	6.5
24½	53.05	1.682	1.0544	5.9
25½	57.75	1.612	1.0448	5.3
27	63.35	1.539	1.0421	5.4
28	68.1	1.485	1.0396	5.5
31	83.0	1.535	1.0318	5.5
35	118.5	1.125	1.0198	4.7
			Mean:	5.65

IX. Effect of Variation of Angle of Incidence

In a recent paper,[9] Farnsworth emphasizes the importance of slight variations in the angle of incidence. An azimuth curve was taken with the normal to the (1–0–0) plane inclined at an angle of 2 or 3 degrees to the direction of motion of the incident primary electrons at an angle θ and voltage indicated by the star in Fig. 4. The curve obtained is the solid one in Fig. 11. The tube was then cut down, the crystal re-aligned, followed by reassembly of the tube, the usual two weeks of baking, and 100 more hours outgassing of the crystal. The azimuth curve was then repeated at the same latitude and voltage, the result being shown by the dotted curve in Fig. 11. The solid curve exhibits peaks very strongly in the (1–0–0) azimuth at 90° and 180°, and weakly at 270° and 0°, but the dotted curve exhibits no peaks at all. The importance of small variations in the angle of incidence is thus again demonstrated.

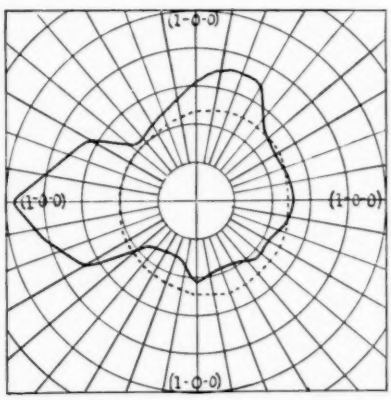

FIG. 11. Azimuth curves showing the effect of slight variations in the angle of incidence.

X. Subsequent Examination of the Crystal

Microscopic examination of the crystal after the work was completed revealed slight pitting of the surface by the bombardment, but the crystal facets flashed up in unison over the entire face even more brightly than they had just after the original etching, indicating that if any recrystallization had occurred, it was ultramicroscopic.

XI. Discussion

A. General

In the following discussion, the observed peculiarities of electron diffraction in tungsten are enumerated, followed in each case by a brief attempt to partly correlate them with the known structure of the tungsten lattice.

(1) Except in the case of the AA' azimuth of the (1–1–2) plane, the beams on the whole are less intense, less sharp in co-latitude and azimuth, and have a slower rate of growth and decay (these expressions were explained in Section VI) than those observed by others for nickel, copper, silver, etc.

The (1–0–0) and (1–1–2) planes of tungsten are somewhat less densely populated than the planes examined in these other metals. For example, the populations of the tungsten (1–1–2) and (1–0–0) planes, the (1–1–1) plane of nickel, and the (1–0–0) planes of silver and copper are approximately in the ratio 81 : 99 : 106 : 121 : 155 respectively. This circumstance might enable the primary electrons to penetrate more deeply into the crystal, and the secondaries originating deep within the metal might suffer a second diffraction or undergo irregular scattering on their way back to the surface. Such successive diffraction might help to account for the generally lessened sharpness and rate of growth and decay and for the increased diffusely scattered background.

(2) In general, the volume interference condition seems to play a more important rôle in tungsten than in other metals. This also could be explained on the basis of deeper penetration, which would tend to increase the intensity of the volume maxima and also to increase their sharpness due to improved resolving power.

(3) A unique behavior is observed in the case of the beams diffracted in the AA' azimuth when the primary beam is incident normally upon the (1–1–2) plane. Here the beams were sharper in co-latitude and azimuth than are usually observed for other materials, and were found at every voltage tried, always at a value of θ agreeing with the volume Eq. (2). In this azimuth of this plane, the surface interference Eq. (1) has negligible effect, or none at all.

The sparse population of the (1–1–2) planes coupled with their small interplanar distance and the unusual staggering of the atoms about the normal pointed out in Section IV might allow penetration of an unusual number of planes by the primaries. From Fig. 1, one can see that the secondaries diffracted at oblique exodence in the B or C azimuths will encounter many obstructing atoms in their journey back to the surface with the results already mentioned in Part 1 of the discussion, but secondaries diffracted at oblique exodence in the A or A' azimuth will find a comparatively free path back to the surface if θ is less than about 35°. This makes the extreme sharpness, great intensity, and the accentuation of the volume interference somewhat more plausible, but fails to account for the absence of destructive interference when Eq. (1) is not satisfied.

The unique behavior is observed with a sparsely populated closely spaced set of planes. The opposite extreme in behavior was observed by Kikuchi with the opposite extreme in structure, though with primary velocities from 10,000 to 85,000 electron-volts. Bombarding films of mica about 10^{-5} cm thick normally to the cleavage planes which are spaced at the relatively great distance of 10A[11] and recording the transmitted secondaries by a photographic plate behind the film, he obtained[12] a so-called "N-pattern" which fits perfectly the surface interference condition applied to the cleavage plane, while the volume condition had no influence which could be even detected. The same phenomenon was noted in mica with x-rays by W. Linnik.[13]

It seems worth noting that while with tungsten the breakdown of the *surface* condition for

[11] Siegbahn, Phys. Rev. **8**, 320 (1916).

[12] Kikuchi, Proc. Imp. Jap. Acad. **4**, 271, 275, 354, 471 (1928); Japanese Journal of Physics **5**, 83 (1928).

[13] Linnik, Nature **123**, 604 (1929).

constructive interference is associated with incidence on relatively empty but closely spaced planes, Kikuchi's observed breakdown of the *volume* condition for constructive interference is associated with relatively full planes which are widely spaced. This suggests that the explanation of both anomalies is somehow contained in the relation of population to interplanar distance.

This problem has already aroused the interest of others. W. L. Bragg[14] suggested that the phenomenon could be "readily explained by the familiar laws of diffraction by a three dimensional grating, assuming a slight random warping of the mica planes," and performed an experiment to demonstrate this possibility. It seems doubtful whether the present results can be explained on the basis of an opposite type of deformation of the tungsten crystal.

The sharpness of the beams in the AA' azimuth of the (1–1–2) plane enables one to compute that the phase waves assumed to be associated with the electrons have an effective lateral extent at right angles to the direction of propagation of at least 30A if one is permitted to apply the usual formulae for resolving power to the phase waves. A similar conclusion was reached by G. P. Thomson.[15]

B. Values for W_a

According to Sommerfeld's theory of metals,[16] we have

$$\phi = W_a - W_i \qquad (7)$$

where ϕ is the usual photoelectric or thermionic work function (4.55 volts for tungsten), W_a is the height of the potential wall at the metal surface, and W_i is the maximum internal energy of the free electrons in the metal. Therefore, if we take the final value of 5.52 volts for W_a yielded by the present experiments, we get W_i = about 1 volt, whereas an application of Sommerfeld's theory to tungsten yields a theoretical value of 5.7 volts.

The only other determination of W_a for tungsten is that of Boas and Rupp[5] who obtained values of 0 and 10 volts for polycrystalline material. As regards consistency, the present results are considerably more satisfactory than those recently given by Farnsworth[9] for a single copper crystal in which case the values of W_a range from 5 to 31 volts. The fact that higher outgassing temperatures could be used with tungsten may account for the more consistent values obtained, and this consistency leads one to attach some possible importance to the difference between the resulting value of W_i and that computed from the Sommerfeld theory. This difference may be due to the limitations of the Sommerfeld theory resulting from the fact that the variations in potential inside the crystal due to the atoms is not considered; or perhaps one is not justified in treating the diffraction from the crystal planes in such a highly idealized way, as though the problem were quite analogous to diffraction of light in optics; or it may be that unsuspected systematic experimental errors are responsible.

In conclusion, the writer wishes to express his sincere appreciation of the invaluable help so willingly offered by Professor C. E. Mendenhall, who directed the work.

[14] Bragg, Nature **124**, 125 (1929).

[15] See Thomson's book, *Wave Mechanics of Free Electrons*, p. 72.

[16] Sommerfeld, Zeits. f. Physik **47**, 31 (1928).

The Fluorescence Yield from the L_{III} Level of Uranium

REGINALD J. STEPHENSON, *Ryerson Physical Laboratory, University of Chicago*

(Received February 3, 1933)

The fluorescence yield, defined as the ratio of the number of fluorescence quanta emitted from the L_{III} level to the total number of incident quanta absorbed in the L_{III} level has been measured for uranium; and the value of 0.67 found. The relative intensities of the α to the β-lines in the K fluorescence spectra of molybdenum have been measured and found to agree with the value from the characteristic spectrum. The relative intensities of the α to the β-lines originating from the L_{III} level have been measured in the fluorescence spectrum of uranium, and found to agree with the value from the characteristic spectrum. The atomic absorption coefficients for uranium for wave-lengths including the L_{III} discontinuity have been measured, and a value for $\delta = 2.27$ found, where δ is the ratio of the absorption coefficients on the short and long wave-length sides of the L_{III} discontinuity.

ACCORDING to the theory of the production of fluorescence x-rays, when an electron in the K energy level absorbs a quantum of x-rays, it is ejected as a photoelectron. An electron from the L or outer levels will then fall into the vacant K level with the emission of K fluorescence radiation. Thus for each quantum of energy absorbed in the K level there should be emitted one quantum of fluorescence K radiation. However, it has been apparent for some years that this simple picture does not give a complete account of the phenomena associated with the reorganization of the atom. In some early experiments on the efficiency of production of fluorescence x-rays, excited by K characteristic radiation, for atoms belonging to the iron group Barkla and Sadler[1] found that only some 30 percent of these atoms ionized in the K level emitted K fluorescence radiation. Barkla[2] and Beatty[3] also found that the excitation of the K series was accompanied by a sudden increase in the emission of the photoelectrons. Auger,[4] using a Wilson cloud-chamber with different inert gases, was able to photograph the tracks of the photoelectrons and measure their energy. He found that in addition to the photoelectron whose energy is given by Einstein's equation $E_{kin} = h\nu - h\nu_K$ for absorption by a K electron; there might be emitted from the same atom an electron of energy approximately $E = h\nu_K - 2h\nu_L$ and others of a similar type. This simultaneous ejection of several β-particles from the same atom has been called the "compound photoelectric effect." By knowing the energy and number of the β-particles, Auger was able to count the number of quanta absorbed in the K level, and the number of fluorescence K quanta emitted. He defined the fluorescence yield for the K level as the ratio of the number of fluorescence K quanta emitted to the total number of incident quanta absorbed in the K level. A similar definition may be applied to the L levels. Using the symbols w_K and w_L to represent the fluorescence yield from the K and L levels, respectively, Auger found the following results:

Auger's Results on Fluorescence Yield in K and L Series.

Atomic No.	Gas	w_K	w_L
19	argon	0.07	
36	krypton	0.51	0.1
54	xenon	0.71	0.25

Kossel[5] has suggested that the low efficiency of the K series emission may be explained on the assumption that the majority of such atoms undergo radiationless reorganizations of the Klein-Rosseland type resulting in the appearance of high-speed photoelectrons. Bothe,[6] on the other hand, has suggested that the results of Barkla

[1] Barkla, Bakerian Lecture, Phil. Trans. **217**, 317 (1917).
[2] Barkla and Philpot, Phil. Mag. **25**, 489 (1923).
[3] Beatty, Proc. Roy. Soc. **A85**, 329 (1911).
[4] Auger, C. R. **177**, 169 (1923); C. R. **180**, 65 (1925); Ann. de Physique **6**, 183 (1926).
[5] Kossel, Zeits. f. Physik **19**, 333 (1923).
[6] Bothe, Phys. Zeits. **26**, 410 (1925).

and Auger can be correlated on the assumption that they are manifestations of the phenomena of "internal absorption." According to this picture K radiation is always emitted in the reorganization of a K ionized atom, but the probability that this radiation shall be absorbed in the L, M, N, etc., levels of the same atom is very much greater than that it shall be absorbed in the same level of some other atom. In other words, the absorption coefficient for the K series radiation in the L, M, N, etc., levels of the "parent" atom is very much greater than for radiation of the same wave-length emitted from some other atom. There appears, however, to be no method of deciding between the two theories from an experimental standpoint. The excitation of the K series radiations in a solid or gas will be accompanied by a sudden increase in the photoelectric emission as a result of the "internal absorption" of the fluorescence radiations in the outer levels of the atoms. This was observed by Barkla[2] and Beatty[3] in the ionization produced relative to air, in methyl bromide, methyl iodide, and selenium hydride, when the wave-length of the radiation was slightly shorter than the K limit of the gas in question. Martin[7] has calculated the value for w_K from these data for bromine, iodine and selenium, and found it to give reasonable results. The importance of this effect in the measurement of relative intensities of x-ray lines with an ionization chamber has been well shown by Allison and Andrew.[8]

Measurements on the fluorescence yield in the K series have been made by Compton[9] and Martin,[7] where it was shown that w_K increases with the atomic number of the element, but does not vary with the wave-length of the incident x-rays. The latter conclusion involves the assumption, in the calculation of the energy of the x-rays, that the energy required to produce a pair of ions in the gas of the ionization chamber is constant and independent of the wave-length of the x-rays. This assumption appears to be fully justified by quite independent experiments.[10]

Since there are three L levels it was decided to make a determination of the fluorescence yield for a single one of these; and accordingly the L_{III} level of uranium was chosen. The method used in this experiment is essentially the same as that adopted by Compton.[9]

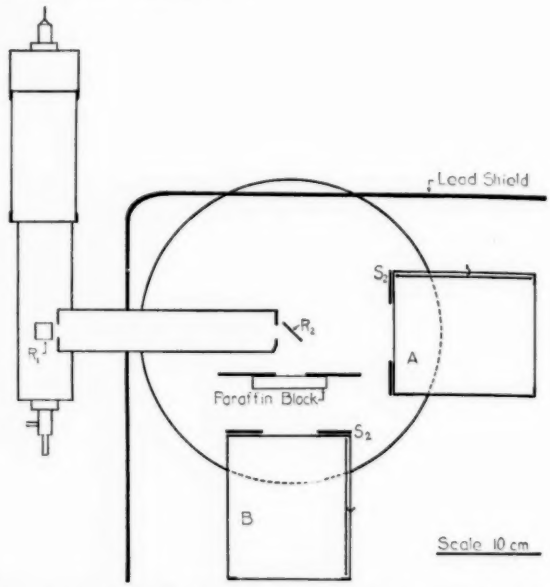

FIG. 1. Diagram of apparatus used for measuring the fluorescence yield from the L_{III} level of uranium.

The wave-lengths of the three L levels of uranium are given by Siegbahn[11] as: $L_I = 0.5680$A; $L_{II} = 0.5913$A; $L_{III} = 0.7208$A; and the wave-length of the molybdenum $K\alpha_1 = 0.7078$A; Mo $K\beta_1 = 0.6309$A; so that if this radiation from Mo is incident on a block of U only the lines arising from the L_{III} level will be excited. Primary x-rays from a rhodium target fell on a block of molybdenum at R_1 producing nearly homogeneous K radiation. A rhodium target was used in the x-ray tube because the wave-lengths of the Rh $K\alpha_1$ and Rh$K\beta_1$ are just a little shorter than the K absorption limit of Mo, and consequently the fluorescence lines from Mo will be excited quite strongly. Fluorescence radiation was used in preference to characteristic, because the former is entirely line radiation.

The fluorescence Mo radiation after passing through collimating slits fell on a piece of U at R_2, and the resulting radiation measured by an ionization chamber placed in position B. The intensity of the direct beam was measured by the ionization chamber in the position A.

[7] Martin, Proc. Roy. Soc. **A115**, 420 (1927).
[8] Allison and Andrew, Phys. Rev. **38**, 441 (1931).
[9] A. H. Compton, Phil. Mag. **8**, 961 (1929).
[10] Crowther and Bond, Phil. Mag. **8**, 961 (1929).
[11] Siegbahn, *Spektroskopie der Röntgenstrahlen*, Second Edition, p. 274.

Calculation of the Fluorescence Yield

Let μ' be the total absorption coefficient of the primary Mo x-rays in the U radiator, then

$$\mu' = \tau' + \sigma'$$

where τ' is the photoelectric absorption, and σ' the absorption due to scattering. In this case the greater part of the photoelectric absorption will be due to the electrons in the L_{III} level, i.e., τ_L'. For the sake of convenience the subscript III will be dropped, and it is to be understood that τ_L and w_L refer only to the L_{III} level of U and not to all of the levels. The Mo fluorescence beam was taken as composed of four lines; α_1, α_2, β_1, β_2, and their relative intensities taken from Meyer's[12] data, namely: $\alpha_1 : \alpha_2 : \beta_1 : \beta_2 = 100 : 50.6 : 23.25 : 3.48$. Each of these lines will make its own contribution to the fluorescence beam from the uranium. Consider first the contribution made by the α_1-line; its intensity is 100/177.3 of the total intensity from molybdenum. The fluorescence beam coming from the uranium is composed of seven lines: α_1, α_2, β_2, β_5, β_6, β_7, l, and each one of these will make its separate contribution to the ionization current derived from the uranium. Allison's values for the relative intensities in the L_{III} characteristic spectrum from U give $\alpha_1 : \alpha_2 : \beta_2 : \beta_5 : \beta_6 : \beta_7 : l = 100 : 11 : 28 : 6.4 : 1.6 : 0.4 : 2.4$. Let us therefore first obtain an expression for the power entering the ionization chamber due only to the U $L\alpha_1$ and excited by the Mo $K\alpha_1$. The wave-lengths and relative intensities of the Mo and U lines were taken from the characteristic spectrum, but as is shown later this appears to be quite justified.

Suppose a beam of x-rays from the Mo of intensity I' and cross section A' traverses a thickness dx of the U radiator. The number of quanta absorbed by the L level and hence the number of photoelectrons ejected from the L level will be

$$dn = (I'A'dx/h\nu')(100/177.3)\tau_L', \qquad (1)$$

where ν' is the frequency of the Mo $K\alpha_1$. Hence the number of fluorescence L quanta escaping from the U atoms, due to the Mo $K\alpha_1$, will be $dn_1 = w_L dn$. The power in the fluorescence beam due to the U $L\alpha_1$ will be $h\nu'' dn_1$, where ν'' is the frequency of the U $L\alpha_1$. Barkla and Sadler have shown that the intensity of the fluorescence beam is the same in all directions. Thus the power in the U fluorescence beam, due to the Mo $K\alpha_1$ and U $L\alpha_1$, uncorrected for absorption; which enters the ionization chamber is

$$dP'' = h\nu'' dn_1 \frac{A''}{4\pi r^2}\tau_L' = h\nu'' w_L P' \tau_L' dx \frac{1}{h\nu'}\frac{A''}{4\pi r^2}\frac{100}{177.3}. \qquad (2)$$

A'' is the area of the diaphragm S_2 and $P' = I'A'$ is the power in the primary Mo beam, and r the distance from the center of the U block to the center of the diaphragm S_2. $A''/4\pi r^2$ is the solid angle which the ionization chamber subtends at the uranium radiator.

If the uranium is set at 45° to the primary molybdenum beam and thus at 45° to the ionization chamber in the position B, then the paths of the primary and the U fluorescence beam in the U radiator will be the same. Let μ' and μ'' be the absorption coefficients of the Mo $K\alpha_1$ and U $L\alpha_1$, respectively, in the uranium. Then the power in the fluorescence beam entering the ionization chamber will be

$$P'' = w_L \frac{A''}{4\pi r^2} P' \tau_L' \frac{\nu''}{\nu'}\frac{100}{149.8}\frac{100}{177.3}\int_0^\infty e^{-(\mu'+\mu'')x}dx = w_L \frac{A''}{4\pi r^2}\frac{\tau_L'}{\mu'+\mu''}\frac{100}{149.8}\frac{100}{177.3}\frac{\lambda'}{\lambda''}P' \cdots, \qquad (3)$$

where 100/149.8 is the fractional intensity of the U $L\alpha_1$ to the total U beam λ' and λ'' are the wave-lengths of the Mo $K\alpha_1$ and U $L\alpha_1$ respectively. Similar expressions will give the contribution from the U $L\alpha_2$, $L\beta_2$, $L\beta_5$, $L\beta_6$, $L\beta_7$, l; these added together give the total contribution due to the Mo $K\alpha_1$. To this must be added the total contribution due to the Mo $K\alpha_2$, $K\beta_1$, $K\beta_2$, and then after making the appropriate corrections for the absorption of each of these lines in

[12] Meyer, Wissenschaftliche Veröffentlichungen aus dem Siemens-Konzen VII, 2 (1929).

Also, Siegbahn, *Spektroskopie der Röntgenstrahlen*, Second Edition.

the gas of the ionization chamber, the sum total will give values proportional to the observed ionization currents.

The absorption coefficients of these various wave-lengths in uranium need to be determined, as well as the value of τ_L. It is also necessary to test whether the relative intensities of lines of the Mo characteristic spectrum agree with those from the fluorescence spectrum. This must also be checked for the lines from the L_{III} level of uranium.

Absorption Coefficients in Uranium

Because of the high absorption of uranium it is impractical to use foil, even if it were available; consequently a solution of uranyl nitrate was employed. A parallel sided cell was made 0.320 cm thick, the front and back faces covered with mica and held in position with rubber gaskets. A single crystal ionization spectrometer was used, the cell being placed between the two defining slits. A motor generator set supplied current at 540 cycles to the primary of a transformer; the secondary current being rectified by kenotrons and then passed into condensers to smooth out the ripple. The high voltage was read on an electrostatic voltmeter and kept constant during the experiment. The current through the x-ray tube was read on a milliammeter and also kept constant, so that the power through the tube remained the same during an experiment. This equipment was used in all the experiments described in this paper.

Solutions of 2, 5 and 10 g of uranyl nitrate crystals dissolved in 100 g of water were used in the cell and the three served as checks. Since the absorption coefficient of water is also found this served as an additional check, the results agreeing very well with the published data.[13]

The results shown in Table I were obtained for the atomic absorption coefficient for uranium. The value of the L_{III} discontinuity, or the ratio of μ_a on the short and long wave-length sides of the L_{III} absorption limit is found from the graph to equal 2.27. Kustner[14] gives the value of 2.2 for the L_{III} discontinuity. From these results it would appear that the wave-length of the L_{III} absorption limit is less than 0.7208A, since the line U $L\beta_1 = 0.7185$A lies on the long wave-length side of the limit.

[13] Dershem, Phys. Rev. **21**, 30 (1923); Hewlett, Phys. Rev. **17**, 284 (1921).

[14] Kustner, Phys. Zeits. **46**, 845 (1932).

Table I. *Atomic absorption coefficients in U.*

Line	λ in A	μ_a
Sr $K\alpha_1$	0.8734	2.90×10^{-20}
U $L\beta_2$	.7531	1.94
Cb $K\alpha_1$	.7446	1.94
U $L\beta_1$	.7185	1.84
U $L\beta_3$	.7088	3.81
U $L\gamma_1$	.6136	2.53

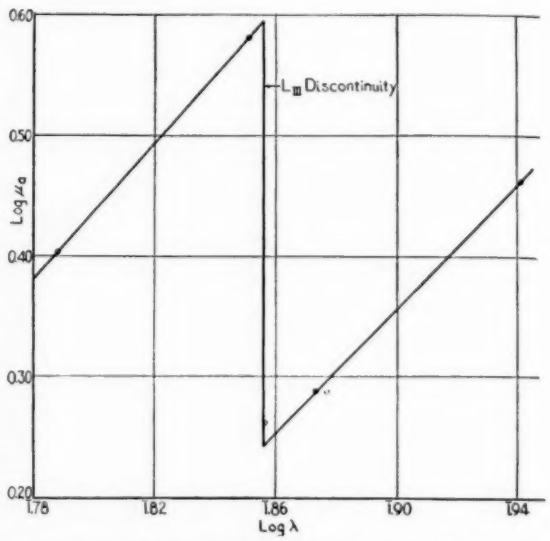

Fig. 2. Graph showing logarithm of atomic absorption coefficient for uranium plotted against logarithm of wave-length (log μ_a as a function of log λ).

The quantity $1.27/2.27 = 0.56$ represents the fraction of the radiation on the short wave-length side of the L_{III} limit which is absorbed photoelectrically in the L_{III} level. Since the scattering term may be assumed negligible, $\mu' = \tau'$ and hence $\tau_L' = 0.56\mu'$.

Relative Intensities of the Mo $K\alpha$ to the Mo $K\beta$ in the Fluorescence Spectrum

A metal x-ray tube with a rhodium target was operated at 40 kv and 10 milliamperes, the molybdenum scatterer being placed immediately in front of the aluminum window of the tube. The distance from the center of the rhodium target to the molybdenum scatterer was approximately 2.5 cm. A single crystal ionization spectrometer was used, the molybdenum fluorescence beam being collimated by two slits 0.8 mm wide, 2.4

cm high, and 25 cm apart. The ionization chamber was made of copper 20.3 cm long with mica windows, and filled with methyl iodide at 20.8 cm pressure. The ratio of the peak intensities of the α_{12} to β_{12} read from the graph is 4.85 to 1.

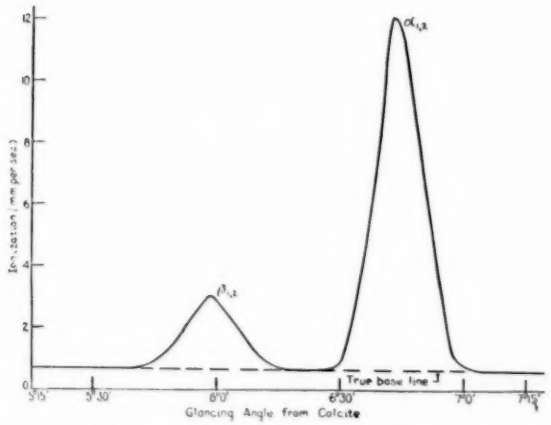

FIG. 3. Graph of intensity against crystal angle for K fluorescence spectrum from molybdenum.

The true base line occurs at 0.048 mm per sec., found by moving the ionization chamber from its correct position for reflection from the crystal. This intensity ratio has to be corrected for: (1) the relative absorption in the air between the scatterer and the window of the ionization chamber, a factor of 1.014; (2) the relative absorption in the mica window of the ionization chamber, a factor of 1.014; (3) the relative absorption in the methyl iodide, a factor of 0.815; (4) the relative absorption in the Mo scatterer, a factor of 1.375; and (5) the reflection coefficients of the two wave-lengths from the calcite crystal, a factor of 0.965. This gives a final result of 5.42 for the relative intensities of the Mo $K\alpha_{12}$, Mo $K\beta_{12}$ in the fluorescence spectrum. In order to check this value with that given by Meyer for these lines in the characteristic spectrum, curves were drawn for the $K\alpha_1$, $K\alpha_2$ with peak intensities of 100 and 50.6 and displaced relative to one another by 2.5 minutes of arc, and similarly for the $K\beta_1$, $K\beta_2$. The value obtained in this manner gave 5.9, which would appear to be within the limits of experimental error. Measurements are at the present time being carried on in this laboratory by Dr. J. H. Williams on relative intensities of lines in the characteristic spectrum, and preliminary results indicate that Meyer's value of β_1 is somewhat low. The calcite crystal which was used here was one previously calibrated by Allison[15] (crystal *VA*) by means of a double crystal spectrometer.

THE RELATIVE INTENSITIES OF THE $L\alpha_{12}$ TO THE $L\beta_2$ LINES IN THE FLUORESCENCE SPECTRUM FROM THE L_{III} LEVEL OF URANIUM

The apparatus used in this experiment was the same as in the previous one, except the rhodium target was replaced by a molybdenum target, and the molybdenum scatterer by a uranium scatterer. The x-ray tube was operated at 40 kv and 20 milliamperes, and the ionization chamber filled with methyl bromide at atmospheric pressure. The true base line occurs at 0.05 mm per sec., found by moving the ionization chamber from its correct position for reflection from the crystal. Lines from the L_I and L_{II} levels appear in the graph but their relative intensities, with respect to the lines from the L_{III} level, cannot be compared with that from primary x-rays from a U target. The ratio of the peak intensities of the α_{12} to β_2 read from the graph is 2.22. Both the

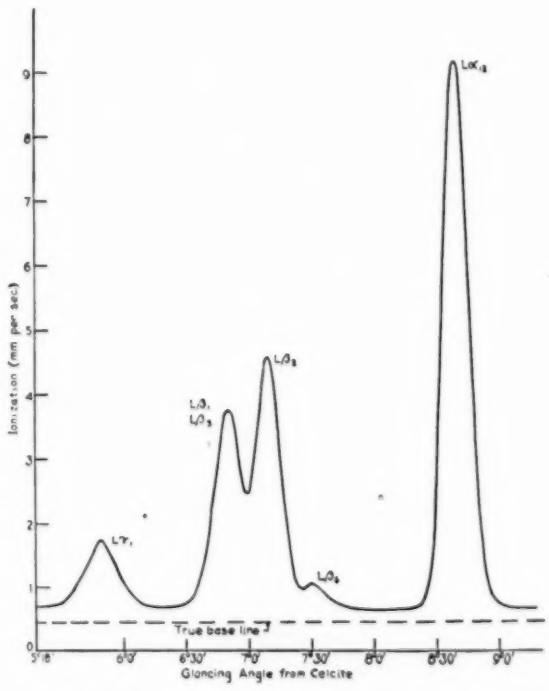

FIG. 4. Graph of intensity against crystal angle for the fluorescence spectrum from the L_{III} level of uranium.

[15] Allison, Phys. Rev. **41**, 1 (1932).

α and β-lines are of shorter wave-length than the K limit of bromine, so that the bromine K radiation will be excited in the ionization chamber and part of this will escape to the walls of the chamber. The method of correction for this follows that given by Allison and Andrew,[8] and introduces a factor of 1.09.

The other corrections follow as in the previous experiment: (1) correction for absorption in the air and mica window, a factor of 1.053; (2) correction for relative absorption in the U, a factor of 1.62; (3) correction for relative reflection from the calcite crystal, a factor of 0.903. This gives a final result of 3.73 for the relative intensities of the U $L\alpha_{12}L\beta_2$, in the fluorescence spectrum.

The relative intensities of these lines in the characteristic spectrum were determined by Allison[16] and his results give the value of 3.78. Thus it would appear that the same relative intensities are obtained for the lines from the L_{III} level in the characteristic spectrum as in the fluorescence spectrum.

Calculation of the Fluorescence Yield from the Uranium L_{III} Level

The diagram of the apparatus used is shown in Fig. 1. The fluorescence molybdenum radiation passed through two circular holes 1 cm in diameter and 20 cm apart, and was visible on a fluorescent screen. The ionization chamber was 10.7 cm in diameter, and 13.2 cm long, and the windows at the front and back were made so that none of the uranium radiation struck the walls or the back of the chamber.

A difficulty was encountered which was due to the radioactivity of the uranium, or rather to the β-particles given out by the radioactive products UX_1, UX_2. The ionization caused by the β-particles was eliminated by interposing a piece of paraffin 1.485 cm thick between the uranium and the ionization chamber. This of course reduced the intensity of the fluorescence beam from the uranium; but not too seriously.

The intensity of the direct beam from the molybdenum was reduced to measurable values by using absorbing screens of silver of known thickness. Silver was chosen because it can be obtained pure, and also no silver K radiation will be excited. The absorption coefficient determined in this manner will be less than the correct absorption coefficient for silver since some of the scattered radiation can enter the ionization chamber.

In a similar manner the absorption coefficient for paraffin cannot be taken directly from tables, but was found approximately by finding the absorption coefficient of paraffin for the direct molybdenum beam. The value found in this experiment for $\lambda=0.698$A, which is weighted mean wave-length from Mo, is 0.384. From data given by Allen[17] the absorption coefficient for paraffin for $\lambda=0.698$A is 0.523. It was therefore assumed that the absorption coefficient for $\lambda=0.876$A, which is the weighted mean wave-length from the uranium, should be, for this experimental arrangement $0.384\times0.901/0.523=0.661$ where 0.901 is the value given by Allen for $\lambda=0.876$. There may be here a large source of error, for the scattering of the molybdenum and the uranium beams will not be the same, but this is some extent taken up by the difference in the geometry of the two beams. The molybdenum beam is more or less a parallel cylindrical one, while the uranium beam is a divergent one.

The intensities observed for the uranium fluorescence beam must then be multiplied by $e^{0.982}$ or 2.67.

Five separate determinations were made with different voltages and currents through the x-ray tube, and different pressures of methyl iodide in the ionization chamber. Sufficient intensity was found when the tube was operated at 30 kv and 10 milliamperes.

From Eq. (3) the contribution from the Mo $K\alpha_1$ and U $L\alpha_1$ is given by substituting $0.56\mu'$ for τ_L'. Similarly, the contribution from the Mo $K\alpha_1$ and U $L\alpha_2$ will be given by replacing 100/149.8 by 11/149.8 in Eq. (3) and letting μ'' be the absorption coefficient of U $L\alpha_2$ in U. Similarly for all the lines. The distance r from the center of the uranium to the center of the diaphragm S_2 was 9.54 cm, and A'' the area of S_2 was 20.27 cm^2. The intensity I'' of the fluorescence radiation from the uranium will be given by

$$I''=w_L(S_1+S_2+S_3+S_4)I'A''/4\pi r^2$$

where S_1, S_2, S_3, S_4 represent the contributions

[16] Allison, Phys. Rev. **32**, 907 (1926).

[17] Allen, Phys. Rev. **28**, 907 (1926)

made by the Mo $K\alpha_1$, $K\alpha_2$, $K\beta_1$, $K\beta_2$ lines, respectively. Typical values of these contributions are $S_1=0.210$, $S_2=0.1065$, $S_3=0.047$ and $S_4=0.008$. These values include the corrections for the absorption of the various wave-lengths in the methyl iodide. Hence

$$I''=0.371 w_L I'/4\pi r^2.$$

I'' and I' are proportional to the ionization currents observed for the uranium fluorescence beam and the direct molybdenum beam, respectively, after each has been corrected for absorption. After correction for absorption in the paraffin, $I''=25.6$ mm per sec. After correction for absorption in the silver, $I'=5822$ mm per sec. Thus

$$w_L=\frac{25.6}{5822}\frac{1}{0.371}\frac{4\pi r^2}{A''}=0.67.$$

The value given above was also the average of all the readings.

Another method of calculation, which is considerably simpler than the one given above is that of taking average values for the wave-lengths and absorption coefficients. The weighted mean average of the wave-length of the molybdenum fluorescence beam is $\lambda'=0.698$A, and for the uranium beam is $\lambda''=0.876$A. These values are taken from the fluorescence spectrum reported in this paper. The values of μ' and μ'', the atomic absorption coefficients of the molybdenum and uranium beams, respectively, in uranium are 3.65×10^{-20}, 2.92×10^{-20}. The calculation then gives $w_L=0.66$.

The fact that these two calculations give values so close to one another, may be taken to show that the intensities of the lines in the characteristic and fluorescence spectra, used here, are very nearly the same. It should be noted even if Meyer's value of β_2 is as much as 5 percent too low, the change in the result for the final value for w_L would not be more than 0.5 percent.

I take great pleasure in thanking Professor S. K. Allison for the suggestion of the problem and his useful advice throughout the course of the work.

Attempts to Observe an Electron Affinity Spectrum

O. OLDENBERG, *Research Laboratory of Physics, Harvard University*

(Received January 18, 1933)

The failure of previous attempts to observe an electron affinity spectrum (emitted by the combination of neutral, electronegative atoms and electrons) is explained by inadequate experimental methods. On the basis of recent results regarding combination spectra of positive ions and electrons, new attempts have been made to observe the electron affinity spectrum of atomic iodine by using three methods (hollow cathode, positive column with addition of a rare gas, glowing filament). No new spectrum was observed. This failure is discussed theoretically. It seems that the capture of electrons by halogen atoms is an improbable process as compared with the combination of positive ions and electrons.

I. PROBLEM AND PREVIOUS WORK

THE *electron affinity* of the halogen atoms, i.e., their ability to form negative ions, is known from various observations: the existence of polar molecules and crystals, the low mobility of the negative particles in their vapors, the negative values of e/m in the "positive ray." The *value* of the electron affinity (i.e., the energy difference between the atom and electron separated and the negative ion) has first been derived by Born[1] from the grating energy of the alkali halogen crystals. Another determination of the electron affinity of the iodine atom, based on the thermal equilibrium at high temperature of CsI vapor, has been made by J. E. Mayer.[2] The iodine atom has an electron affinity of 74.2 ± 1.5 k cal.

These results establish the *existence* of the negative ions and its *energy of formation*. They do not give evidence, however, by what process this ion is formed. Franck[3] suggested that a neutral gas atom as well as a positive ion, capturing a free electron, might radiate the energy of formation plus the kinetic energy the electron had before this process. The corresponding spectrum, therefore, would consist of a continuous band starting from the frequency given by the energy of electron affinity, spreading to short waves. The intensity distribution within this continuous band would depend upon the kinetic energy distribution of the electrons (modified by some probability factor for the capture also depending on the kinetic energy). The observation of this spectrum would be important in that it would give evidence of the elementary process, and in addition yield by its long wave-length limit a straightforward determination of the energy of electron affinity.

All previous attempts to observe electron affinity spectra of gaseous atoms or molecules have failed. Two continuous bands observed in the *positive column of the electric discharge* through iodine vapor have been ascribed to the process under discussion. Both of them turned out later to belong to the band spectrum of the iodine molecule.[4] These failures in observing the electron affinity spectrum in the positive column can be understood on the basis of more recent information. In this source of light even the combination of *positive ions* and electrons—in spite of the Coulomb force acting—does not play an important part, the reason being that only *very slow electrons* have an appreciable chance to be caught by ions.[5] By analogy we conclude that in the positive column most electrons are too fast to be captured by *neutral iodine atoms.*

Von Angerer and Mueller[6] investigated *absorp-*

[1] M. Born, *Problems of Atomic Dynamics*, Cambridge, 1926, p. 170.

[2] J. E. Mayer, Zeits. f. Physik **61**, 798 (1930); J. E. Mayer and Lindsay Helmholz, Zeits. f. Physik **75**, 29 (1932).

[3] J. Franck, Zeits. f. Physik **5**, 428 (1921); cf. K. Fajans, Verh. d. D. Phys. Ges. **21**, 714 (1919).

[4] W. Steubing, Ann. d. Physik **64**, 673 (1921); J. Franck, Zeits. f. Physik **5**, 428 (1921); W. Gerlach and F. Gromann, Zeits. f. Physik **18**, 239 (1923); O. Oldenberg, Zeits. f. Physik **25**, 136 (1924).

[5] R. Seeliger, Phys. Zeits. **30**, 346 (1929).

[6] E. von Angerer and A. Müller, Phys. Zeits. **26**, 643 (1925) and L. A. Müller, Ann. d. Physik **82**, 64 (1927).

tion spectra of alkali halogen compounds. In their vapors at high temperature a considerable concentration of negative halogen ions is to be expected. The neutralization of these negative ions ($I^- \rightarrow I + \epsilon$) requires the energy of electron affinity. The question is: does the neutralization take place by the action of light? Continuous bands were observed, which the authors interpreted later, however, as belonging to the neutral alkali halogen molecules. Their failure to observe electron affinity spectra might be due to the masking of a faint absorption by another stronger one.

Franck and Scheibe[7] have interpreted continuous absorption bands observed in the solutions of the alkali halogen compounds in water as electron affinity spectra of the negative halogen ion losing the excess electron under the influence of light. This hypothesis has recently been modified, however, by Franck and Haber.[8] They assume that the electron is not *liberated* but that it *jumps* from the halogen ion to a water molecule which in the same process splits up into H and OH^-. The spreading of the continuous spectrum, therefore, is not related to the velocity distribution of the electrons liberated but is the same phenomenon as the broadening of all spectral lines in liquids. This result does not solve the original, simple problem: the electron affinity spectrum of the undisturbed atom. This can be solved only by observing the gaseous state.[9]

So we come to the conclusion that as yet the problem has been attacked under conditions that from our present standpoint seem to be unfavorable. Therefore, the failure to observe the spectrum under discussion is not necessarily to be interpreted as due to the *nonexistence* of this spectrum. It will be worth while to search for it under more favorable conditions.

II. Experiments

(a) Hollow cathode method

Recent successes in producing combination spectra of *positive ions* and electrons[10] suggest various methods for producing the electron affinity spectrum of *neutral halogen atoms*. In the inside of a hollow cathode of a discharge tube containing helium Paschen[11] discovered marked continuous spectra connected with well developed line series of the helium atom. As only slow electrons are able to recombine with ions it must be concluded that the concentration of slow electrons in the hollow cathode is considerable. This is largely due to the fact that no rapid acceleration exists, because, from symmetry, the electric field will be small along the axis of the hollow cathode. The corresponding experiment carried through with iodine vapor completely dissociated by heat should give a chance to observe the electron affinity spectrum—slow electrons being present due to the properties of the hollow cathode, and iodine atoms due to the thermal dissociation of the vapor.

The iodine atom is particularly suited for this experiment, because iodine is the only halogen vapor that can be dissociated to nearly 100 percent at easily accessible temperatures.[12] Any new spectrum, therefore, that might come out under special conditions will be likely to belong to the iodine *atom*. The only remainder of the *molecular* spectrum that is known to appear in spite of complete dissociation is the band with the long

[7] J. Franck and G. Scheibe, Zeits. f. physik. Chemie (A) Haberband **22** (1928); G. Scheibe, Ber. d. Dtsch. Chem. Ges. **59**, 1321 (1926).

[8] J. Franck and F. Haber, Ber. d. preuss. Ak. d. Wiss; Phys. math. Klasse **XIII**, 8 (1931).

[9] In this argument it has been assumed that the electron affinity spectrum consists only of the continuous band without showing sharp lines, in other words that the negative ion has no definite excited states. As the electron affinity is understood on the basis of the great stability of a completed group of electrons, there seems to be no reason to assume a *stable* negative ion with the excess electron in an *excited* state. It might be as stable as the negative ion of any other atom having no pronounced electron affinity. No corresponding atomic spectrum (line spectrum of a negative ion) has been observed. Bartlett (Nature **125**, 459 (1930)) estimates that the Cl^- ion has no stable excited states at all below its neutralized state. Since he applies an extrapolation method, it might be safer to conclude that excited states, if there are any, should be very near the ionized state and therefore almost unstable. This result does not agree with Mecke's tentative interpretation of certain intense band spectra of BeH and MgH as due to negative molecular ions (Zeits. f. Physik **72**, 155 (1931)).

[10] A survey has been given by R. Seeliger, Phys. Zeits. **30**, 329 (1929).

[11] F. Paschen, Sitzungsber. d. Preuss. Akad. d. Wiss., p. 207 (1927); cf. R. A. Sawyer, Phys. Rev. **36**, 44 (1930).

[12] G. E. Gibson and W. Heitler, Zeits. f. Physik **49**, 465 (1928); cf. W. G. Brown, Phys. Rev. **38**, 708 (1931).

wave-length limit 3460A. This is well outside the region between 3740 and 3910A in which, according to Mayers determination, we must search for the spectrum under discussion. It happens that this spectral range is appreciably free from intense bands even for a large concentration of molecules.

The discharge tube was made of quartz with tungsten electrodes.[13] Care has been taken that the inside of the hollow cathode was observed not against the glowing wall of the oven as a background but, instead, against a quartz window. As it is known to be difficult to keep the iodine pure in the electric discharge, a continuous flow of iodine vapor was supplied. Iodine vapor reservoirs with different pressures were attached one on each side of the discharge tube. The resulting flow of vapor washed all impurities away from the region of the electrodes and discharge. From time to time the whole system was evacuated after freezing the iodine.

The *results* have been negative. Under no conditions (pressure varied up to 8 mm, current up to 90 m.a.) has a new continuous spectrum been observed. The plates showed mainly the line spectrum of the iodine atoms with faint traces of tungsten lines. In addition the I_2 band 3460 came out with high intensity. It will be discussed in another note. Several plates showed traces of the known diffuse bands of the I_2 molecule.

An argument against the hollow cathode method is that it might fail under the present conditions, because most of the free electrons might be captured by the atomic iodine immediately after leaving the cathode so that no free electrons would be present near the axis. In order to test this possibility, all parts of the hollow cathode discharge, particularly those parts in the neighborhood of the metal, have been carefully investigated by the spectrograph without any positive result. Only intensity differences within the line spectrum appeared.[14]

The presence of free electrons was checked by another method. Their disappearance by immediate capture would produce a fundamental change in the discharge, as compared, for example, with the discharge through hydrogen or nitrogen. The conductivity is largely due to ionization by impacts of *free electrons*. This process cannot be simply replaced by impacts of *ions* only, particularly at high pressure. The reason for this is that only the light electrons keep their kinetic energy in the numerous *elastic* impacts not leading to excitation and ionization and thus can gradually gain energy from the electric field. The heavy ions, on the other hand, give up some kinetic energy in every elastic impact. In order to store up in a heavy ion the kinetic energy required for ionization in spite of collisions, enormous fields are necessary particularly at high pressure. Moreover for ionizing an atom by impact, the heavy ion must have a much larger kinetic energy than the electron which requires just the limiting value of the ionization energy.[15] Hence the potential difference between the electrodes in a discharge tube from which all free electrons are taken away will be very large compared with the potential difference, e.g., in the hydrogen or nitrogen discharge. The comparison of potential differences, therefore, for atomic iodine and hydrogen or nitrogen will give evidence whether or not an appreciable number of free electrons still exist in the iodine discharge. In the same discharge tube for the same pressure (5 mm) and temperature (1000°C), the current-potential-curve for iodine yielded even smaller values of potential difference than in hydrogen. We must conclude that there was some concentration of free electrons left. It is true that this observation was concerned not only with the potential drop in the positive column itself but that in the measurement the cathode drop was included. Actually in the positive column the potential drop in iodine (although mainly molecular) has been found[16] to be somewhat higher than in nitrogen but of the same order (75 instead of 43 volts/cm). Hence it seems certain that in the discharge through atomic iodine the concentration of free electrons might be reduced by the formation of negative ions, but it cannot be very small as compared with the better known discharges through hydrogen or

[13] For technical detail of the electric discharge in iodine cf. H. F. Fruth (Phys. Rev. **31**, 614 (1928). Special stopcock grease has been used as advised by M. Bodenstein.

[14] E. Müller (Ann. d. Physik **14**, 851 (1932)) proved that glowing platinum in iodine vapor emits electrons, not negative ions.

[15] J. Franck, Zeits. f. Physik **25**, 312 (1924); G. Joos and H. Kulenkampf, Phys. Zeits. **25**, 258 (1924).

[16] Matthies, Ann. d. Physik **18**, 493 (1905).

nitrogen.[17] The failure to observe the electron affinity spectrum cannot be due to the complete absence of free electrons.

(b) Positive column in a mixture with helium

It still might seem questionable whether the negative results of the experiments just discussed is due to the nonexistence of the electron affinity spectrum or to unknown properties of the hollow cathode discharge in the halogens. It is desirable, therefore, to search for the same spectrum under other widely different conditions that are also known to be favorable for recombination spectra of ions and electrons. Intense spectra of this kind have been discovered recently by Krefft[18] in the positive column of the electric discharge through metallic vapors with the addition of rare gases. For a group of metals Krefft was able to compare the probability with which they emit the recombination spectra. Under most conditions the radiation emitted from the positive column of the ordinary discharge is known to be due to previous *excitation* by electron impact but not to *recombination* of ions and electrons,[19] the reason being that the concentration of *slow* electrons, which alone have a good chance to recombine, is too small. Under the conditions of Krefft's experiment, however, it is not easy to understand the large concentration of *slow* electrons indicated by the intense combination spectra of ions and electrons (continuous bands connected with series limits). It seems possible that with He added the conditions are particularly favorable for the slowing down of electrons, because, as Sommermeyer[20] found out, the energy input in the electric discharge through He is largely used up for the numerous purely elastic collisions between the electrons and He atoms.[21] In the present experiments, therefore, He of 7 mm pressure has been added to atomic iodine (iodine vapor heated to 1050°C). The positive column was projected "end on" on the slit of the spectrograph. The pressure of the iodine was varied between 0.2 and 1.1 mm. Not a trace of a new continuous spectrum was observed although the exposure was long enough to bring out some traces of the bands of molecular iodine. This negative result points again to a low intrinsic probability of the combination of the neutral iodine atoms with free electrons taking place with radiation.

(c) Glowing filament method

In order further to test the negative result of the experiments discussed it seemed desirable to try still another experiment. A straightforward method for producing electrons with very low velocity at a considerable concentration has been very successfully applied by Mohler.[22] He observed recombination spectra in the close neighborhood of a glowing filament, where the velocity distribution of the electrons is mainly determined by the temperature of the metal from which they have just been evaporated without being accelerated as yet by the electric field. In a quartz tube with iodine vapor heated to 1000°C a glowing tungsten filament was used; tungsten interferes least with the atomic iodine and, therefore, gives the purest conditions.

Again no new continuous spectrum came out. This observation, however, does not give as good evidence as the hollow cathode method because the exposure could not be extended to a considerable length of time because of the superimposed spectrum of the glowing filament. It is not possible to screen it off so completely that in a very

[17] This conclusion is supported by the small probability of the formation of negative ions in (molecular) iodine derived from electrical measurements by W. Hey and A. Leipunski (Zeits. f. Physik **66**, 669 (1930)); cf. F. L. Mohler, Phys. Rev. **26**, 614 (1925) and L. B. Loeb, J. Frank. Inst. **197**, 45 (1924).

[18] H. Krefft, Phys. Zeits. **32**, 948 (1931); Zeits. f. Physik **77**, 752 (1932).

[19] Cf. J. Franck and P. Jordan, *Anregung von Quantensprungen durch Stoesse*, Berlin, 98 (1926).

[20] Sommermeyer, Ann. d. Physik **13**, 315 (1932); cf. H. Kessel, Zeits. f. Physik **70**, 614 (1931).

[21] Results of Mohler (Bull. Am. Phys. Soc. **7**, No. 7, p. 8 (1932)) just published suggest another reason for the slowing down of electrons in the positive column. Mohler observed combination spectra of positive ions and electrons in the positive column of a discharge through pure caesium at a considerable pressure. It might be that the exceptionally low value of the excitation potential of caesium (1.38 volts) together with the large probability of the lowest quantum transition in the alkali atoms is responsible for a large concentration of slow electrons. Also from this point of view it seems worth while to investigate the positive column in atomic iodine at various pressures because the iodine atom has an excitation potential as low as 0.94 volts (L. A. Turner, Phys. Rev. **27**, 406 (1926)) although with a much smaller probability of transition.

[22] F. L. Mohler, Phys. Rev. Sup. **1**, 221 (1929).

long exposure it gives no continuous background even in the near ultraviolet.

From the three groups of experiments discussed it will be concluded that the neutral iodine atom has a smaller chance than a positive ion to capture a free electron and radiate the energy liberated although the energy value of this process is about the same as the ionization energy of caesium whose ions show an intense recombination spectrum. It must be admitted, however, that this negative result cannot be proved by experiments with the same certainty as a positive observation. The mechanism of the discharge is not known so completely that we can with full certainty predict the most favorable condition for a certain elementary process. In particular it might be that still slower electrons than those appearing in the discharges just discussed show a larger tendency of combining with neutral halogen atoms.[23]

III. Theoretical Discussion

In order to explain the failure in all attempts to observe the electron affinity spectrum two reasons will be discussed, one dealing with the velocity of the electrons in the discharge, the other with the process of combination itself.

A great difference between the two cases of combination—positive ions and neutral halogen atoms capturing electrons—will be due to the long range over which the Coulomb force of the *ion* affects free electrons, whereas the *halogen*, being a neutral atom, is surrounded by a field which, although unknown in detail, certainly becomes negligible within a very small distance. Therefore classically the electron to be captured must approach the halogen atom much more closely than the positive ion with the result that the group of electrons which can be captured by the halogen atoms will be comparatively small.

This comparison, however, between combination processes, the energy of which is radiated, must take into account the selection rules. According to these rules the angular momentum of the electron can change in the radiation process only by the quantized amount $h/2\pi$. Let us consider electrons with the average value of the kinetic energy. The capture of an electron by a *positive ion* will frequently happen over a comparatively large distance because of the long range of the Coulomb field. In this case the electron will have a large angular momentum with regard to the ion. After emitting the quantum $h/2\pi$ it will still retain an appreciable value and, therefore, go to a quantum orbit of the neutralized atom with large azimuthal quantum number. A frequency will be emitted belonging to a high *subordinate* series. The continuum connected with a *principal* series, however, will be emitted by the smaller group of electrons passing the ion with smaller angular momentum, i.e., at a smaller distance. This smaller number of processes will give rise to a fainter spectrum. This argument holds only if we deal with electronic temperatures such that the electrons have angular momenta of the order of magnitude $h/2\pi$ when passing the ions at distances of the order of magnitude of atomic dimensions. Actually for an electron temperature of 5000°C, an electron which has the most probable velocity and an angular momentum with respect to the ion of $h/2\pi$, will pass the ion at a distance of 2×10^{-8} cm; this is well within the range of atomic dimensions. On this basis we understand the fact, reported by Krefft, that in the combination spectra of *positive ions* and electrons the continuum connected with the principal series is much less intense than the one connected with the first subordinate series.

In the electron affinity spectrum of the halogen atoms, as discussed in Section I, we expect to observe only the continuum representing the *principal* series. It is not surprising that because of the more constricted field of force of the halogen atoms, the probability of this process comes out still smaller than for the positive ions, although the energy with which the halogen keeps the electron is of the same order.

This interpretation, based on the velocity distribution of electrons in the discharge, does not preclude the inverse process, the separation of the excess electrons from the negative ions by absorption of light, provided the ions are produced in sufficient concentration. For the initial state of this process, the negative ion, is independent of

[23] Recombination spectra of positive iodine ions and free electrons were not observed either. This is not surprising as Krefft, too, failed to observe this type of spectrum for certain groups of elements.

the velocity distribution of electrons. Therefore, it does not contradict the theory that in *absorption* in solutions the electron affinity spectrum has actually been observed by Scheibe, although modified by the water to such an extent that no conclusion can be drawn regarding the same absorption process (its wave-length and its probability) in the vapor. The concentration brings in another difference between vapors and solutions in water. For example, in a 1/100 normal solution of KI the I^- ions have a partial pressure of 1/4 atmosphere; that is a very large pressure as compared with the value in electric discharges.

The theoretical result discussed, regarding the halogen atom in the gaseous state, might be modified in one respect by a recent result derived from wave mechanics by Jen.[24] As yet it has been assumed from analogy with the behavior of *positive ions* that the electron affinity spectrum of certain *neutral atoms* it if exists at all will have a large intensity near its long wave-length limit. A different result, however, has been derived by Jen. In any case (positive ion or neutral atom) the effective cross section for the capture of electrons approaches infinity as a limit with decreasing kinetic energy of the electrons; the *concentration* of slow electrons, however, approaches zero as a limit. The *intensity observed* (product of probability factor and concentration factor) comes out with a finite limiting value. For the electron affinity spectrum of hydrogen—contrary to the spectrum of combination of positive ions—the theoretical *intensity* curve shows a pronounced maximum at a considerable distance from the limit. Hence it might be difficult to observe the theoretical long wave-length limit (defined by the energy of electron affinity) and to identify the spectrum, even if the maximum were intense enough to be photographed.

Jen's theory certainly does not lead to the result that the capture of an electron by a neutral atom resulting in radiation is a "forbidden" process. It seems hardly possible, however, to estimate from wave mechanics the actual intensity of the electron affinity spectrum of *hydrogen;* and we certainly must not correlate Jen's theoretical results quantitatively with observations in the *halogen* vapors.

The main result is that the chance for observing electron affinity spectra in certain parts of the electric discharge seems to be a great deal smaller than the chance for observing combination spectra of positive ions and electrons.[25]

[24] C. K. Jen, Phys. Rev. **42**, 588 (1932). Cf. the following paper. His results are partly supported by the probability for the formation of negative ions as derived from electrical measurements by W. Hey and A. Leipunski (Zeits. f. Physik **66**, 669 (1930)). Their results, however, do not apply directly because their experiments were performed with molecular iodine vapor.

[25] It is interesting to compare the negative result of the present spectroscopic investigation with the results of Hogness and Harkness (T. R. Hogness and R. W. Harkness, Phys. Rev. **32**, 784 (1928)), who investigated the ionization processes of iodine by the mass-spectrograph. Working with molecular iodine they had no chance to investigate the atomic process under discussion ($I+\epsilon \rightarrow I^-$). They found out, however, that negative atomic ions I^- are formed by neutral molecules capturing electrons and breaking up at the same time into a neutral atom and a negative ion ($I_2+\epsilon \rightarrow I+I^-$). Not even I_2^- ions are formed simply by neutral molecules I_2 capturing free electrons but by a more complicated process.

The Continuous Electron Affinity Spectrum of Hydrogen

C. K. JEN, *Research Laboratory of Physics, Harvard University*

(Received January 18, 1933)

A wave-mechanical calculation has been made of the intensity distribution in the continuous emission spectrum due to the capture of electrons by normal hydrogen atoms and the coefficient of absorption in the corresponding absorption spectrum due to the neutralization of negative hydrogen ions. Approximate wave functions for the continuous range of upper energy levels have been combined with the discrete state wave function for H^- given by Hylleraas to give the matrix components for the desired transitions. The computed results are graphically illustrated and their significance discussed. It is shown that an experimental attempt to find the electron affinity emission spectrum of normal hydrogen atoms may encounter at least two difficulties: (1) insufficient intensity compared to that in experiments on the recombination between H^+ ions and electrons, and (2) spectral distribution such that the spectral limit is too diffuse for positive identification. The relation of these results to the interpretation of experiments on the electron affinity spectrum of halogen atoms is discussed.

INTRODUCTION

FOLLOWING the first proposal by Franck,[1] many attempts have been made to determine the electron affinity of electronegative elements by spectroscopic means. Certain unidentified continuous spectra have often been taken as those related with electron affinity, but such identifications have proved to be either false or uncertain.[2] The recent experiments of Oldenberg on the emission spectrum of iodine atom also point to a negative result.* A theoretical explanation for this experimental failure is obviously demanded. However, a complete answer to the problem is difficult because of the complexity of the atoms involved. As a start we propose to treat the electron affinity spectrum of the hydrogen atom, which is the simplest of such problems, and hope to furnish probable explanations for the more complicated halogen atoms.

If free electrons are present in the midst of normal hydrogen atoms, there may be a probability of combination between them to form negative hydrogen ions. The change of energy in such a transition is released as radiation, which, if spectroscopically observed, is expected to form a continuous emission spectrum extending toward the short wave-length side from an edge whose frequency is determined by the electron affinity of the atom. Conversely, a continuous absorption spectrum will be formed when negative hydrogen ions are broken up into neutral atoms and electrons under the influence of light.

The electron affinity of a hydrogen atom has been calculated by Hylleraas[3] and Bethe[4] from a general treatment of the two-electron problem. In spite of the discordant theoretical results[5] which had appeared previously and the absence of sufficient experimental data, their calculations seem to be quite definite and convincing, especially in view of the remarkable success of Hylleraas' method on other examples of the two-electron problem.[6] With the help of their characteristic wave function of a negative hydrogen ion and our present approximate solution of the wave equation in the continuous state, we shall calculate the matrix component of transition for the continuous spectrum, from which the emission intensity and absorption coefficient can be readily deduced.

* O. Oldenberg, Phys. Rev. **43**, 534 (1933).

[1] J. Franck, Zeits. f. Physik **5**, 428 (1921).

[2] W Steubing, Ann. d. Physik **64**, 673 (1921).
O. Oldenberg, Zeits. f. Physik **25**, 136 (1924).
E. V. Angerer und Müller, Phys. Zeits. **26**, 643 (1925).

[3] E. A. Hylleraas, Zeits. f. Physik **60**, 624 (1930).

[4] H. Bethe, Zeits. f. Physik **57**, 815 (1929).

[5] L. Pauling, Phys. Rev. **29**, 285 (1927).
H. Brück, Zeits. f. Physik **51**, 707 (1928).

[6] E. A. Hylleraas, Zeits. f. Physik **65**, 209 (1930).

I. Approximate Solution of the Wave Equation in the Continuous State

The Schrödinger differential equation for two electrons acting in the field of a single fixed proton charge is

$$\nabla_1^2\psi+\nabla_2^2\psi+\{E_T+2(1/r_1+1/r_2-1/r_{12})\}\psi=0, \tag{1}$$

where E_T, the total energy, is measured in terms of Rh and the r's are in terms of $a=h^2/4\pi^2me^2$.

Since the above equation cannot be solved exactly by any ordinary process, we shall resort to a method of approximation. It may be assumed that the electron in the normal state of hydrogen is not appreciably disturbed by the external electron so that the interaction term is considered to affect the potential function of the latter only. Separation of variables is thus made possible.

Let

$$\psi=F_0(i)f(j), \qquad E_T=E_0+\epsilon, \tag{2}$$

where $F_0(i)$ and E_0 denote respectively the characteristic wave function and energy value of the electron belonging to the hydrogen atom in the normal state; $f(j)$ and ϵ denote respectively the continuous wave function and energy of the external electron. The letters i and j are used to designate the "inner" and "outer" electrons; either of them may be numbered as 1 and the other as 2.

Eq. (1) is then separated into

$$\nabla_i^2F_0(i)+(E_0+2/r_i)F_0(i)=0, \tag{3}$$

$$\nabla_j^2f(j)+\{\epsilon+2U(r_j)\}f(j)=0. \tag{4}$$

The normalized characteristic solution of Eq. (3) for the lowest energy level is

$$F_0(i)=\pi^{-\frac{1}{2}}e^{-r_i}. \tag{5}$$

The solution for Eq. (4) may be sought first by the usual method of separation of variables in spherical coordinates. The angular component of $f(j)$ has the usual expression $P_l^m(\cos\theta_j)e^{im\phi j}$ while the radial component, $R_{\epsilon,l}(r_j)$, must satisfy the differential equation

$$d^2(r_jR)/dr_j^2+\{\epsilon+2U(r_j)-l(l+1)/r_j^2\}(r_jR)=0, \tag{6}$$

where l is an integer.

Now we must find an expression for $U(r_j)$, which consists of the potential energy due to nuclear attraction and the interaction energy. To a close approximation, the interaction term is the average of $1/r_{ij}$ over all the configuration space of the inner electron. The result is

$$U(r_j)=\frac{1}{r_j}-\int_\infty\frac{F_0^2(i)d\tau_i}{r_{ij}}. \tag{7}$$

The integral is readily carried out by expanding $1/r_{ij}$ in spherical harmonics with the result

$$U(r_j)=(1+1/r_j)e^{-2r_j}. \tag{8}$$

Even with the above expression, a direct solution for Eq. (6) is still quite difficult. However, Eq. (8) can be very roughly represented by

$$U(r_j)\sim Z^*/r_j \tag{9}$$

where Z^* is a constant (less than one in this case) and is to be interpreted as the effective nuclear number with respect to the external electron. Z^* can be adjusted to make the expression in Eq. (9) fit a limited portion of the curve represented by Eq. (8). As it will be shown later, l in Eq. (6) must be 1 by the selection rule for the transition under consideration, so that the term $l(l+1)/r_j^2$ predominates for $r_j\ll1$. This means that we will only have to secure reasonable fitting for large values of r_j. The numerical determination for Z^* will be discussed later.

By our above assumption Eq. (6) becomes

$$d^2(r_jR)/dr_j^2+\{\epsilon+2Z^*/r_j-l(l+1)/r_j^2\}(r_jR)=0. \tag{10}$$

It is well known that the above differential equation is satisfied by the Laplace contour integral[7] which can in turn be transformed into

$$-2iR_{\epsilon,\,l}(r_j)=r_j^{\,l}\int_{-i(\epsilon)^{\frac{1}{2}}}^{i(\epsilon)^{\frac{1}{2}}}e^{\zeta r_j}(\zeta+i\epsilon^{\frac{1}{2}})^{l+iZ^*\epsilon^{-\frac{1}{2}}}(\zeta-i\epsilon^{\frac{1}{2}})^{l-iZ^*\epsilon^{-\frac{1}{2}}}d\zeta. \tag{11}$$

The solution for $f(j)$ is therefore simply the continuous wave function for the hydrogen atom with an effective atomic number Z^* instead of 1. The normalization of such a function can be carried by the method of Fues[8] as follows:

$$\int_\infty d\tau_j f^*_{\epsilon_2}(j)\int_{\epsilon_1}^{\epsilon_1+\Delta\epsilon_1}f_\epsilon(j)d\epsilon=1 \text{ or } 0 \tag{12}$$

according as $\epsilon_1<\epsilon_2<\epsilon_1+\Delta\epsilon_1$ or not. The result is identical to that of Fues:

$$f_{\epsilon,\,l,\,m}(j)=\left[\frac{(2l+1)}{2}\frac{(l-m)\,!}{(l+m)\,!}\right]^{\frac{1}{2}}\frac{e^{(3\pi/2)(Z^*/\epsilon^{\frac{1}{2}})}}{\pi[2(\epsilon)^{\frac{1}{2}}]^{l+\frac{1}{2}}|\,\Gamma(l+1+i(Z^*/\epsilon)^{\frac{1}{2}})\,|}R_{\epsilon,\,l}(r_j)P_l^{\,m}(\cos\theta_j)e^{im\phi_j}. \tag{13}$$

$F_0(i)f_{\epsilon,\,l,\,m}(j)$ is a particular solution for the wave function in the continuous state. Since i, j can be either 1, 2 or 2, 1, there are two linearly independent solutions, the proper normalized linear combinations are, of course, the symmetric and antisymmetric ones,[9]

$$\psi_{\epsilon,\,l,\,m}(\mathrm{H}^0+e)=2^{-\frac{1}{2}}\{F_0(1)f_{\epsilon,\,l,\,m}(2)\pm F_0(2)f_{\epsilon,\,l,\,m}(1)\}. \tag{14}$$

The bracket $(\mathrm{H}^0+\mathrm{e})$ is now added to denote the wave function of a normal hydrogen atom and an external electron before capture, in order to distinguish it from the discrete wave function. In the present special case, however, the characteristic wave function for H^- (see next section) is symmetric; the antisymmetric function represented by the lower sign in Eq. (14) can be omitted because it contributes nothing to the matrix component.

II. Characteristic Wave Function of H^- Obtained by Hylleraas

By a variational method Hylleraas[6] obtained for the lowest energy level of H^- an approximate characteristic function in the following form,

$$\psi(\mathrm{H}^-)=Ce^{-\alpha(r_1+r_2)}\{1+\beta r_{12}+\gamma(r_1-r_2)^2\}, \tag{15}$$

where α, β, γ are constants and C is the normalization constant which can readily be shown to be

$$C=\alpha^3/\pi\left[1+6\beta^2+\frac{35}{8}\frac{\beta}{\alpha}+\frac{3\gamma}{\alpha^2}+\frac{77}{8}\frac{\beta\gamma}{\alpha^3}+\frac{9\gamma^2}{\alpha^4}\right]^{\frac{1}{2}}.$$

The presence of the factor r_{12} in Eq. (15) is somewhat troublesome when we come to the integration. But we can eliminate the difficulty by the following expansion

$$r_{12}=\hat{r}\sum_{\nu=0}^{\infty}\left(\frac{x^2}{2\nu+3}-\frac{1}{2\nu-1}\right)x^\nu P_\nu(\cos\Theta), \tag{16}$$

where

[7] L. Schlesinger, *Einführung in die Theorie der gewöhnlichen Differential-gleichungen auf funktionentheoretischer Grundlage*, § 67.

[8] E. Fues, Ann. d. Physik **81**, 281 (1926).

[9] E.g., A. Sommerfeld, *Wave Mechanics*, p. 229.

$$P_\nu(\cos\Theta)=\sum_{\mu=-\nu}^{\nu}\frac{(\nu-|\mu|)!}{(\nu+|\mu|)!}P_\nu^{\mu}(\cos\theta_1)P_\nu^{\mu}(\cos\theta_2)e^{i\mu(\phi_1-\phi_2)}, \tag{17}$$

$$\cos\Theta=\cos\theta_1\cos\theta_2+\sin\theta_1\sin\theta_2\cos(\phi_1-\phi_2),$$

r= larger of the two radii, r_1 and r_2; x= ratio of the smaller to the larger radius.

III. The Square of the Matrix Component of Transition

The matrix component of transition formed by $\psi_{\epsilon,\,l,\,m}(H^0+e)$ and $\psi(H^-)$ in the directions x, y, z of the Cartesian coordinates may be defined as

$$\left.\begin{matrix}X_{\epsilon,\,l,\,m}\\ Y_{\epsilon,\,l,\,m}\\ Z_{\epsilon,\,l,\,m}\end{matrix}\right\}=\int\int_{\infty}\psi^*_{\epsilon,\,l,\,m}(H^0+e)\left\{\begin{matrix}x_1+x_2\\ y_1+y_2\\ z_1+z_2\end{matrix}\right\}\psi(H^-)dx_1dy_1dz_1dx_2dy_2dz_2. \tag{18}$$

Let $M^2_{\epsilon,\,l,\,m}$ be the square of the amplitude of the total matrix component per unit energy range. Then the sum over all allowable values of l, m is

$$\sum_{l,\,m}M^2_{\epsilon,\,l,\,m}=\sum_{l,\,m}\{|X_{\epsilon,\,l,\,m}|^2+|Y_{\epsilon,\,l,\,m}|^2+|Z_{\epsilon,\,l,\,m}|^2\}. \tag{19}$$

The three components can be evaulated when we transform Eq. (18) in terms of spherical coordinates and make use of the expressions derived for $\psi_{\epsilon,\,l,\,m}(H^0+e)$ and $\psi(H^-)$. We immediately find that $M^2_{\epsilon,\,l,\,m}$ vanishes except for $l=1$ and $m=0$ or ±1. Therefore the external electron must have an angular momentum quantum number 1 in order to have a chance to be captured by the atom.

Summing up the contributions due to the three different values of m, we arrive at the result

$$\sum_{l,\,m}M^2_{\epsilon,\,l,\,m}=\frac{8\pi}{9}\frac{c^2}{\epsilon^3}\frac{e^{3\pi Z^*/\epsilon^{\frac12}}}{|\Gamma[2+i(Z^*/\epsilon^{\frac12})]|^2}|W|^2,\quad l=1;\ m=-1,\,0,\,+1 \tag{20}$$

where

$$W=\int\int_{\infty}e^{-\{(1+\alpha)r_1+\alpha r_2\}}[3r_2\{1+\gamma(r_1-r_2)^2\}+\beta\hat{r}\{r_1(x^3/5-x)+r_2(x^2+3)\}]$$
$$\cdot\left[\int_{-i(\epsilon)^{\frac12}}^{i(\epsilon)^{\frac12}}e^{\zeta r_2}(\zeta+i(\epsilon)^{\frac12})^{1+iZ^*/\epsilon^{\frac12}}(\zeta-i(\epsilon)^{\frac12})^{1-iZ^*/\epsilon^{\frac12}}d\zeta\right]r_1^2dr_1r_2^3dr_2. \tag{21}$$

The integration of Eq. (21) is effected first by inverting the order of integration and then applying the theorem of residues for the evaluation of complex integrals. The process is essentially similar to that used by Fues[8] and Sugiura,[10] except that here we have to consider also the residue at infinity. Omitting all detailed steps, we write the final result as follows:

$$W=\frac{24^2\pi}{(1+\alpha)^3}\frac{Z^*(Z^{*2}+\epsilon)}{1-e^{2\pi Z^*/\epsilon^{\frac12}}}\left[\left\{\frac{\beta(\alpha+Z^*)}{(1+\alpha)^4Z^*(Z^{*2}+\epsilon)}-\left(\frac13+\frac{4\gamma}{(1+\alpha)^2}\right)\frac{(Z^*-2\alpha)}{(\alpha^2+\epsilon)^3}\right.\right.$$
$$+\frac{\{30\gamma-5\beta(1+\alpha)\}}{3(1+\alpha)(\alpha^2+\epsilon)^4}\left[\alpha^2+2Z^*\alpha+\frac25(1-Z^{*2})\right]+\frac{30\gamma}{(\alpha^2+\epsilon)^5}\left[\frac23\alpha^3-Z^*\alpha^2+\frac25(Z^{*2}-\epsilon)\alpha\right.$$
$$\left.\left.+\frac{Z^*}{45}(7\epsilon-2Z^{*2})\right]\right\}\exp\left[-\frac{2Z^*}{\epsilon^{\frac12}}\tan^{-1}\frac{\epsilon^{\frac12}}{\alpha}\right]-\beta\left\{\frac{\alpha+Z^*}{(1+\alpha)^4Z^*(Z^{*2}+\epsilon)}-\frac{2(2\alpha+3-Z^*)}{(1+\alpha)^3(Z^{*2}+\epsilon)}\right.$$
$$\left.+\frac{2}{(1+\alpha)^2\{(2\alpha+1)^2+\epsilon\}^2}+\frac{2(4\alpha+2-Z^*)}{3(1+\alpha)\{(2\alpha+1)^2+\epsilon\}^3}\right\}\exp\left[-\frac{2Z^*}{\epsilon^{\frac12}}\tan^{-1}\frac{\epsilon^{\frac12}}{2\alpha+1}\right]\Bigg]. \tag{22}$$

[10] Y. Sugiura, Scient. Pap. of Inst. of Phys. and Chem. Res. (Tokyo), No. 193 (1929).

IV. Intensity of Emission, Effective Cross Section of Combination, and the Atomic Coefficient of Absorption for H^-

(a) To calculate the total intensity of emission one must assume a definite distribution of electrons while they are mixed with the atoms. Since we are here dealing with neutral atoms only, we shall assume that their effect on the distribution of electrons can be neglected for the present purpose. This cloud of free electrons may be considered to behave exactly like an ideal gas in a fixed enclosure, having for the aggregate an electron temperature, T_e. Hence, we can apply the results of the quantum statistics for free electrons.

From the preceding section it can be shown[10] that $(a^2/Rh)\sum_{l,m}M^2_{\epsilon,l,m}dE$ represents the amplitude squared of the matrix component for the transition of an electron having its energy lying between E and $E+dE$. Here a^2/Rh is the conversion factor from the units used in the preceding sections into c.g.s. units; $E=Rh\epsilon$. Therefore $(e^2a^2/Rh)\sum_{l,m}M^2_{\epsilon,l,m}dE$ is to be interpreted as the square of the amplitude of electric moment. If g_E is the number of free electron states in the energy interval between E and $E+dE$, then $(e^2a^2/g_ERh)\sum_{l,m}M^2_{\epsilon,l,m}dE$ is the weighted mean of the amplitude squared of the electric moment. We need only to multiply this by the total number of electrons in dE to obtain the total amplitude squared of the electric moment. By the well-known quantum statistics,[11] the total number of electrons in the energy interval between E and $E+dE$ is equal to $g_E\cdot\mathfrak{F}$ where $\mathfrak{F}$ is the average number of electrons per state. Therefore the total amplitude squared of the electric moment is

$$(e^2a^2\mathfrak{F}Rh)\sum_{l,m}M^2_{\epsilon,l,m}dE. \tag{23}$$

Now the electric moment vibrates with a frequency ν determined by the equation

$$h\nu=E+e\Phi, \tag{24}$$

where Φ = electron affinity of the normal hydrogen atom. By referring to the classical electrodynamics for the radiation from a dipole oscillator, we can get the following wave-mechanical equivalent for the intensity of the continuous spectrum:

$$I(\nu)d\nu=N^0\cdot\frac{64\pi^4\nu^4e^2a^2}{3c^3Rh}\mathfrak{F}\sum_{l,m}M^2_{\epsilon,l,m}dE, \tag{25}$$

where $hd\nu=dE$, by Eq. (24); $I(\nu)d\nu$ = time rate of emission energy in ergs per sec. per cc in the frequency interval between ν and $\nu+d\nu$; N^0 = number of normal hydrogen atoms per cc. The $\mathfrak{F}$-function may be assumed to be that of an ideal electron gas obeying the new statistics of Fermi and Dirac, namely

$$\mathfrak{F}=1/ce^{E/kT_e}-1, \tag{26}$$

where T_e = electron temperature, and C = function of T_e and electron density. Fermi[12] showed that for very large T_e,* C is so large that $Ce^{E/kT}\gg1$. Hence we have the Maxwell's distribution and the $\mathfrak{F}$-function is accordingly

$$\mathfrak{F}=[N^eh^3/(2\pi mkT_e)^{\frac{3}{2}}]e^{-E/kT_e}, \tag{26a}$$

where N^e is the number of electrons per cc. Combining Eqs. (25) and (26a), we have

$$\frac{I(\nu)}{N^0N^e}=\frac{64\pi^4\nu^4e^2a^2}{3c^3R}\cdot\frac{h^3}{(2\pi mkT_e)^{\frac{3}{2}}}e^{-E/kT_e}\sum_{l,m}M^2_{\epsilon,l,m}. \tag{27}$$

(b) The effective cross section of combination for an atom (q) may be defined as the cross section of a small sphere such that the number of electrons with velocity v striking the surface of the sphere will be equal to the number of electrons with the same velocity actually captured by the atom. If $n(E)dE$ is the number of electrons per cc in the energy interval between E and $E+dE$ (according to Maxwell's distribution), then

$$n(E)dE=[2\pi N^eE^{\frac{1}{2}}/(\pi kT_e)^{\frac{3}{2}}]e^{-E/kT_e}dE, \tag{28a}$$

$$I(\nu)d\nu=N^0h\nu\cdot qvn(E)dE. \tag{28b}$$

Solving for q, we get

$$q=[16\pi^3h\nu^3/3(mv)^2c^3]e^2a^2\sum_{l,m}M^2_{\epsilon,l,m}. \tag{29}$$

[11] E.g., G. Birtwistle, *The New Quantum Mechanics*, Chap. XXIX. E. Fermi, Zeits. f. Physik **36**, 902 (1926).

[12] E. Fermi, Zeits. f. Physik **36**, 902 (1926).

* We are here interested only in large T_e. (See Section V.)

(c) The atomic coefficient of absorption (k) for H^- may be similarly defined as the effective cross section of H^- for the capture of quanta of radiation. The number of quanta captured, or the number of H^- atoms dissociated, per second per cc in the frequency interval between ν and $\nu+d\nu$ is clearly

$$kc\rho d\nu/h\nu$$

where $\rho d\nu$ = radiation energy density in the same frequency interval.

Assuming thermal equilibrium between emission and absorption processes (extension of Einstein's method to transitions between continuous and discrete states), Kramers[13] and Milne[14] derived the following relation between q and k

$$q/k = 2gh^2\nu^2/m^2v^2c^2, \qquad (30)$$

where g is the statistical weight of the lower energy state in this case, $g(H^-)=1$. The explicit expression for k in terms of the square of the matrix component of transition is

$$k = (8\pi^3\nu/3cRh)e^2a^2\textstyle\sum_{l,m} M^2_{\epsilon,\,l,\,m}. \qquad (31)$$

V. Numerical Computations

The three constants in the H^- wave function given by Hylleraas are in the units here used: $\alpha=0.770$, $\beta=0.308$, and $\gamma=0.119$. To fit the expression in Eq. (9) with that in Eq. (8) for large values of the radial variable, Z^* may take any value ranging between 0 and 0.5, depending upon which portion of the curve is to be fitted best. Various values of Z^* in this range have been tried in the present calculation. Except for slight differences in numerical magnitudes, they give approximately the same distribution of $\sum_{l,m} M^2_{\epsilon,\,l,\,m}$ as a function of the energy parameter ϵ. For illustration, we have chosen for Z^* a value of 0.42, although much smaller values will equally serve the purpose. The values for $\sum_{l,m} M^2_{\epsilon,\,l,\,m}$ are not critical to the variation of Z^*, so that the general interpretation of results about to be obtained will not necessarily depend upon any particular value of Z^*.

The electron affinity of the normal hydrogen atom is given by Hylleraas as 0.715 v, with which we can calculate the frequency of radiation for any kinetic energy of the electron (by Eq. (24)).

Now, we will consider the order of magnitude of the electron temperature (T_e). Langmuir and

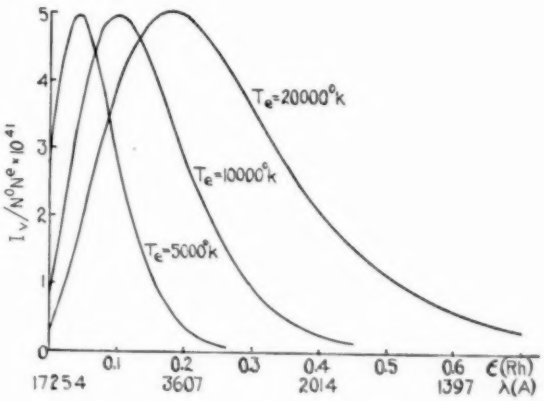

Fig. 1. Intensity distribution at different electron temperatures.

Mott-Smith[15] find a temperature of about 30,000°C at 2×10^{-4} mm pressure in discharges through mercury vapor. Kopfermann and Ladenburg[16] find convincing evidence for statistical equilibrium in discharges through neon at 1 mm

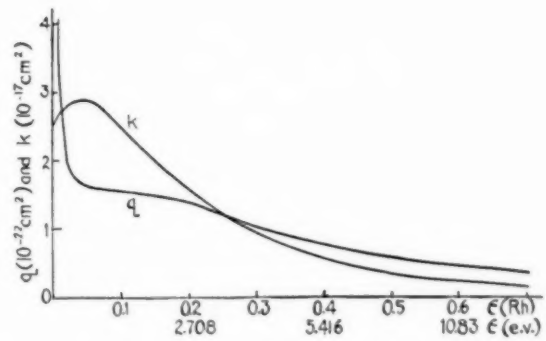

Fig. 2. Effective cross section of combination (q) and coefficient of absorption for H^- (k).

pressure with an electron temperature of about 22,000°C. From these evidences and others, it seems certain that the electron temperature under electrical discharge conditions must be

[13] H. A. Kramers, Phil. Mag. **46**, 836 (1923).

[14] E. A. Milne, Phil. Mag. **47**, 209 (1924).

[15] J. Langmuir and H. Mott-Smith, Gen. Elec. Rev. **27**, 449 (1924).

[16] H. Kopfermann and R. Ladenburg, Naturwiss. **5**, 513 (1931).

quite high. In the present calculations of the emission spectrum we shall choose several different values of electron temperature to illustrate its effect upon the general distribution of emission intensities.

The accompanying graphs (Figs. 1 and 2) show the results of computation for the emission intensities at different electron temperatures, the effective cross section of combination, and the coefficient of absorption for H^-.

Conclusion

(a) Discussion of results

The computed results show that the intensity per unit frequency interval in the emission spectrum has a low but finite value at the long wave limit. There is a point toward the short wave side of the limit where the intensity has its maximum value, which is displaced more and more away from the limit as the electron temperature is raised. Thus, at a very high electron temperature (e.g., 20,000°K) the intensity at the limit may be more than ten times smaller than the maximum value whose spectral position is considerably away from the limit (see Fig. 1). If the absolute magnitude of the intensity is low, then the limit would be so faint that it is beyond recognition. The identification of the continuous spectrum and the subsequent determination of electron affinity by the position of the limit would become very difficult.

The curve for the effective cross section of combination (see Fig. 2) is similar in appearance to that of the recombination between H^+ and electrons obtained by Stueckelberg and Morse,[17] except that the order of magnitude of the former is much smaller and it does not diminish as rapidly for high-velocity electrons. It must be mentioned here that the present calculations are based on random distribution of electrons while Stueckelberg and Morse assumed a unidirectional stream of electrons. For a more exact comparison, we have calculated the effective cross section in exact accordance with Stueckelberg and Morse's method. The resulting value is not shown in the figure, but is about 100–500 times smaller than for their case. If the concentration of the corresponding reaction quantities (i.e., the number of H^- atoms and electrons in one case and the number of H^+ atoms and electrons in the other) are the same, the emission intensities would bear the same ratio. Hence the intensity of the electron affinity spectrum for normal hydrogen atoms is expected to be generally very low.

The curve for the atomic coefficient of absorption (see Fig. 2) has a maximum near the limit of the continuous absorption spectrum. The magnitude of the coefficient is generally higher than the values for caesium given by Mohler[18] (possibly by as much as 100-fold). If there is sufficient concentration of H^- ions present, it should be possible (apart from the experimental difficulties) to obtain a continuous absorption spectrum due to the photo-ionization of H^- ions.

(b) Application of the results to the electron affinity spectrum of halogen atoms

The halogen atoms are known to have great affinity for electrons and their negative ions have a stable external configuration similar to the inert gases. If the negative ions are formed by an elementary process of combination between neutral atoms and electrons, the emission spectrum of halogen atoms should be very roughly similar to that of hydrogen. On this qualitative basis we expect that the conclusions obtained for hydrogen may partially apply to the continuous spectrum of halogen atoms.

In his recent experiments, Oldenberg found no trace of an electron affinity spectrum for the iodine atom under widely varying experimental conditions. The possibility of having a distribution of intensities such that the maximum intensity is far separated from the spectral limit becomes less for the iodine atom because of the slower change of the ν^4-factor at a larger electron affinity (about 3.2 volts). It seems that the only other alternative is to assume that the intensity of emission is too faint to be experimentally detectable; or in other words, the combination between neutral iodine atoms and electrons with simultaneous emission of radiation is comparatively an improbable process—a conclusion reached by Oldenberg.

Strictly speaking, however, we are not justified to make quantitative comparisons between the

[17] E. C. G. Stueckelberg and P. M. Morse, Phys. Rev. **36**, 16 (1930).

[18] F. L. Mohler, Phys. Rev. Sup. **1**, 2 (1929).

two cases for at least two reasons. First, the present calculations for hydrogen are based upon very rough wave functions in the continuous state; hence the solution is far from being rigorous and exact. The results may be expected, at best, to be only approximately correct for hydrogen and must not be applied directly to the halogen atoms, which presumably have quite different potential functions. Secondly, the difference in magnitudes of electron affinity between the halogen atoms and hydrogen is quite large—the halogen atoms have electron affinities in the range of 3–4 volts against about 0.7 v for hydrogen. The influence of the magnitude of electron affinity comes in when one deals with the ν^4-factor in the expression for intensity. Under these circumstances we cannot expect to have a simple quantitative relation between the two problems.

The writer is very much indebted to Professor E. C. Kemble for invaluable advice.

Note on Kowalewski's Top in Quantum Mechanics

OTTO LAPORTE, *University of Michigan*

(Received February 14, 1933)

It is well known that in classical mechanics algebraic integrals of the top equations only exist in the cases of Euler (asymmetric top, no electric moment), of Lagrange (symmetric top, electric moment parallel to the axis of figure) and of Kowalewski. The latter case is that of a symmetric top whose two equal moments of inertia are twice as large as the third ($A=B=2C$) with an electric moment perpendicular to the axis of figure. The quantum mechanical analogue to Euler's and Lagrange's cases being well known, Kowalewski's case was tried. If ϑ, ψ, φ are the Euler angles, $Q_{\mathrm{I}}=Q_1+iQ_2$, $Q_{\mathrm{II}}=Q_1-iQ_2$ linear combinations of the momenta around the principal axes and

$$U=Q_{\mathrm{I}}^2+4C\mu \sin \vartheta e^{-i\Psi},$$

then Kowalewski's integral becomes:

$$UU^*+U^*U+4h^2(Q_{\mathrm{I}}Q_{\mathrm{II}}+Q_{\mathrm{II}}Q_{\mathrm{I}})=\text{Diag. Matrix},$$

which differs from the classical result by the symmetrization and by the last term proportional to h^2.

I. INTRODUCTION

THERE are two cases where the classical equations for the rotation of a rigid heavy body around a fixed point may be integrated readily by separation of variable of the Hamiltonian in question: Firstly the case of Lagrange, the case of a symmetric top ($A=B\neq C$) with the center of gravity on the axis of figure. Secondly the case of Euler, the case of a totally asymmetric top ($A\neq B\neq C$) with the center of gravity coinciding with the fixed point of rotation. However in 1888 Sonya Kowalewski[1] succeeded in solving another case of top motion, namely that of a symmetric top whose two equal moments of inertia are twice as large as the third ($A=B=2C$) and whose center of gravity lies in the plane of the two equal moments, or perpendicular to the axis of figure. Kowalewski only was able to integrate this case because she discovered (in addition to the energy and momentum integrals) a third algebraic integral which brought the number of first integrals up to three, as in the cases of Euler and Lagrange.

It is of interest to note that in 1907 it was proved by Husson[2] that a third algebraic integral only exists in the aforementioned cases of Euler, Lagrange and Kowalewski or in special cases of these.

The quantum mechanical analogue of Lagrange's case, namely that of a symmetric top molecule with the electric moment parallel to the axis of figure was treated by Reiche and Rademacher,[3] by Kronig and Rabi,[4] and by Manneback.[5] Euler's case, the asymmetric top, was treated quantum-mechanically by Wang,[6] by Kramers and Ittmann,[7] and by Klein.[8] In the present paper we show that the quantum mechanical analogue of the Kowalewski top also possesses a third algebraic integral. Thus it is to be expected that a complete solution of the problem is possible in spite of the inseparability of Hamiltonian of the problem.

II. THE FUNDAMENTAL EQUATIONS OF KOWALEWSKI'S TOP

For the sequel the reader is referred to the Leiden dissertation of H. B. G. Casimir[9] where more detailed derivations of the equations of rotation in quantum mechanics are given.

The independent variables are the Euler angles.

[1] S. Kowalewski, Acta Mathematica **12**, 177 (1888).

[2] E. Husson, Ann. Fac. Science Toulouse **8**, 73 (1906).

[3] F. Reiche and H. Rademacher, Zeits. f. Physik **39**, 444 (1926); **41**, 453 (1927).

[4] R. deL. Kronig and J. J. Rabi, Phys. Rev. **29**, 262 (1927).

[5] C. Manneback, Phys. Zeits. **28**, 72 (1927).

[6] S. C. Wang, Phys. Rev. **34**, 243 (1929).

[7] H. A. Kramers and G. P. Ittmann, Zeits. f. Physik **53**, 553 (1929); **58**, 217 (1929); **60**, 663 (1930).

[8] O. Klein, Zeits. f. Physik **58**, 730 (1929).

[9] H. B. G. Casimir, *Leiden Dissertation*, 1931.

The notation of Whittaker's Analytical Dynamics is used so that if $OXYZ$ is a right-hand system fixed in space and $Oxyz$ a right-hand system fixed in the body and if OK is the nodal line then

$$\sphericalangle zOZ=\vartheta;\quad \sphericalangle YOK=\varphi;\quad \sphericalangle yOK=\psi.$$

It is not necessary to write down all nine direction cosines (cf. Whittaker, page 10), all we need are the cosines of the angles formed by the vertical Z

$$\begin{aligned}&\text{with } x\text{: } \gamma_1=-\sin\vartheta\cos\psi,\\ &\text{with } y\text{: } \gamma_2=\ \ \sin\vartheta\sin\psi,\\ &\text{with } z\text{: } \gamma_3=\ \ \cos\vartheta.\end{aligned}\tag{1}$$

As axis of figure we choose the z axis. Let the electric moment be in the direction of the x axis, so that the potential energy is

$$V=\mu\gamma_1=-\mu\sin\vartheta\cos\psi.\tag{2}$$

As momenta we have Q_1, Q_2, Q_3, the momenta around the axes of the principal moments of inertia. Now it is essential for the following, that both for the Q and for the γ we always use the following complex combinations:

$$\begin{aligned}&Q_{\mathrm{I}}=Q_1+iQ_2;\quad \gamma_{\mathrm{I}}=\gamma_1+i\gamma_2=-\sin\vartheta e^{-i\psi},\\ &Q_{\mathrm{II}}=Q_1-iQ_2;\quad \gamma_{\mathrm{II}}=\gamma_1-i\gamma_2=-\sin\vartheta e^{+i\psi}.\end{aligned}\tag{3}$$

As operators upon functions of the Euler angles the Q look as follows[10]:

$$\begin{aligned}Q_{\mathrm{I}}&=-ihe^{-i\psi}\left\{\frac{1}{\sin\vartheta}\left(\cos\vartheta\frac{\partial}{\partial\psi}-\frac{\partial}{\partial\varphi}\right)+i\frac{\partial}{\partial\vartheta}\right\},\\ Q_{\mathrm{II}}&=-ihe^{+i\psi}\left\{\frac{1}{\sin\vartheta}\left(\cos\vartheta\frac{\partial}{\partial\psi}-\frac{\partial}{\partial\varphi}\right)-i\frac{\partial}{\partial\vartheta}\right\},\\ Q_3&=-ih\frac{\partial}{\partial\psi}.\end{aligned}\tag{4}$$

From these formulae the exchange relations of the Q with each other and with the γ may be derived; or they may be obtained by generalizing, in the well-known way their Poisson brackets of classical mechanics. Using the abbreviation of Born and Jordan[11]

$$(i/h)(xy-yx)=[x,y]\tag{5}$$

we put down, for future reference, the following table of exchange relations:[12]

$$\begin{aligned}&[Q_{\mathrm{I}},Q_3]=iQ_{\mathrm{I}}, &&\text{(a)}\quad [Q_k,\gamma_k]=0, &&\text{(h)}\\ &[Q_{\mathrm{II}},Q_3]=-iQ_{\mathrm{II}}, &&\text{(b)}\quad [Q_{\mathrm{I}},\gamma_3]=i\gamma_{\mathrm{I}}, &&\text{(i)}\\ &[Q_{\mathrm{I}},Q_{\mathrm{II}}]=-2iQ_3, &&\text{(c)}\quad [Q_{\mathrm{II}},\gamma_3]=-i\gamma_{\mathrm{II}}, &&\text{(k)}\\ &[Q_{\mathrm{I}}^2,Q_3]=2iQ_{\mathrm{I}}^2, &&\text{(d)}\quad [Q_3,\gamma_{\mathrm{I}}]=-i\gamma_{\mathrm{I}}, &&\text{(l)}\\ &[Q_{\mathrm{II}}^2,Q_3]=-2iQ_{\mathrm{II}}^2, &&\text{(e)}\quad [Q_3,\gamma_{\mathrm{II}}]=i\gamma_{\mathrm{II}}, &&\text{(m)}\\ &[Q_{\mathrm{I}}Q_{\mathrm{II}},Q_3]=0, &&\text{(f)}\quad [Q_{\mathrm{I}},\gamma_{\mathrm{II}}]=-2i\gamma_3, &&\text{(n)}\\ &[\gamma_k,\gamma_l]=0, &&\text{(g)}\quad [Q_{\mathrm{II}},\gamma_{\mathrm{I}}]=2i\gamma_3, &&\text{(o)}\\ &&&\quad [Q_{\mathrm{I}}^2,\gamma_{\mathrm{II}}]=-2i(Q_{\mathrm{I}}\gamma_3+\gamma_3Q_{\mathrm{I}}), &&\text{(p)}\\ &&&\quad [Q_{\mathrm{II}}^2,\gamma_{\mathrm{I}}]=+2i(Q_{\mathrm{II}}\gamma_3+\gamma_3Q_{\mathrm{II}}). &&\text{(q)}\end{aligned}$$

If we put $A=B=2C$ we obtain as Hamiltonian[13]:

$$H=(1/8C)(Q_{\mathrm{I}}Q_{\mathrm{II}}+Q_{\mathrm{II}}Q_{\mathrm{I}})+(1/2C)Q_3^2+\tfrac{1}{2}\mu(\gamma_{\mathrm{I}}+\gamma_{\mathrm{II}}).\tag{6}$$

H put equal to the diagonal matric E is the first of the three algebraic integrals. The second is due to the fact that H does not contain the Euler angle φ explicitly: thus

$$p_\varphi=\tfrac{1}{2}(\gamma_{\mathrm{II}}Q_{\mathrm{I}}+\gamma_{\mathrm{I}}Q_{\mathrm{II}})+\gamma_3Q_3=\text{Diag. Matrix.}\tag{7}$$

III. Kowalewski's Integral

We now have to work with the Euler equations of the top which are obtained from the consideration, that the time derivative of any matric function f is given by $\dot{f}=[H,f]$. We then obtain, using repeatedly the exchange relations:

$$\begin{aligned}4C\dot{Q}_{\mathrm{I}}&=-i(Q_3Q_{\mathrm{I}}+Q_{\mathrm{I}}Q_3)+4iC\mu\gamma_3,\\ 4C\dot{Q}_{\mathrm{II}}&=+i(Q_3Q_{\mathrm{II}}+Q_{\mathrm{II}}Q_3)-4iC\mu\gamma_3,\\ 4C\dot{Q}_3&=\qquad\qquad 2iC\mu(\gamma_{\mathrm{I}}-\gamma_{\mathrm{II}}),\end{aligned}\tag{8}$$

$$\begin{aligned}4C\dot{\gamma}_{\mathrm{I}}&=-2i(Q_3\gamma_{\mathrm{I}}+\gamma_{\mathrm{I}}Q_3)+i(Q_{\mathrm{I}}\gamma_3+\gamma_3Q_{\mathrm{I}}),\\ 4C\dot{\gamma}_{\mathrm{II}}&=+2i(Q_3\gamma_{\mathrm{II}}+\gamma_{\mathrm{II}}Q_3)-i(Q_{\mathrm{II}}\gamma_3+\gamma_3Q_{\mathrm{II}}),\\ 4C\dot{\gamma}_3&=-\tfrac{1}{2}i\{(Q_{\mathrm{I}}\gamma_{\mathrm{II}}+\gamma_{\mathrm{II}}Q_{\mathrm{I}})-(Q_{\mathrm{II}}\gamma_{\mathrm{I}}+\gamma_{\mathrm{I}}Q_{\mathrm{II}})\}.\end{aligned}\tag{9}$$

[10] Casimir, p. 57, Eq. (18).

[11] M. Born and P. Jordan, *Elementare Quantenmechanik*, Berlin, 1930, p. 23, Eq. (7).

[12] Casimir, p. 44, Eqs. (1) to (6).

[13] Casimir, p. 45, Eqs. (10).

Except for the symmetrizations Eqs. (8) and (9) are exactly the same as in classical mechanics. We multiply the first Eq. (8) with Q_I from the left and then again with Q_I from the right and thus obtain the time derivative of the square of Q_I:

$$4C(Q_I^2)^{\cdot} = -i(Q_I^2Q_3+2Q_IQ_3Q_I+Q_3Q_I^2) + 4iC\mu(Q_I\gamma_3+\gamma_3Q_I).$$

The last term of this equation is eliminated by means of (9.1). Applying exchange rule (a), (d) and (l) we have:

$$C(Q_I^2-4\mu C\gamma_I)^{\cdot} = -iQ_3(Q_I^2-4\mu C\gamma_I)-ih(Q_I^2-2\mu C\gamma_I) \quad (10.1)$$

$$= -i(Q_I^2-4\mu C\gamma_I)Q_3+ih(Q_I^2-2\mu C\gamma_I). \quad (10.2)$$

We shall use both forms later on. We now treat the second Eq. (8) and the second Eq. (9) in a completely analogous manner and obtain:

$$C(Q_{II}^2-4\mu C\gamma_{II})^{\cdot} = iQ_3(Q_{II}^2-4\mu C\gamma_{II})-ih(Q_{II}^2-2\mu C\gamma_{II}) \quad (11.1)$$

$$= i(Q_{II}^2-4\mu C\gamma_{II})Q_3+ih(Q_{II}^2-2\mu C\gamma_{II}). \quad (11.2)$$

We introduce the abbreviations:

$$\begin{aligned} Q_I^2-4\mu C\gamma_I &= U, \\ Q_{II}^2-4\mu C\gamma_{II} &= U^*, \\ UU^*+U^*U &= T. \end{aligned} \quad (12)$$

We compute

$$\dot{T} = \dot{U}U^*+U\dot{U}^*+\dot{U}^*U+U^*\dot{U}. \quad (13)$$

It now simplifies the calculation of $\dot{T}$ considerably if in the first term of this expression one uses (10.2) for $\dot{U}$ and in the last term (10.1) for $\dot{U}$. Similarly in the second term of (13) we will use (11.1) for U^* and in the third term (11.2) for U^*. We then have:

$$\begin{aligned} -iC\dot{T} = &\{-(Q_I^2-4\mu C\gamma_I)Q_3+h(Q_I^2-2\mu C\gamma_I)\}(Q_{II}^2-4\mu C\gamma_{II}) \\ &+(Q_I^2-4\mu C\gamma_I)\{Q_3(Q_{II}^2-4\mu C\gamma_{II})-h(Q_{II}^2-2\mu C\gamma_{II})\} \\ &+\{(Q_{II}^2-4\mu C\gamma_{II})Q_3+h(Q_{II}^2-2\mu C\gamma_{II})\}(Q_I^2-4\mu C\gamma_I) \\ &+(Q_{II}^2-4\mu C\gamma_{II})\{-Q_3(Q_I^2-4\mu C\gamma_I)-h(Q_I^2-2\mu C\gamma_I)\}. \end{aligned}$$

Evidently all terms which are not proportional to h cancel. We are left with:

$$C\dot{T} = h^2\{[Q_I^2-2\mu C\gamma_I,\ Q_{II}^2-4\mu C\gamma_{II}]+[Q_{II}^2-2\mu C\gamma_{II},\ Q_I^2-4\mu C\gamma_I]\}.$$

The terms containing Q in the fourth order cancel each other in the two exchange brackets. So do the terms containing products of γ. We then have:

$$\dot{T} = -2h^2\mu\{[Q_I^2,\ \gamma_{II}]+[Q_{II}^2,\ \gamma_I]\}.$$

Applying exchange rule (p) and (q) we finally get:

$$\dot{T} = 4ih^2\mu(Q_I\gamma_3+\gamma_3Q_I-Q_{II}\gamma_3-\gamma_3Q_{II}). \quad (14)$$

Leaving this equation for the moment we now return to the Euler Eqs. (8). We propose to multiply (8.1) with Q_{II} first from the left and then from the right and similarly (8.2) with Q_I both from the left and right sides. These four equations are then added:

$$\begin{aligned} &4C(Q_IQ_{II}+Q_{II}Q_I)^{\cdot} \\ &= i(-Q_{II}Q_3Q_I-Q_{II}Q_IQ_3-Q_3Q_IQ_{II} \\ &\quad -Q_IQ_3Q_{II}+Q_IQ_3Q_{II}+Q_IQ_{II}Q_3 \\ &\quad +Q_3Q_{II}Q_I+Q_{II}Q_3Q_I) \\ &\quad +4i\mu C(Q_{II}\gamma_3+\gamma_3Q_{II}-Q_I\gamma_3-\gamma_3Q_I). \end{aligned} \quad (15)$$

In the first parenthesis on the right side the first and last as well as the fourth and fifth term cancel. The remaining four terms of the first parenthesis may be written:

$$[[Q_I,\ Q_{II}],\ Q_3]$$

which vanishes because of (c). Combining (14) and (15) we find:

$$\dot{T} = -4h^2(Q_IQ_{II}+Q_{II}Q_I)^{\cdot}$$

or integrating and using (13):

$$UU^*+U^*U+4h^2(Q_{\mathrm{I}}Q_{\mathrm{II}}+Q_{\mathrm{II}}Q_{\mathrm{I}})=\text{Diag. Matrix.} \tag{16.1}$$

Taking into account (12) and (3) one may write this:

$$(Q_{\mathrm{I}}^2-4\mu C\gamma_{\mathrm{I}})(Q_{\mathrm{II}}^2-4\mu C\gamma_{\mathrm{II}})+(Q_{\mathrm{II}}^2-4\mu C\gamma_{\mathrm{II}})(Q_{\mathrm{I}}^2-4\mu C\gamma_{\mathrm{I}})+4h^2(Q_{\mathrm{I}}Q_{\mathrm{II}}+Q_{\mathrm{II}}Q_{\mathrm{I}})=\text{Diag. Matrix.} \tag{16.2}$$

or

$$(Q_1^2-Q_2^2+4\mu C\sin\vartheta\cos\psi)^2+(Q_1Q_2+Q_2Q_1-4\mu C\sin\vartheta\sin\psi)^2+4h^2(Q_1^2+Q_2^2)=\text{Diag. Matrix.} \tag{16.3}$$

Eqs. (16) represent the quantum mechanical analogue of the Kowalewski Integral, which in classical mechanics simply is: $UU^*=\text{const.}$ It is interesting that the simplest quantum-like generalization, namely symmetrization of U and U^* is not sufficient to obtain an integral; the term proportional to h^2 has to be added. Nor is it possible to embody this correction term in the definition of U as one might attempt in order to preserve the classical form as closely as possible.

Eqs. (6), (7) and (16) form the three first integrals of the problem. By means of these (or rather their classical counterparts) Kowalewski showed that the problem could be completely solved and reduced to hyperelliptic integrals. It remains to be seen whether or not a similar reduction is possible also in quantum mechanics.

Transport Phenomena in Einstein-Bose and Fermi-Dirac Gases. I

E. A. UEHLING AND G. E. UHLENBECK, *University of Michigan*

(Received February 13, 1933)

The theory of gases in nonstationary states, given by Lorentz and Enskog, is generalized for the quantum statistics to give the hydrodynamical equations and the distribution function in first and second approximation, and formal expressions for the viscosity and heat conductivity coefficients. These results are valid for all statistics and for all degrees of degeneration. Two essential points contribute to this generality: (a) Exact expressions independent of statistics and degeneration can be given for the coordinate and time derivatives of the coefficient A of the equilibrium distribution function in terms of the pressure and temperature gradients and time derivatives, though a closed expression for this coefficient as a function of v and T is known only in limiting cases; (b) The function W of the general equation of state for ideal gases in all statistics

$$pv=(RT/M)W(v^3T)$$

is adiabatically invariant. Numerical values of the viscosity and heat conductivity coefficients, which should come out of the formal theory on the introduction of special assumptions about the molecular forces, have not yet been obtained. It is our hope that these results, when found, may furnish an experimental test of the existence of Einstein-Bose statistics in real gases, as is required by theory.

INTRODUCTION

§1

One may distinguish broadly two methods of treating the problem of viscosity and heat conductivity of an ideal gas. The first of these is an inexact method according to which an equilibrium distribution function is considered to be descriptive of the state within the gas, subject only to the condition that the five quantities, the density, the temperature, and the three components of mass velocity are functions of position. The conception of the mean free path is fundamental in this theory.

According to the second and more nearly exact method, which is due mainly to Maxwell and Chapman on the one hand, and to Lorentz and Enskog[1] on the other, one recognizes the fact that the above assumption regarding the equilibrium distribution function is not valid, since the latter does not fulfill the fundamental Boltzmann continuity equation. We propose to generalize this method so as to include the Einstein-Bose and the Fermi-Dirac as well as the Maxwell-Boltzmann statistics.

§2

In this generalization we will follow Lorentz and Enskog, rather than Maxwell and Chapman. An understanding of the method used may be obtained from a consideration of the electron theory of metals of Lorentz.[2] The essential points in this theory follow.

The fundamental Boltzmann equation in this case, where one assumes the existence of a steady state, the dependence on one coordinate only, and elastic collisions between the electrons and fixed ions with no interaction among the electrons themselves, takes the form:

$$r_x\frac{\partial f}{\partial x}+X\frac{\partial f}{\partial r_x}=nR^2r\int\{f(r_x'r_y'r_z')-f(r_xr_yr_z)\}\cos\vartheta d\Omega, \tag{1}$$

where ϑ is the angle between the direction of the line of centers in collision and the electron velocity r; $d\Omega$ is the element of solid angle within which the direction of the line of centers must lie; n is

[1] Maxwell, *Collected Works II*, p. 1; Lorentz, *Theory of Electrons*, Note 29, p. 266, Ges. Abh. I, p. 72, *Vorträge über die kinetische Theorie der Materie und Electrizität*, p. 185; Chapman, Phil. Trans. **216 A**, 279 (1915); **217 A**, 115 (1916); Enskog, *Kinetische Theorie der Vorgänge in mässig verdünnten Gasen, Dissertation*, Upsala, 1917. Also see Jeans, *Dynamical Theory of Gases*, Chapters VIII and IX.

[2] Lorentz, Reference 1.

the number of ions per unit volume; R is the sum of the radii of the electron and ion; and X is the acceleration due to the external electric field. Primes denote quantities which are to be taken *after* collision.

In the determination of the distribution function which fulfills this equation one can distinguish the following steps:

(a) *The principle of solution.* One assumes:

$$f=f^{(0)}(1+\varphi), \tag{2}$$

where $f^{(0)}$ is the equilibrium distribution function, and φ is a small perturbation term. Introducing (2) into (1), and retaining only first order quantities, one obtains, since $f^{(0)}$ is a function only of r:

$$r_x\frac{\partial f^{(0)}}{\partial x}+X\frac{\partial f^{(0)}}{\partial r_x}=nR^2rf^{(0)}\int(\varphi'-\varphi)\cos\vartheta d\Omega. \tag{3}$$

(b) *Conditions imposed on* φ. Eq. (3) is in an inhomogeneous integral equation of the second kind with a symmetric kernel. Because the homogeneous equation has a solution (namely φ_1 = const.), the necessary condition that the inhomogeneous equation has a solution is that the left member of the equation is orthogonal to φ_1. This condition is identically fulfilled. To make the solution of (3) perfectly definite, one may impose on φ the auxiliary condition:

$$\int\varphi d\Omega=0. \tag{4}$$

One finds that this implies:

$$\int f^{(0)}\varphi dr_x dr_y dr_z=\int r^2 f^{(0)}\varphi dr_x dr_y dr_z=0,$$

which means physically, that the density and temperature are determined by the mean values formed with the equilibrium distribution function just as in the equilibrium state.

(c) *Reduction of the left member.* Introducing

$$f^{(0)}=A(x)e^{-h(x)r^2}$$

where $h(x)=m/2kT(x)$, one obtains for the left member:

$$r_x(d\ln A/dx-r^2dh/dx-2hX)Ae^{-hr^2}. \tag{5}$$

(d) *"Ansatz" for* φ *and its verification.* The form of the left member suggests the solution:

$$\varphi=r_x\chi(r),$$

which fulfills condition (4). Introducing this expression into the right member of (3), one finds upon integration that the latter becomes proportional to r_x, giving the final result:

$$\chi(r)=\frac{1}{\pi nR^2}\left(r^2\frac{dh}{dx}-\frac{d\ln A}{dx}+2hX\right)\frac{1}{r},$$

from which all further conclusions regarding the heat and electric conductivity follow.[3]

This description is intended to show only the analogy between the method of the Lorentz theory of metals and the generalized Enskog theory of gases. Points (a) to (d) of the Lorentz theory given in §2 correspond to points §5 to §8 in the theory of gases generalized to include the quantum statistics which is to follow. A *strict* analogy does not exist. One would have to consider in the Lorentz theory also nonstationary states, and extend the theory of gases to include also mixtures in order to see the former as a special case of the latter.

The General Hydrodynamical Equations

§3

For Einstein-Bose and Fermi-Dirac gases in a nonsteady state, one may write the general Boltzmann equation in the form:

$$\frac{\partial f}{\partial t}+D(f)=\int d\phi_1\int gw(\vartheta g)d\Omega\{f'f_1'(1+\theta f)(1+\theta f_1)-ff_1(1+\theta f')(1+\theta f_1')\}, \tag{6}$$

[3] A well-known defect of the Lorentz theory is that it gives no account of the Joulian heat, since only elastic collisions between the electrons and immovable ions are considered. This is probably the reason, also, for the following difficulty. If one attempts to find the next approximation to the distribution function, one obtains an integral equation of the same type as (3). But now the left member is *not* orthogonal to the solution of the homo-

where

$$D(f)=v_\alpha(\partial f/\partial x_\alpha)+X_\alpha(\partial f/\partial v_\alpha). \quad (7)$$

In these expressions $v_i(v_xv_yv_z)$ are the three components of the absolute velocity, $X_i(XYZ)$ are the three components of the external force per unit mass, and the usual summation convention has been used.[4] The function $w(\vartheta g)d\Omega$ represents the effective cross section for a collision which changes the direction of the relative velocity g of two molecules by the angle ϑ, such that this velocity after collision g' lies within an element of solid angle $d\Omega=\sin\vartheta d\vartheta d\varphi$, where φ is the azimuthal angle about g. The subscript 1 denotes functions and variables pertaining to the second molecule in the collision, over which the integration takes place, and the primes denote functions and variables which are to be taken after the collision. The differential $d\phi$ has the usual interpretation:

$$d\phi=VG(m/h)^3dv_xdv_ydv_z, \quad (8)$$

where G is an eventual weight-factor, and V is included for dimensional reasons, but is to be considered as having the value unity to agree with the meaning of f as giving the number of particles per phase cell in coordinate-momenta space of which the space part has unit volume.

Eq. (6) includes (namely for $\theta=0$) the Boltzmann equation of the classical statistics[5] as a special case. It differs from the latter in the Einstein-Bose statistics ($\theta=+1$) and in the Fermi-Dirac statistics ($\theta=-1$) only in the "collision" term of the right member. The essential points of difference in this term are: (1) the use of the appropriate "Stoszzahlansatz," and (2) the necessity of determining the transition probability function, $w(\vartheta g)$, quantum-mechanically, and of taking into account the identity of the molecules in this determination, as was first done by N. F. Mott in his theory of collisions between two electrons.[6] That the "streaming" terms of the left member need not be changed in the quantum theory, has been proved in general by Nordheim and Kikuchi.[7] As usual, the principle of microscopic reversibility has been used in the derivation of the collision term in Eq. (6).

Just as in the classical case[8] one can derive from Eq. (6) a general transport equation for a function $F(xyzv_xv_yv_zt)$. Specializing F to be successively m, mv_x, mv_y, mv_z, and $\frac{1}{2}mv^2$, one obtains the *general hydrodynamical equations:*

$$\left.\begin{aligned} &d\rho/dt+\rho(\partial u_\alpha/\partial x_\alpha)=0, && \text{a}\\ &\rho(du_i/dt)=\rho X_i-\partial p_{i\alpha}/\partial x_\alpha, && \text{b}\\ &\rho\frac{d(Q/\rho)}{dt}+\frac{\partial q_\alpha}{\partial x_\alpha}=-p_{\alpha\beta}S_{\alpha\beta}, && \text{c}\end{aligned}\right\} \quad (9)$$

where $u_i(uvw)$ and $q_i(q_xq_yq_z)$ are the components of the mass-velocity and heat current, respectively:

$$\text{(a) } u_i=\bar{v}_i, \quad \text{(b) } q_i=\tfrac{1}{2}\rho\overline{U_iU^2} \quad (10)$$

and where, furthermore

$$U_i=v_i-u_i; \quad U^2=U_x^2+U_y^2+U_z^2 \quad (11)$$

denotes the relative velocity. The functions p_{ij} and S_{ij} are the components of the stress and the rate of pure strain tensors, respectively:

$$\text{(a) } p_{ij}=\rho\overline{U_iU_j}, \quad \text{(b) } S_{ij}=\tfrac{1}{2}\left(\frac{\partial u_i}{\partial x_j}+\frac{\partial u_j}{\partial x_i}\right). \quad (12)$$

Finally, Q denotes the energy of heat motion per unit volume:

$$Q=\tfrac{1}{2}\rho U^2=\tfrac{1}{2}(p_{xx}+p_{yy}+p_{zz})=3p/2 \quad (13)$$

and d/dt denotes the total time derivative:

$$d/dt=\partial/\partial t+u_\alpha(\partial/\partial x_\alpha). \quad (14)$$

§4

One obtains the hydrodynamical equations in *first approximation* by calculating the ten mean value quantities, (10b), (12a) and (13) with the aid of the equilibrium distribution function $f^{(0)}$. Since the latter depends only on U^2, one obtains[9]:

$$p_{ij}=p\delta_{ij}, \quad q_i=0,$$

geneous equation as a consequence of which the inhomogeneous equation has *no* solution. In the theory of gases one does *not* encounter an analogous difficulty.

[4] Greek letters are used for dummy indices.

[5] Compare e.g., Jeans, *Dynamical Theory of Gases*, p. 210.

[6] Proc. Roy. Soc. **A126**, 259–267 (1930).

[7] Nordheim and Kikuchi, Zeits. f. Physik **60**, 652 (1930).

[8] Compare Enskog, reference 1, pp. 14–19; Jeans, reference 1, Chapter IX.

[9] The equation: $Q=3p/2$ or $pv=2\epsilon/3$, where ϵ is the energy per unit mass, and v is the specific volume, follows, also, from an application of the general virial theorem to an ideal gas. It is, itself, often called the virial theorem.

whereupon (9) reduces to:

$$\left.\begin{aligned} &d\rho/dt+\rho(\partial u_\alpha/\partial x_\alpha)=0, && \text{a}\\ &\rho(du_i/dt)=\rho X_i-(\partial p/\partial x_i), && \text{b}\\ &\frac{d}{dt}\left(\frac{p}{\rho}\right)=-\frac{2}{3}\frac{p}{\rho}\frac{\partial u_\alpha}{\partial x_\alpha}. && \text{c}\end{aligned}\right\} \quad (15)$$

The energy equation (15c) can be put into another form by introducing the equation of state:

$$p/\rho=(RT/M)W(T\rho^{-\frac{2}{3}}), \quad (16)$$

which holds in all statistics. M denotes the molecular weight, ρ is the density, and W is a function of the argument $T\rho^{-\frac{2}{3}}$ which is a different function for the different statistics, but is in each case an *adiabatic invariant.*[10] The latter property makes it possible to remove W from the differential operator d/dt when (16) is introduced into (15c). Thus the energy equation becomes:

$$dT/dt=-\tfrac{2}{3}T(\partial u_\alpha/\partial x_\alpha). \quad (15c')$$

In Note 1 it will be shown that an expression for the velocity of sound in first approximation, that is, neglecting viscosity and heat conductivity, follows immediately from (15).

The Nonsteady State Distribution Function

§5. The principle of solution of the Boltzmann equation

In order to proceed with the theory of gases, one needs to know the deviation of the actual distribution function from the equilibrium state. For this determination one must obtain a solution of Eq. (6). As in the Lorentz theory outlined in §2, one assumes a solution of the form:

$$f=f^{(0)}(1+\varphi), \quad (17)$$

which, upon introduction into Eq. (6) and simplification with the aid of the principle of detailed balancing,[11] yields the inhomogeneous integral equation:

$$\partial f^{(0)}/\partial t+D(f^{(0)})=-I(\chi) \quad (18)$$

where

$$\chi=\varphi/(1+\theta f^{(0)}) \quad (19)$$

$$I(\chi)=\int d\phi_1\int gw(\vartheta g)d\Omega\cdot f^{(0)}f_1^{(0)}(1+\theta f^{(0)\prime})(1+\theta f_1^{(0)\prime})(\chi+\chi_1-\chi'-\chi_1'). \quad (20)$$

One can show that Eq. (18) has the following properties: (a) It is reducible to the form of an inhomogeneous integral equation of the second kind[12]; (b) the kernel of this equation is symmetric; (c) the kernel is invariant with respect to rotations in U_i-space. Furthermore, the operator I has certain properties, which will be required later. Using the notation:

$$[F, G]=\int FI(G)d\phi,$$

one finds by the same reasoning as is used in deriving the H-theorem:

$$[F, G]=\tfrac{1}{4}\int d\phi\int d\phi_1\int gw(\vartheta g)d\Omega\cdot f^{(0)}f_1^{(0)}(1+\theta f^{(0)\prime})(1+\theta f_1^{(0)\prime})\cdot(F+F_1-F'-F_1')(G+G_1-G'-G_1'), \quad (21)$$

from which follows:

$$\left.\begin{aligned} &[F, G]=[G, F], && \text{a}\\ &[F, G+H]=[F, G]+[F, H], && \text{b}\\ &[F, bG]=b[F, G], && \text{c}\\ &[F, F]\geqq 0, && \text{d}\end{aligned}\right\} \quad (22)$$

where b is a function independent of all variables of integration.

[10] Uhlenbeck and Uehling, Phys. Rev. **39**, 1014 (1932).

[11] This principle follows, as is well known, from the previously assumed principle of microscopic reversibility and a generalized H-theorem. Comp. Nordheim, Proc. Roy. Soc. **A119**, 689 (1928); Pauli, Sommerfeld Festschrift, p. 30.

[12] This reduction is accomplished by a series of transformations of variables, in a manner analogous to that used by Enskog in the classical case (Reference 1, pp. 140–148).

§6. Conditions imposed on φ

Consider the homogeneous equation following from (18):

$$I(\psi)=0. \tag{18a}$$

Multiplying with $\psi d\phi$ and integrating, one obtains: $[\psi, \psi]=0$. From the properties of this operator this equality exists only if:

$$\psi+\psi_1-\psi'-\psi_1'=0. \tag{23}$$

Eq. (23), according to the number, momentum and energy conservation theorems, has as its solution a linear combination of the functions[13]:

$$\psi_1=1;\ \psi_2=r_x;\ \psi_3,=r_y;\ \psi_4,=r_z;\ \psi_5,=r^2. \tag{24}$$

In order, therefore, that the inhomogeneous Eq. (18) may have a solution, the left member must be orthogonal to the five functions (24). As consequences of this orthogonality one finds that the five parameters ρ, T, u, v and w on which the equilibrium distribution function $f^{(0)}$ depends, must, for the purpose of solution of Eq. (18), be functions of x, y, z and t which fulfill the hydrodynamical equations in *first* approximation (15).[14] To make the solution of Eq. (18) definite one may impose on φ or χ the five conditions:

$$\int \psi_i f^{(0)}\varphi d\phi=\int \psi_i f^{(0)}(1+\theta f^{(0)})\chi d\phi=0, \qquad (i=1, 2, \cdots 5) \tag{25}$$

which interpreted physically express the fact that the parameters ρ, T, u, v and w of the equilibrium distribution function may be interpreted physically as the density, temperature, and the three components of mass velocity, respectively, just as in the equilibrium state. One can show, in a manner analogous to that used by Enskog in the classical case (reference 1, p. 27–31), that if one has determined the arbitrary constants in the general solution of Eq. (18) such that the conditions (25) are fulfilled, at the time $t=0$, they will remain fulfilled for all values of the time.

§7. Introduction of new variables and reduction of the left member

One may introduce the equilibrium distribution function:

$$f^{(0)}=\frac{1}{(1/A)\exp{(m/2kT)U^2-\theta}} \tag{26}$$

into the left member of Eq. (18). The five parameters, ρ, T, u, v and w on which this function depends are defined by the equations:

$$\left.\begin{aligned}
\rho&=m\int f^{(0)}d\phi,\\
u_i&=\frac{1}{\rho}\int m r_i f^{(0)}d\phi,\\
\epsilon&=\frac{3}{2}\frac{p}{\rho}=\frac{3}{2}\frac{RT}{M}W(T\rho^{-\frac{2}{3}})\\
&=\frac{1}{\rho}\int\frac{1}{2}m U^2 f^{(0)}d\phi.
\end{aligned}\right\} \tag{27}$$

Transforming, also, to dimensionless variables $\xi_i(\xi\eta\zeta)$ where $\xi_i=(r_i-u_i)c^{\frac{1}{2}}$; $\tau^2=\xi^2+\eta^2+\zeta^2$ and $c=m/2kT$, Eq. (18) becomes:

$$\frac{f^{(0)2}}{Ae^{-\tau^2}}\left[\frac{d\ln A}{dt}+\frac{\tau^2}{T}\frac{dT}{dt}+\frac{1}{c^{\frac{1}{2}}}\xi_\alpha\left\{\frac{\partial\ln A}{\partial x_\alpha}-2c\left(X_\alpha-\frac{\partial u_\alpha}{\partial t}\right)+\frac{\tau^2}{T}\frac{\partial T}{\partial x_\alpha}\right\}+2\xi_\alpha\xi_\beta\frac{\partial u_\alpha}{\partial x_\beta}\right]=-I(\chi). \tag{28}$$

Now one may prove, as is done in Note 3, that in all statistics and for all degrees of degeneration the following relations exist:

$$\left.\begin{aligned}
&\frac{d\ln A}{dt}=\frac{dW}{dt}+W\left(\frac{1}{\rho}\frac{d\rho}{dt}-\frac{3}{2}\frac{1}{T}\frac{dT}{dt}\right) && \text{a}\\
&\frac{\partial\ln A}{\partial x_i}=\frac{p}{nkT}\left(\frac{1}{p}\frac{\partial p}{\partial x_i}-\frac{5}{2}\frac{1}{T}\frac{\partial T}{\partial x_i}\right). && \text{b}
\end{aligned}\right\} \tag{29}$$

Since W is adiabatically invariant, and since it has been proved that a solution of Eq. (18) exists only if ρ and T fulfill the hydrodynamical equations (15a) and (15c′) in first approximation, one finds that $d\ln A/dt$ vanishes. Furthermore, one obtains from (15b) and (29b) the result:

[13] That (24) are the only solutions of (23), one can prove strictly for spherically symmetric molecules (compare Jeans, Reference 1, p. 25), to which this theory is restricted.

[14] See Note 2 for the proof of this result.

$$\frac{\partial \ln A}{\partial x_i} - 2c\left(X_i - \frac{du_i}{dt}\right) = -\frac{5}{2}\frac{p}{nkT}\frac{1}{T}\frac{\partial T}{\partial x_i}.$$

Introducing also the value of dT/dt from (15c′) the equation

$$\frac{f^{(0)2}}{Ae^{-\tau^2}}\left\{\frac{1}{c^{\frac{1}{2}}}\frac{1}{T}\xi_\alpha\frac{\partial T}{\partial x_\alpha}\left(\tau^2-\frac{5}{2}\frac{p}{nkT}\right)+\left(\xi_\alpha\xi_\beta-\frac{\tau^2}{3}\delta_{\alpha\beta}\right)\left(\frac{\partial u_\alpha}{\partial x_\beta}+\frac{\partial u_\beta}{\partial x_\alpha}\right)\right\} = -I(\chi) \tag{30}$$

is obtained.[15]

Dimensionless variables and functions will be introduced, also, into the operator $I(\chi)$. One may decompose the transition probability function in the following arbitrary manner

$$w(\vartheta\gamma) = \tfrac{1}{4}s^2\cdot\sigma(\gamma)\cdot u(\vartheta\gamma),$$

where

$$g = \gamma(2/c)^{\frac{1}{2}},$$

s is a constant having the dimensions of a length and in the case of spherical molecules being the actual collision radius, $\sigma(\gamma)$, is a dimensionless function, and $u(\vartheta\gamma)$ is a dimensionless probability function representing the scattering into an element of solid angle per unit angle divided by the average scattering per unit solid angle. In the case of a classical collision between two spherical molecules the functions σ and u are simply unity. In the case of a classical collision between molecules repelling inversely as the νth power of the distance, where $\nu > 1$, u is independent of γ, and σ depends on γ and on the temperature T. Finally introducing the variables ξ_i, the differential becomes

$$d\phi_1 = VG(m/h)^3c^{-\frac{1}{2}}dw_1; \quad dw_1 = d\xi_1 d\eta_1 d\zeta_1.$$

In these variables and functions

$$I(\chi) = (2^{\frac{1}{2}}s^2A^2VG/c^2)(m/h)^3I'(\chi), \tag{31}$$

where

$$I'(\chi) = \frac{1}{4A^2}\int dw_1\int d\Omega\cdot\gamma\sigma^2(\gamma)u(\vartheta\gamma)\,(\chi+\chi_1-\chi'-\chi_1')\cdot f^{(0)}f_1{}^{(0)}(1+\theta f^{(0)\prime})(1+\theta f_1{}^{(0)\prime}). \tag{32}$$

One finds that the bracket expression $[F, G]$ defined with the operator I' has the same properties (22) as the expression defined with the operator I.

§8. The "Ansatz" for χ and its verification

Since it is linear, and the integration in $I'(\chi)$ is over only the velocity components ξ_i, Eq. (30) may be decomposed by choosing for the solution:

$$\chi = -\frac{c^{\frac{1}{2}}}{2^{\frac{1}{2}}s^2AVG}\left(\frac{h}{m}\right)^3\frac{1}{T}\frac{\partial T}{\partial x_\alpha}\pi_\alpha - \frac{c^2}{2^{\frac{1}{2}}s^2AVG}\left(\frac{h}{m}\right)^3\left(\frac{\partial u_\alpha}{\partial x_\beta}+\frac{\partial u_\beta}{\partial x_\alpha}\right)\pi_{\alpha\beta}, \tag{33}$$

where π_i and $\pi_{ij} = \pi_{ji}$ are nine new unknown functions, which fulfill respectively the nine integral equations:

$$\left.\begin{aligned}\frac{f^{(0)2}}{A^2e^{-\tau^2}}\xi_i\left(\tau^2-\frac{5}{2}\frac{p}{nkT}\right) &= I'(\pi_i), \quad \text{a}\\ \frac{f^{(0)2}}{A^2e^{-\tau^2}}\left(\xi_i\xi_j-\frac{\tau^2}{3}\delta_{ij}\right) &= I'(\pi_{ij}). \quad \text{b}\end{aligned}\right\} \tag{34}$$

In a manner analogous to the Lorentz theory (see d in §2), one can show that π_i and π_{ij} have the forms:

$$\left.\begin{aligned}\pi_i &= \xi_i\chi_a(\tau), \quad \text{a}\\ \pi_{ij} &= (\xi_i\xi_j - \tau^2\delta_{ij}/3)\chi_b(\tau). \quad \text{b}\end{aligned}\right\} \tag{35}$$

The problem is reduced in this way to the determination of the two unknown functions $\chi_a(\tau)$ and $\chi_b(\tau)$, The procedure differs, however, from that in the Lorentz theory in that it is not possible in this case to obtain closed expressions for these functions. They may be obtained only by a method of successive approximations after definite assumptions regarding the nature of the

[15] In the classical case, $p = nkT$ and $f^{(0)} = Ae^{-\tau^2}$; the left member of this equation then agrees completely with the result of Enskog. (Reference 1, Eq. 53.)

molecular interactions have been introduced; i.e., after the functions $\sigma(\gamma)$ and $u(\vartheta\gamma)$ have been specified.

One can prove that the functions π_i and π_{ij} have the forms given by (35) as follows. One verifies that the left members of both (34a and b) are orthogonal to the five functions ψ_i of (24), and, therefore, orthogonal as well to the functions

$$\psi_1=1;\ \psi_2=\xi;\ \psi_3=\eta;\ \psi_4=\zeta;\ \psi_5=\tau^2, \quad (24a)$$

which as before represent the solutions of the homogeneous equation. The forms of π_i and π_{ij} may be made definite by imposing on both the five conditions:

$$\int \psi_j f^{(0)}(1+\theta f^{(0)})\pi dw=0 \quad (36)$$

as consequences of which χ will fulfill conditions (25). As further consequences of conditions (36) Eqs. (34a and b) each have one and only one solution. Finally, one uses the fact that Eqs. (34a and b) have properties analogous to those of Eq. (18) discussed in §5; namely: (a) they are linear integral equations of the second kind, (b) the kernel is symmetric, (c) the kernel is *invariant with respect to rotations in ξ_i-space.* In fact, one can show that:

$$I'(\pi)=k(\tau)\pi(\xi_i)+\int dw'\pi(\xi_i')K(\tau\tau'\epsilon), \quad (37)$$

where ϵ is the angle between the two vectors ξ_i and ξ_i', which have the magnitude τ and τ'. This is the essential point in the proof. One may proceed now in different ways. The most simple method perhaps is verification. This is accomplished when one has proved that integrals of the type:

$$\int dw'\xi_i' f(\tau\tau'\epsilon)=\xi_i F(\tau) \quad (38a)$$

and of the type:

$$\int dw'\left(\xi_i'\xi_j'-\frac{\tau'^2}{3}\delta_{ij}\right)f(\tau\tau'\epsilon) = \left(\xi_i\xi_j-\frac{\tau^2}{3}\delta_{ij}\right)G(\tau). \quad (38b)$$

The proof of these results can be given geometrically (see Note 4).[16]

The auxiliary conditions (36) are fulfilled by (35b) identically, and by (35a) when $\chi_a(\tau)$ fulfills:

$$\int \tau^4 f^{(0)}(1+\theta f^{(0)})\chi_a(\tau)d\tau=0. \quad (39)$$

It is always possible to satisfy this condition by adding to $\chi_a(\tau)$ a suitable constant.

§9. The distribution function

In terms of the unknown functions $\chi_a(\tau)$ and $\chi_b(\tau)$ the nonsteady state distribution function may be written with the aid of Eqs. (17), (19), (33), (35a and b) in the following manner:

$$f=f^{(0)}\left[1-\frac{c^{\frac{1}{2}}f^{(0)}e^{\tau^2}}{2^{\frac{1}{2}}s^2A^2VG}\left(\frac{h}{m}\right)^3\frac{1}{T}\frac{\partial T}{\partial x_\alpha}\xi_\alpha\chi_a(\tau)-\frac{c^2f^{(0)}e^{\tau^2}}{2^{\frac{1}{2}}s^2A^2VG}\left(\frac{h}{m}\right)^3\left(\frac{\partial u_\alpha}{\partial x_\beta}+\frac{\partial u_\beta}{\partial x_\alpha}\right)\left(\xi_\alpha\xi_\beta-\frac{\tau^2}{3}\delta_{\alpha\beta}\right)\chi_b(\tau)\right]. \quad (40)$$

This expression reduces to that of Enskog[17] for the Maxwell-Boltzmann statistics in which: (1) the equilibrium distribution function is $f^{(0)}=Ae^{-\tau^2}$; (2) $\chi_a(\tau)$ and $\chi_b(\tau)$ are determined by Eqs. (34a and b) with $p=nkT$, $\theta=0$, and classical values of $\sigma(\gamma)$ and $u(\varphi\gamma)$; (3) account is taken of the weight factor by which the A of Enskog's equations differs from the A used here.

Formal Expressions for the Viscosity and Heat Conductivity Coefficients

§10. The heat conductivity coefficient

In order to obtain this coefficient it will be necessary to derive one of the components of the heat current. By using the definition (10b), the expression (40) for the distribution function, and transforming to dimensionless variables, one obtains

[16] A second method is by means of the resolvent of (37). One can show that the resolvent as well as the kernel is a function only of τ, τ' and ϵ. Writing down the formal solutions of (34a and b) and using (38) one finds again that the solutions must have the form (35).

[17] Enskog, Reference 1, Eq. (65), p. 41.

$$q_x = -\lambda(\partial T/\partial x), \tag{41}$$

where:

$$\lambda = \frac{m}{(2c)^{\frac{1}{2}}s^2A^2}\frac{1}{T}\int f^{(0)2}e^{\tau^2}\xi^2\tau^2\chi_a(\tau)dw. \tag{42}$$

For the purpose of the numerical calculation of this coefficient, one may transform this expression; first, by adding a term which is identically zero by virtue of the auxiliary conditions on $\chi_a(\tau)$, giving

$$\lambda = \frac{m}{(2c)^{\frac{1}{2}}s^2A^2}\frac{1}{T}\int f^{(0)2}e^{\tau^2}\xi\left(\tau^2 - \frac{5}{2}\frac{p}{nkT}\right)\xi\chi_a(\tau)dw$$

and then, by introducing a simplification obtained when one substitutes for a part of the integrand its value given by the integral Eq. (34a) in $\chi_a(\tau)$. Thus, one arrives at the final result:

$$\lambda = \frac{m}{(2c)^{\frac{1}{2}}s^2}\frac{1}{T}[\xi\chi_a(\tau), \xi\chi_a(\tau)]. \tag{43}$$

That λ is always positive follows from the property (22d) of the bracket expressions.

§11. The viscosity coefficient

In order to obtain this coefficient, one may determine either p_{xy} or the deviation of p_{xx} from p. Using the definitions (12a) and (13), introducing the distribution function (40), and transforming to dimensionless variables, one obtains in the latter case:

$$p_{xx} - p = -\frac{2\mu}{3}\left(2\frac{\partial u}{\partial x} - \frac{\partial v}{\partial y} - \frac{\partial w}{\partial z}\right), \tag{44}$$

where:

$$\mu = \frac{3m}{2^{\frac{1}{2}}c^{\frac{1}{2}}s^2A^2}\int f^{(0)2}e^{\tau^2}\left(\xi^2 - \frac{\tau^2}{3}\right)\left(\xi^2 - \frac{\tau^2}{3}\right)\chi_b(\tau)dw. \tag{45}$$

By using the integral Eq. (34b) for χ_b, this can be written:

$$\mu = \frac{2m}{2^{\frac{1}{2}}c^{\frac{1}{2}}s^2}\left[\left(\xi^2 - \frac{\tau^2}{3}\right)\chi_b(\tau), \left(\xi^2 - \frac{\tau^2}{3}\right)\chi_b(\tau)\right], \tag{46}$$

from which one finds, as in the case of the heat conductivity coefficient, that the viscosity coefficient is always positive.

In the other case one obtains in the same manner:

$$p_{xy} = -\mu\left(\frac{\partial v}{\partial x} + \frac{\partial u}{\partial y}\right), \tag{47}$$

where:

$$\mu = \frac{2m}{(2c)^{\frac{1}{2}}s^2A^2}\int f^{(0)2}e^{\tau^2}\xi^2\eta^2\chi_b(\tau)dw$$

$$= \frac{2m}{(2c)^{\frac{1}{2}}s^2}[\xi\eta\chi_b(\tau), \xi\eta\chi_b(\tau)]. \tag{48}$$

A partial integration of these expressions shows that (46) and (48) are identical.

§12. The hydrodynamical equations in second approximation

The preceding derivation shows that the stress tensor components have the same form in the quantum as in the classical statistics. Eqs. (44) and (47) for these components may be combined in the form:

$$p_{ij} = [p + (2\mu/3)(\partial u_a/\partial x_a)]\delta_{ij} - 2\mu S_{ij}. \tag{49}$$

Introducing these expressions and Eq. (41) for the heat current components into the general hydrodynamical Eq. (9). one obtains the hydrodynamical equations with viscosity and heat conduction:

$$\left.\begin{aligned}
&d\rho/dt + \rho(\partial u_a/\partial x_a) = 0, && \text{a}\\
&\rho\frac{du_i}{dt} = \rho X_i - \frac{\partial p}{\partial x_i} + \frac{1}{3}\frac{\partial^2 u_a}{\partial x_i \partial x_a} + \mu\frac{\partial^2 u_i}{\partial x_a \partial x_a} - \frac{2}{3}\frac{\partial u_a}{\partial x_a}\frac{\partial \mu}{\partial x_i} + 2S_{ia}\frac{\partial \mu}{\partial x_a}, && \text{b}\\
&\frac{3}{2}\rho\frac{d(p/\rho)}{dt} - \frac{\partial}{\partial x_a}\left(\lambda\frac{\partial T}{\partial x_a}\right) = -pS_{aa} + 2\mu(S_{a\beta}S_{a\beta} - \tfrac{1}{3}S_{aa}^2). && \text{c}
\end{aligned}\right\} \tag{50}$$

Ordinarily μ may be considered as a constant, since the variations in T and ρ, on which μ depends,[18] are generally small. When this is the case, the last two terms of Eq. (50b) vanish, and this equation then takes the usual form.[19] Introducing $Q=3p/2$ into the energy Eq. (50c), one finds that it gives the rate of increase of heat energy per unit volume due to: (a) conduction of heat from adjacent elements, (b) the work done per unit of time by the internal (scalar) pressure, and (c) the work done in the distortion of the volume element.

§13. Conclusion

The formal part of the theory is now completed. To proceed further, and thus obtain explicit expressions for the viscosity and heat conductivity coefficients as functions of the temperature and density, one must introduce special assumptions regarding the molecular forces. With the introduction of these assumptions, the transition probability function $w(\vartheta\gamma)$ may be determined from the quantum-mechanical collision theory, whereupon the functions $\sigma(\gamma)$ and $u(\vartheta\gamma)$ of the integral equations are completely specified. The integral Eqs. (34) may be solved then numerically. Enskog has developed a method of solution in the classical case which may be extended, also, to the quantum statistics. These questions will be considered in a following paper.

Note 1

In order to derive the equation for the velocity of sound from (15), one assumes that the conditions are such that the velocity components and the deviation of the density ρ from its equilibrium value are small quantities of the first order, and that no outside forces exist. Then the density may be written in terms of a condensation factor s: $\rho=\rho_0(1+s)$, where ρ_0 is its equilibrium value. Retaining only quantities of the first order (15a and b) become:

$$\partial s/\partial t=-\partial u_\alpha/\partial x_\alpha, \tag{51}$$

$$\rho_0(\partial u_i/\partial t)=-\partial p/\partial x_i \cong -K(\partial s/\partial x_i), \tag{52}$$

where K is the coefficient of volume elasticity $\rho(dp/d\rho)$. Eliminating u_i or s, one obtains the wave equation for s or u_i with the velocity:

$$C^2=K/\rho_0=(dp/d\rho)_{\rho=\rho_0}. \tag{53}$$

Now assuming that the frequency is sufficiently high so that one may neglect heat conduction, this differential quotient may be taken under strictly adiabatic conditions. The first order energy equation gives such a determination of this expression. Under the conditions assumed it becomes:

$$\left(\frac{p}{\rho}\right)_0\frac{\partial u_\alpha}{\partial x_\alpha}=-\frac{3}{2}\frac{\partial}{\partial t}\left(\frac{p}{\rho}\right). \tag{54}$$

Now using Eq. (51), integrating, and solving for p, one obtains:

$$p=\tfrac{1}{3}(p/\rho)_0\rho(1+2\rho/\rho_0), \tag{55}$$

from which follows:

$$C^2=(dp/d\rho)_{\rho=\rho_0}=(5/3)p_0/\rho_0 \tag{56}$$

in accordance with the thermodynamic calculation of $(dp/d\rho)_{\text{adiab.}}$.[20]

Note 2

From the theory of integral equations the conditions:

$$\int\psi_i[\partial f^{(0)}/\partial t+\mathcal{D}(f^{(0)})]d\phi=0 \qquad (i=1, 2, \cdots 5) \tag{57}$$

must exist in order that the inhomogeneous Eq. (18) may have a solution. This follows, also, upon multiplying both sides of (18) by $\psi_i d\phi$ and integrating. The right member then becomes $[\psi_i, \chi]$ which is zero according to (21) and (23).

In Eq. (57) $f^{(0)}$ represents the equilibrium distribution function in the six-dimensional phase space (x_i, r_i). Since it is a function only of the relative velocities, $U_i=r_i-u_i$, it is convenient to change to axes which move with the volume-element of the gas. The differential quotients then become:

$$\frac{\partial f^{(0)}}{\partial t}=\frac{\partial' f^{(0)}}{\partial t}-\frac{\partial u_\alpha}{\partial t}\frac{\partial' f^{(0)}}{\partial U_\alpha},$$

$$\frac{\partial f^{(0)}}{\partial x_i}=\frac{\partial' f^{(0)}}{\partial x_i}-\frac{\partial u_\alpha}{\partial x_i}\frac{\partial' f^{(0)}}{\partial U_\alpha},$$

$$\frac{\partial f^{(0)}}{\partial r_i}=\frac{\partial' f^{(0)}}{\partial U_i},$$

and Eq. (57) may be written, omitting the primes:

$$\int\psi_i\left[\frac{df^{(0)}}{dt}-\frac{\partial f^{(0)}}{\partial U_\alpha}\frac{du_\alpha}{dt}+U_\alpha\frac{\partial f^{(0)}}{\partial x_\alpha}-U_\beta\frac{\partial f^{(0)}}{\partial U_\alpha}\frac{\partial u_\alpha}{\partial x_\beta}+X_\alpha\frac{\partial f^{(0)}}{\partial U_\alpha}\right]d\phi=0 \qquad (i=1, 2, \cdots 5). \tag{58}$$

If these conditions are valid for the five ψ_i of (24), they must be valid, also, for ψ_i equal to m, mU_x, mU_y, mU_z, and mU^2. Substituting these values successively into this equation, and using (27), one obtains the first order hydrodynamical Eqs. (15).

[18] Only in the classical case is μ independent of ρ.

[19] See Lamb, *Hydrodynamics*, Fifth Edition, p. 546.

[20] Compare Uhlenbeck and Uehling, Phys. Rev. **39**, 1014 (1932).

NOTE 3

From the definitions (27) one obtains

$$\left.\begin{aligned} n &= \rho/m = VG(2\pi mkT/h^2)^{\frac{3}{2}}F_{\frac{1}{2}}, && \text{a} \\ p &= \tfrac{2}{3}Q = \tfrac{2}{3}\epsilon\rho = VGkT(2\pi mkT/h^2)^{\frac{3}{2}}F_{\frac{3}{2}}, && \text{b} \end{aligned}\right\} \quad (59)$$

where F_s is the Sommerfeld integral:

$$F_s(A) = \frac{1}{\Gamma(s+1)}\int_0^\infty f^{(0)}(z)z^s dz = \frac{1}{\Gamma(s+1)}\int_0^\infty \frac{z^s dz}{(1/A)e^z - \theta}$$

$$z = \tau^2 = (m/2kT)U^2.$$

The result:

$$p/nkT = F_{\frac{3}{2}}/F_{\frac{1}{2}} \quad (60)$$

follows as an immediate consequence of these equations. Also, from the definition of F_s, one obtains the relation:

$$A(dF_s/dA) = F_{s-1}. \quad (61)$$

Considering p and T as functions of the time and the coordinates, one obtains from (59b) the equation

$$\frac{dF_{\frac{3}{2}}}{dt} = F_{\frac{3}{2}}\left(\frac{1}{p}\frac{dp}{dt} - \frac{5}{2}\frac{1}{T}\frac{dT}{dt}\right).$$

On the other hand, Eq. (61) gives:

$$\frac{dF_{\frac{3}{2}}}{dt} = A\frac{d\ln A}{dt}\cdot\frac{dF_{\frac{3}{2}}}{dA} = F_{\frac{1}{2}}\frac{d\ln A}{dt}.$$

Combining these results and using the equation of state (16), one obtains Eq. (29a). In a similar manner one obtains Eq. (29b).

NOTE 4

Interpret $f(\tau\tau'\epsilon)$ as a density distribution in the ξ_i'-space. (See Fig. 1.) This function will have rotational symmetry around the axis OP, the direction of τ, and it will depend only on this direction and not on the special choice of the coordinate axes ξ_i'. To prove (38a) we remark that the left member represents the coordinates of the center of gravity, which, because of the rotational symmetry, must lie on the line OP. Therefore these coordinates, and accordingly the left member of (38a) must be proportional to ξ_i. Since $f(\tau\tau'\epsilon)$ is invariant with respect to rotations of the ξ_i' axis, the proportionality factor must be a function only of τ.

In order to prove (38b) one may consider the integral

$$\int dw'\xi_i'\xi_j' f(\tau\tau'\epsilon) = A_{ij}$$

as representing the moments and products of inertia of the density function $f(\tau\tau'\epsilon)$ in the ξ_i'-space. Because of rotational symmetry, the ellipsoid of inertia is a rotational ellipsoid about the axis OP. Taking O as the center of this ellipsoid, and p and q as the lengths of the main axes, one may write for its equation

$$OR^2/p^2 + RQ^2/q^2 = 1.$$

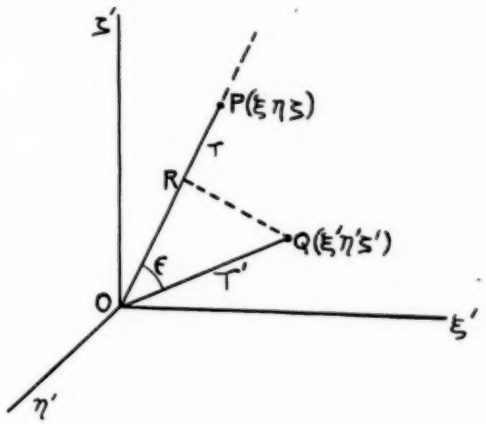

FIG. 1.

Designating the direction cosines of OP by $\lambda_i(\lambda_1\lambda_2\lambda_3)$ one obtains $OR = \lambda_\alpha\xi_\alpha'$, whereupon the equation of the ellipsoid becomes, since $RQ^2 = OQ^2 - OR^2$

$$\left(\lambda_\alpha\lambda_\beta + \frac{p^2}{q^2-p^2}\delta_{\alpha\beta}\right)\xi_\alpha'\xi_\beta' = \frac{p^2q^2}{q^2-p^2}.$$

But the equation of the inertial ellipsoid is also

$$A_{\alpha\beta}\xi_\alpha'\xi_\beta' = \text{const.}$$

Therefore

$$\int dw'\xi_i'\xi_j' f(\tau\tau'\epsilon) \sim \lambda_i\lambda_j + \frac{p^2}{q^2-p^2}\delta_{ij}$$

$$\sim \xi_i\xi_j + \frac{p^2}{q^2-p^2}\tau^2\delta_{ij}$$

$$\int dw'\left(\xi_i'\xi_j' - \frac{\tau'^2}{3}\delta_{ij}\right)f(\tau\tau'\epsilon) \sim \left(\xi_i\xi_j - \frac{\tau^2}{3}\delta_{ij}\right)$$

and the proportionality factor as before can depend only on τ.

Effect of Etching on the Relative Intensities of the Components of Double Laue Spots Obtained from a Quartz Crystal

M. Y. COLBY AND SIDON HARRIS, *Department of Physics, University of Texas*

(Received January 20, 1933)

Laue patterns obtained from a quartz crystal of dimensions 100×6×2 millimeters taken through the 2 millimeter direction are given. One face of the crystal was highly polished and the other face was etched. The pattern obtained when the etched face of the crystal was next to the photographic film exhibited a weaker inner component for spots close to the origin; the pattern obtained when the etched face of the crystal was next to the source of x-rays exhibited a stronger inner component for spots close to the origin. The pattern obtained when the etched face of the crystal was next to the photographic film and the crystal was oscillating piezoelectrically along the direction of the long dimension showed no appreciable difference from the pattern obtained with the crystal in this same position when at rest. An explanation of the recent results obtained by J. M. Cork is offered.

A NUMBER of investigations on quartz plates oscillating piezoelectrically along the direction of thickness of the plates caused by the longitudinal effect[1] have been recently reported.[2, 3, 4, 5, 6] The results obtained showed that the intensities of the Laue spots were greatly increased by the piezoelectric oscillations. J. M. Cork found that the Laue pattern obtained when both sides of the quartz plate were etched with hydrofluoric acid exhibited double spots with the inner components showing more intensity for the spots close to the origin. He found that the spots farther out exhibited components of more nearly equal intensity. One purpose of the present work was to further investigate this phenomenon. As Fox and Cork had failed to observe any effect on the lines obtained by the Bragg method caused by piezoelectric oscillation produced by the longitudinal effect, and as the authors[7] have succeeded in obtaining an effect on the lines obtained by this method caused by piezoelectric oscillations in a long quartz crystal produced by the transverse effect, it was thought that a Laue pattern obtained from this same crystal oscillating in the manner described above would be of interest.

The crystal used was an X-cut crystal of dimensions 100×6×2 millimeters. The long dimension was in the Y direction. A detailed account of how the crystal was cut is given in a previous paper.[7] The Laue patterns were made by passing x-radiation obtained from a Mo target excited by 30 kv through the crystal in the 2 millimeter direction. The photographic films were placed at a distance of approximately two centimeters from the crystal. One face of the crystal was highy polished and the other face was etched with hydrofluoric acid.

The pattern obtained with the etched face of the non-oscillating crystal next to the film is shown in Fig. 1A. It is readily seen that the spots close to the origin are double in nature and that the inner component of most of the spots thus situated is weaker in intensity than the outer component. This result would indicate that the reflecting power of the surface closest to the film was weaker than the reflecting power of the surface closest to the source of x-rays; this result was to be expected. The spots farther out from the origin show considerably less difference in the intensities of their components. This result may be explained by the fact that the radiation reflected from the surface of greater reflecting power has to pass through more of the crystal in

[1] The terminology here used is taken from *Piezo-Electric Terminology*, by W. G. Cady, The Inst. of Radio Eng. **18**, No. 12 (1930).

[2] Y. Sakisaka, Jap. Jour. Phys. **4**, 171 (1927).

[3] G. W. Fox and P. H. Carr, Phys. Rev. **37**, 1622 (1931).

[4] G. W. Fox and J. M. Cork, Phys. Rev. **38**, 1420 (1931).

[5] C. S. Barrett and C. E. Howe, Phys. Rev. **38**, 2290 (1931); **39**, 889 (1932).

[6] J. M. Cork, Phys. Rev. **42**, 749 (1932).

[7] M. Y. Colby and Sidon Harris, Phys. Rev. **42**, 733 (1932).

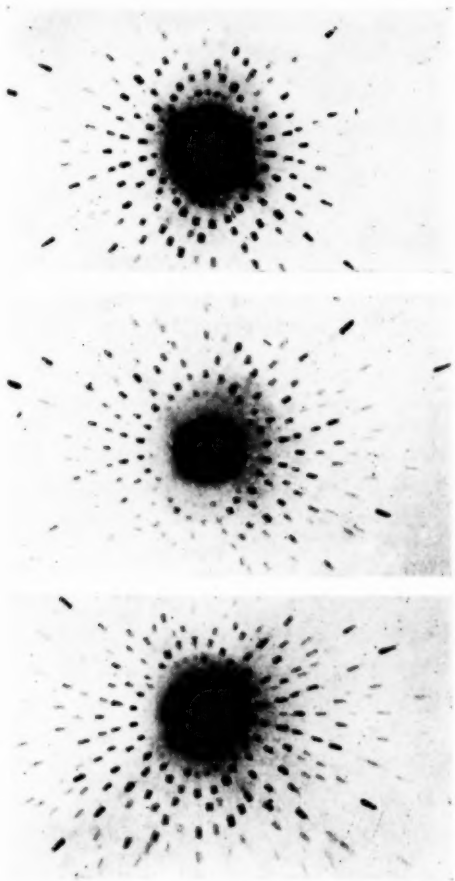

FIG. 1. A, pattern with etched face of non-oscillating crystal next to film. B, same with etched face of crystal next to x-ray source. C, pattern with crystal in position of A, but oscillating.

reaching the photographic film than does the radiation which is reflected from the face of weaker reflecting power. It will be observed that the inner ends of the remote spots are stronger than the outer ends. Here, the radiation reflected from the surface of greater reflecting power has to traverse so much more of the crystal in reaching the photographic film than does the radiation reflected from the surface of weaker reflecting power that the radiation reaching the film reflected from the former face is actually weaker in intensity than the radiation reaching the film reflected from the latter face.

The pattern obtained with the etched face of the non-oscillating crystal next to the source of x-rays is shown in Fig. 1B. It is readily seen that the relative intensities of the components of the spots close to the origin are in the reverse order in which they occur in Fig. 1A. This fact shows that the differences in intensities of the components of spots close to the origin is due to differences in the reflecting powers of the two surfaces of the crystal. Thus the result of J. M. Cork might be explained by supposing that, although both sides of his crystal had been etched, the reflecting power of the face nearest the film was stronger than the reflecting power of the face nearest the source of x-rays, and that the reflecting power of both faces was still greater than the reflecting power of the inner layers of the crystal. His result might be explained in this manner without elaboration of the usual Laue theory.

The pattern shown in Fig. 1C was obtained when the crystal was in the same position that it was when the pattern shown in Fig. 1A was taken; however, in the case of Fig. 1C, the crystal was oscillating piezoelectrically in a direction parallel to the long dimension under the influence of the transverse effect. Very little difference, if any, can be observed in the two patterns. When the crystal is oscillating in this fashion, a loop of pressure exists through the crystal in the center of the long dimension. The x-rays were passed through the crystal at this point. It might be supposed, then, that the reflecting power of the etched face should be increased more than the reflecting power of the polished face, and that the difference between the two components of the spots close to the origin should be decreased by oscillations of this fashion. It might be further expected that the reflecting power of the inner layers of the crystal would be uniformly increased and consequently the blackening between the two components of the double spots would be relatively increased by oscillations of this fashion. This point requires further investigation.

On the Interpretation of Heat in Relativistic Thermodynamics

R. C. TOLMAN, *California Institute of Technology* AND H. P. ROBERTSON, *Princeton University*

(Received January 3, 1933)

This article investigates the interpretation of the right-hand side of the relativistic second law of thermodynamics

$$\left(\phi_0 \frac{dx^\mu}{ds}\right)_\mu (-g)^{\frac{1}{2}} dx^1 dx^2 dx^3 dx^4 \geqq \frac{dQ_0}{T_0}$$

and shows that the quantity dQ_0 can be interpreted as the heat—measured by a local observer at rest in the fluid at the point of interest—which flows relative to the fluid into an element of the fluid having the instantaneous proper volume dV_0 during the proper time dt_0, where these quantities are chosen so as to satisfy the numerical equality $dV_0 dt_0 = (-g)^{\frac{1}{2}} dx^1 dx^2 dx^3 dx^4$ and the quantity T_0 is taken as the temperature ascribed to this heat by the local observer.

§1. INTRODUCTION

THE analogue in relativistic thermodynamics of the usual second law of thermodynamics may be conveniently written in either of the two equivalent forms[1]

$$\left(\phi_0 \frac{dx^\mu}{ds}\right)_\mu (-g)^{\frac{1}{2}} dx^1 dx^2 dx^3 dx^4 \geqq \frac{dQ_0}{T_0} \quad (1)$$

or

$$\frac{\partial}{\partial x^\mu}\left(\phi_0 \frac{dx^\mu}{ds}(-g)^{\frac{1}{2}}\right) dx^1 dx^2 dx^3 dx^4 \geqq \frac{dQ_0}{T_0}, \quad (2)$$

where the sign "is greater than" ($>$) applies to irreversible processes and the sign "is equal to" ($=$) applies to reversible processes.

The quantity ϕ_0 occurring in these expressions is the proper density of entropy as measured by a local observer at rest at the point of interest with respect to the thermodynamic fluid or working substance which is under consideration. The quantities dx^μ/ds are the components of the macroscopic "velocity" of this fluid at the point of interest. And the quantity dQ_0/T_0 may be described as the heat which flows into the element of the fluid and during the time denoted by $dx^1 dx^2 dx^3 dx^4$, divided by its temperature—both of these quantities being measured in proper coordinates.

In the applications of relativistic thermodynamics which have so far been made, there has been no flow of heat relative to the fluid under consideration, so that the term dQ_0/T_0 has actually been zero. These applications have been in the first place to cases of static *thermodynamic equilibrium*[2] where the heat flow was zero on account of the condition of static equilibrium. In the second place, applications have been made to the *reversible* expansion and contraction of certain models of the universe[3] in which there has been no flow of heat from one portion of the material filling the model to another owing to uniformity of conditions throughout the models considered. In the third place, applications have also been made to the *irreversible* expansion and contraction of models of the universe[4] in which, however, there was still no flow of heat from one portion of the material to another,—again on account of the assumed homogeneity of the models.

In general, nevertheless, the expression of the relativistic second law given by (1) and (2) should be valid when the heat flow does not happen to be equal to zero. And the purpose of the present note is to make as clear as may be a correct method in the general case for the specification of the quantity dQ_0/T_0.

[1] Tolman, Proc. Nat. Acad. **14**, 268 (1928); ibid. **14**, 701 (1928); Phys. Rev. **35**, 896 (1930).

[2] Tolman, Proc. Nat. Acad. **14**, 353 (1928); ibid. **17**, 153 (1931); Phys. Rev. **35**, 904 (1930); Tolman and Ehrenfest, Phys. Rev. **36**, 1791 (1930).

[3] Tolman, Phys. Rev. **37**, 1639 (1931); ibid. **38**, 797 (1931); ibid. **38**, 1758 (1931).

[4] Tolman, Phys. Rev. **39**, 320 (1932); Tolman and Ward, Phys. Rev. **39**, 835 (1932).

§2. Invariance of dQ_0/T_0 with Respect to Coordinate Transformations

Examining the expression for the relativistic second law in the form given by (1), it will be noted that the two factors $(\phi_0\ dx^\mu/ds)_\mu$ and $(-g)^{\frac{1}{2}}dx^1dx^2dx^3dx^4$, which are multiplied together to give the left-hand side of the expression, are both of them invariant scalars. The first of these factors $(\phi_0\ dx^\mu/ds)_\mu$ is a scalar since it is the *contracted covariant derivative* of a vector and it will have a numerical value which is the same in all coordinate systems. The second of the factors $(-g)^{\frac{1}{2}}dx^1dx^2dx^3dx^4$ is the known expression in *natural measure* for the four-dimensional volume specified by the range $dx^1dx^2dx^3dx^4$, and hence is also a scalar, having a value proportional to the designated range, but otherwise independent of the coordinate system.

As a result of this invariant scalar character of the left-hand side of (1), it is evident from the principle of covariance that the right-hand side of the expression must also be a similar invariant scalar, since otherwise the postulated law would not lead to the same results when applied in different coordinate systems. Hence the quantity dQ_0/T_0 must itself have a value, which is of course proportional to the four-dimensional volume $(-g)^{\frac{1}{2}}dx^1dx^2dx^3dx^4$, but is otherwise independent of the coordinate system. This result is very useful, since it permits us to obtain a general determination of the quantity dQ_0/T_0 by first employing a specially chosen coordinate system in which the interpretation will be quite simple and clear.

§3. Determination of dQ_0/T_0 by Using "Co-Moving" Coordinates

To obtain a coordinate system which will make the interpretation easy, we may take for the space-like coordinates x^1, x^2, x^3 a three-dimensional network of lines permanently connecting adjacent macroscopically identifiable points of the fluid under consideration and moving with the fluid, and take for the time-like coordinate x^4 the readings of a set of natural clocks which have been distributed to a sufficient number of different points throughout the fluid and are then allowed to move therewith. The possibility of obtaining such a coordinate system would appear guaranteed by the specifications for setting it up, and such systems which might be called "co-moving coordinates" are often very useful.

With such coordinates, it is evident that the fluid will always be permanently everywhere at rest with respect to the space-like coordinates, so that we can write

$$dx^1/ds=dx^2/ds=dx^3/ds=0 \tag{3}$$

for the spatial components of its macroscopic "velocity." Furthermore, for the temporal component we can write

$$dx^4/ds=1 \tag{4}$$

since increments in coordinate time and proper time have been made the same by our specification of x^4 with the help of natural clocks moving with the fluid.

Substituting (3) and (4) in the relativistic second law as given in the form (2), we then find that this reduces to the simple expression

$$\frac{\partial}{\partial x^4}(\phi_0(-g)^{\frac{1}{2}})dx^1dx^2dx^3dx^4 \geqq \frac{dQ_0}{T_0} \tag{5}$$

and because of the mutual independence of the coordinates this can be rewritten in the form

$$\frac{\partial}{\partial x^4}(\phi_0(-g)^{\frac{1}{2}}dx^1dx^2dx^3)dx^4 \geqq \frac{dQ_0}{T_0}. \tag{6}$$

To see more clearly, moreover, the significance of this result we may now introduce the evidently valid substitutions

$$dt_0=dx^4;\quad dV_0=(-g)^{\frac{1}{2}}dx^1dx^2dx^3, \tag{7}$$

where dt_0 is an element of proper time as measured by a local observer at rest in the fluid at the point of interest, and dV_0 is the proper spatial volume, associated with the four-dimensional region $dx^1dx^2dx^3dx^4$, as measured by this same local observer. Introducing (7) in (6), we can then write

$$\frac{\partial}{\partial t_0}(\phi_0 dV_0)dt_0 \geqq \frac{dQ_0}{T_0}. \tag{8}$$

The interpretation of dQ_0/T_0 with the help of this result is then quite simple. Since ϕ_0 is the density of entropy as measured by a local ob-

server at rest in the fluid, and dV_0 is the spatial volume as measured by this observer of a small region through the boundaries of which no fluid is passing, the left-hand side of the expression gives the change which the local observer finds in the time dt_0 in the entropy of a definite small element of the fluid. In accordance with the principle of equivalence, however, this change which a local observer finds in the entropy of a system small enough so that gravitational curvature can be neglected must be related to the heat that flows into the system in the way given by the ordinary second law of thermodynamics. Hence we can now conclude that dQ_0 is the heat as measured by the local observer that flows in the time dt_0 into the element of fluid instantaneously contained in the proper volume dV_0, and T_0 is the temperature associated with this heat. Furthermore, as a result of our previous discussion in §2 of the invariance of dQ_0/T_0 to coordinate transformations, we are thus furnished with a correct value to use for this quantity in any coordinate system, provided of course that we allow for the proportionality between the magnitude of dQ_0/T_0 and the magnitude $(-g)^{\frac{1}{2}}dx^1dx^2dx^3dx^4$ of the four-dimensional volume associated with the specified coordinate range.

Hence, returning to our general expression for the relativistic second law, which is valid in any coordinate system

$$\left(\phi_0 \frac{dx^\mu}{ds}\right)_\mu (-g)^{\frac{1}{2}}dx^1dx^2dx^3dx^4 \geqq \frac{dQ_0}{T_0} \qquad (9)$$

we may now state that the quantity dQ_0 occurring in this expression can be taken as the heat—measured by a local observer at rest in the fluid at the point of interest—which flows into an element of the fluid having the instantaneous proper volume dV_0 during the proper time dt_0, where these quantities are chosen so as to satisfy the numerical equality

$$dV_0dt_0 = (-g)^{\frac{1}{2}}dx^1dx^2dx^3dx^4 \qquad (10)$$

and the quantity T_0 is taken as the temperature ascribed to this heat by the local observer. We are thus provided with a perfectly definite interpretation of all the quantities occurring in the relativistic second law which will satisfy the principle of covariance by leading to the same results no matter what coordinate system is used, and which satisfies the principle of equivalence by reducing, as we have seen with the help of a specially convenient coordinate system, to the ordinary second law for an infinitesimal portion of the fluid.

§4. Determination of dQ_0/T_0 by Using Natural Coordinates

In accordance with the above specifications for determining a correct value to use in the relativistic second law for the flow of heat dQ_0 into the element and during the time denoted by $dx^1dx^2dx^3dx^4$, it will be noted that this quantity is to be obtained from measurements by a local observer of the rate at which heat flows into a specified element of the fluid. Hence this quantity is to be regarded as corresponding to a flow of heat measured relative to boundaries at rest in the fluid, rather than in some way relative to boundaries at rest with respect to the spatial coordinates that are actually being employed, as might at first sight have seemed plausible. Since this conclusion was obtained, however, with the help of a coordinate system specially chosen so that boundaries at rest with respect to the fluid were also at rest with respect to the spatial coordinates, it will be illuminating to show that we should also be led to the same interpretation for dQ_0/T_0 using a system of coordinates with respect to which the fluid is not at rest.

To obtain such a demonstration, we shall now use a set of coordinates x, y, z, t with respect to which the fluid is not at rest, but which are so chosen as to be *natural coordinates* for the point of interest. In accordance with the principle of equivalence such natural coordinates for any desired spacetime point can always be found, and with respect to them the principles of special relativity as expressed in their usual form may be taken as valid in the immediate neighborhood of the point in question. Hence, by choosing these coordinates, we shall be able to employ the principles of thermodynamics as developed for the special theory of relativity by Planck and Einstein in arriving at the desired interpretation.

Making use of these natural coordinates x, y, z, t, we shall evidently have

$$(-g)^{\frac{1}{2}} = 1$$

and

$$\frac{\partial}{\partial x}(-g)^{\frac{1}{2}}=\frac{\partial}{\partial y}(-g)^{\frac{1}{2}}=\frac{\partial}{\partial z}(-g)^{\frac{1}{2}}=\frac{\partial}{\partial t}(-g)^{\frac{1}{2}}=0 \quad (11)$$

at the point of interest. Hence by substituting into the relativistic second law of thermodynamics in the form given by (2), we can now write the left-hand side of that expression in our present coordinates in the form

$$\left[\frac{\partial}{\partial x}\left(\phi_0\frac{dx}{ds}\right)+\frac{\partial}{\partial y}\left(\phi_0\frac{dy}{ds}\right)+\frac{\partial}{\partial z}\left(\phi_0\frac{dz}{ds}\right)+\frac{\partial}{\partial t}\left(\phi_0\frac{dt}{ds}\right)\right]dxdydzdt \quad (12)$$

where dx/ds, dy/ds, and dz/ds are the components of the macroscopic velocity of the fluid at the point of interest with respect to proper time, and by a simple substitution we can rewrite this in the form

$$\left[\frac{\partial}{\partial x}\left(\phi_0\frac{dt}{ds}\frac{dx}{dt}\right)+\frac{\partial}{\partial y}\left(\phi_0\frac{dt}{ds}\frac{dy}{dt}\right)+\frac{\partial}{\partial z}\left(\phi_0\frac{dt}{ds}\frac{dz}{dt}\right)+\frac{\partial}{\partial t}\left(\phi_0\frac{dt}{ds}\right)\right]dxdydzdt, \quad (13)$$

where dx/dt, dy/dt and dz/dt give the components of the velocity of the fluid as ordinarily expressed in terms of the coordinate time t.

In accordance with the special theory of relativity, however, entropy is an invariant for the Lorentz transformation, and hence entropy density will be affected by the Lorentz factor of contraction ds/dt in such a way that we can substitute

$$\phi=\phi_0(dt/ds), \quad (14)$$

where ϕ is the density of entropy at the point of interest taken with respect to our present system of coordinates x, y, z, t.

Substituting (14) into (13), and writing for simplicity u, v, and w for the three components of velocity dx/dt, dy/dt and dz/dt, we then obtain

$$\left[\frac{\partial}{\partial x}(\phi u)+\frac{\partial}{\partial y}(\phi v)+\frac{\partial}{\partial z}(\phi w)+\frac{\partial\phi}{\partial t}\right]dxdydzdt \quad (15)$$

and by performing the indicated differentiations and rearranging the order, this can be rewritten in the form

$$\left[\frac{\partial\phi}{\partial t}+u\frac{\partial\phi}{\partial x}+v\frac{\partial\phi}{\partial y}+w\frac{\partial\phi}{\partial z}+\phi\left(\frac{\partial u}{\partial x}+\frac{\partial v}{\partial y}+\frac{\partial w}{\partial z}\right)\right]dxdydzdt. \quad (16)$$

Finally, noting the significance of the various terms in (16), we may now rewrite this expression for the left-hand side of the relativistic second law in the simple form

$$(d\phi/dt)dVdt+\phi(d/dt)(dV)dt, \quad (17)$$

where we have written dV for the volume of the element of fluid, instantaneously contained in the region $dxdydz$, and have written $d\phi/dt$ for the total rate of change in entropy density as we follow the moving fluid. Hence in natural coordinates the left-hand side of the relativistic second law is seen to be equal to the change that takes place in time dt in the entropy of the element of fluid instantaneously contained in the region $dxdydz$, and we can write for these coordinates

$$\left(\phi_0\frac{dx^\mu}{ds}\right)_\mu(-g)^{\frac{1}{2}}dx^1dx^2dx^3dx^4=\frac{d}{dt}(\phi dV)dt. \quad (18)$$

In accordance, however, with special relativistic thermodynamic theory we can relate this change in the entropy, of the little thermodynamic system consisting of this element of fluid, to heat flow and temperature by the expression

$$d/dt\,(\phi dV)dt\geqq dQ/T, \quad (19)$$

where dQ is the heat absorbed by the element at temperature T and in the time dt referred to our present coordinates. Furthermore, since the ratio of heat to temperature is an invariant for the Lorentz transformation, we can also take

$$dQ/T=dQ_0/T_0, \quad (20)$$

where dQ_0 is the absorbed heat as measured in

proper coordinates and T_0 is the proper temperature of the element. Moreover, in accordance with the Lorentz contraction for volume elements and Lorentz dilation for time intervals we can write

$$dVdt = dV_0 dt_0, \tag{21}$$

where dV_0 is the volume of this element as measured in proper coordinates and dt_0 is the proper time during which the heat absorption takes place.

Hence combining (18), (19) and (20), we have now obtained, also using our present coordinates, the result

$$\left(\phi_0 \frac{dx^\mu}{ds}\right)_\mu (-g)^{\frac{1}{2}} dx^1 dx^2 dx^3 dx^4 \geqq \frac{dQ_0}{T_0}, \tag{22}$$

where, in accordance with (21), dQ_0 is to be taken as the heat—measured by a local observer at rest in the fluid at the point of interest—which flows into an element of the fluid having the instantaneous proper volume dV_0 during the proper time dt_0, these quantities being chosen so as to satisfy the numerical equality

$$dV_0 dt_0 = dVdt = (-g)^{\frac{1}{2}} dx^1 dx^2 dx^3 dx^4. \tag{23}$$

Thus, using natural coordinates, we have satisfactorily obtained the same interpretation of the quantities occurring in the relativistic second law as was obtained in the preceding section using co-moving coordinates. And the treatment gives the desired illustration of the fact that our interpretation of dQ_0 as heat flowing through a boundary stationary in the fluid was not a result of our original special choice of coordinates in which the fluid was at rest.

§5. Conclusion

Before concluding, two further remarks may be made concerning the interpretation of the relativistic second law, which may be illuminating.

In accordance with the treatment given in the last section it is to be noted that the quantities ϕ, ϕu, ϕv and ϕw must be regarded as *total* densities of entropy and entropy flux at the point of interest, since otherwise, for example, the left-hand side of expression (19) could not have been interpreted as the change in the total entropy of the specified element of fluid and correlated as was done with the influx of heat. This implies that we are to treat our thermodynamic fluid from a macroscopic point of view and take ϕ as the total entropy associated and moving along with unit volume of that material, rather than to try to employ a microscopic point of view and take ϕ as entropy belonging in some way solely to the molecules of the fluid with an additional quantity belonging to the radiation in the space between them. Similar remarks apply to ϕ_0 and $\phi_0 dx^\mu/ds$. It will be noted that the correct procedure is in entire agreement with ordinary thermodynamic practice and with the spirit of thermodynamics as a macroscopic phenomenological science.

In laying down a correct method for determining the magnitude of the heat flux divided by temperature dQ_0/T_0 which corresponds to the infinitesimal element of fluid and time denoted by $dx^1 dx^2 dx^3 dx^4$, it will have been noted that we have merely specified that the local observer should measure the proper heat dQ_0 entering an element of the fluid of instantaneous proper volume dV_0 during the proper time dt_0, where dV_0 and dt_0 are chosen so as to satisfy the numerical equality

$$dV_0 dt_0 = (-g)^{\frac{1}{2}} dx^1 dx^2 dx^3 dx^4 \tag{21}$$

and have not introduced any specifications as to the shape of the four-dimensional region $dV_0 dt_0$. This, however, will be seen to be legitimate since the heat flux is directly proportional to the product of volume and time, independent of shape except for higher order differentials which can be neglected on shrinking the four-dimensional region down to the point of interest.

It is hoped that the treatment which we have given in this article will help to make the interpretation of the relativistic second law clear. The considerations presented are in agreement with the results obtained in previous applications of relativistic thermodynamics where there was no flow of heat relative to the fluid under consideration, and should be specially helpful when further applications are made to systems in which a flow of heat relative to the fluid does take place.

The Effect of Tension on the Electrical Resistance of Single Antimony Crystals

MILDRED ALLEN, *Research Laboratory of Physics, Harvard University*

(Received February 9, 1933)

The adiabatic tension coefficient of resistance of single antimony crystals has been determined for various orientations. Since antimony crystals have the same type of symmetry as bismuth, the curves connecting the coefficient with the primary and secondary orientations have the same general shape as in the case of bismuth and again uphold the theory put forth by Bridgman. The observed values of the coefficients for antimony when the tension and current are parallel to the trigonal axis and perpendicular to it are different both in magnitude and in sign, whereas in the case of bismuth the two were both negative and very nearly equal in magnitude. The six coefficients necessary completely to determine the behavior of the resistance when deforming forces are applied to the antimony crystals have been found (1) without correcting for strain and (2) correcting for the changes arising from the strain produced by the tension.

IN a previous paper[1] the author has studied experimentally the effect of tension on the electrical resistance of single *bismuth* crystals. The experimental dependence of the tension coefficient on the principal and secondary orientations of the crystals with respect to the cylindrical axis was later found by Professor Bridgman[2] to be in agreement with a geometrical theory based on the symmetry of the crystal. The object of the present paper is to examine the effect of tension on the resistance of single crystals of *antimony* which has the same type of symmetry as bismuth and to see whether the results obtained are consistent with the theory. The values of the six tension coefficients are found numerically, both as observed directly and as corrected for the change in resistance due to the strains in the crystal produced by the tension.

PROCEDURE

Experimentally the procedure is somewhat more difficult than in the case of bismuth. The specific resistance of antimony is roughly one third that of bismuth so that the resistance of a similar piece of antimony is approximately one third as great. Furthermore, since the tension coefficient of resistance of polycrystalline antimony is of the order of one tenth[3] that of polycrystalline bismuth, it is to be assumed that the tension coefficients of antimony will be of the order of one tenth of those of bismuth. Consequently, the absolute change in resistance to be measured will be about one thirtieth that studied in the case of bismuth. This is counteracted in some degree by the fact that twice and even four times as great a tension (force per unit area) as had been necessary to use with bismuth was here safely applied. On the other hand, antimony is more brittle and so is more difficult to handle.

Therefore the apparatus had to be studied afresh to see in what way the sensitivity could be increased—and preferably to about ten times its previous value. Considerable increase in sensitivity was obtained by using twice as large, and sometimes four times as large, a current as in the work with bismuth. The most obvious way further to increase the precision of the method was to use a more sensitive galvanometer, but even the new Leeds and Northrup galvanometer was rated to have only twice the voltage sensitivity of the older galvanometer already in use. It was pointed out in the previous paper[1] that when the *deflection* method was used the voltage sensitivity of the galvanometer depended on the resistance r of the compensating circuit Q across which the galvanometer was connected and was in fact proportional to the sum of this resistance r and the resistance of the galvanometer itself. It is thus of advantage to use a small r. Moreover, in comparing small changes of re-

[1] Mildred Allen, Phys. Rev. **42**, 848 (1932).
[2] P. W. Bridgman, Phys Rev. **42**, 858 (1932).
[3] P. W. Bridgman, Proc. Amer. Acad. **57**, 41 (1922).

sistance it seemed desirable to attempt to use the galvanometer so that its voltage sensitivity remained constant. This was effected by choosing r as 3 ohms plus half the length of the slide wire in the auxiliary circuit, and by roughly balancing the potential fall across the crystal against the auxiliary potential difference by varying the large resistance governing the current in the auxiliary circuit. The final precise balancing could then be carried out by moving the contact on the slide wire a small distance. For this reason the large resistance in the auxiliary circuit Q was chosen to be a 10,000 ohm variable radio resistance. The voltage sensitivity of the galvanometer, with the scale at 5 meters as before, was 2.15×10^{-7} volts per cm. Readings then were satisfactorily large as they varied from 0.15 cm to 4.00 cm. With this *deflection* method it proved to be possible to measure the tension coefficients to within about 1×10^{-6} in absolute value where the coefficient itself varied from $+9.0\times10^{-6}$ to -35.0×10^{-6}. The *null* method used before was discarded, since the changes of resistance were too small to give more than a millimeter's displacement on the balancing slide wire of the main circuit; its only use in this set of experiments was to check the sign of the change of resistance.

A further precaution was to decrease the size of the air chamber containing the crystal and the surrounding copper cylinder, so that temperature equilibrium was obtained more rapidly. The substitution of a mercury thermostat for the metal one and of a Burgess vacuum switch for the tilting mercury switch made the temperature less variable and entirely independent of the room temperature. This greater stability of temperature was of importance in measuring the markedly smaller effect and was reflected in the character of the deflection runs made with alternate readings with and without tension, Fig. 1, which in this work with antimony usually showed a definite periodic variation. This periodicity must arise primarily from the periodic changes in temperature produced by the regular increases and decreases in heating current governed by the thermostat. In addition there is usually to be noted a small gradual displacement of the whole curve up or down, and this drift in a given direction can reasonably be ascribed to the zero drift of the galvanometer and to the unequal changes of voltage in the two balancing circuits arising very probably from the polarization of the dry cell of the auxiliary circuit Q. As is seen in Fig. 1 this drift is very small when temperature equilibrium has been thoroughly established before beginning to take readings.

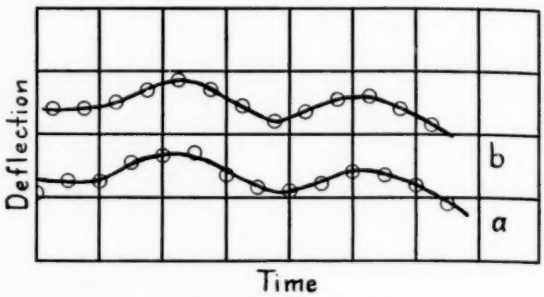

FIG. 1. a without tension; b with tension.

The crystals used were of Kahlbaum antimony. Some of them had been made and used by Professor Bridgman and were generously put by him at the writer's disposal; they had diameters of approximately 1/8″. Others were crystallized by the writer, following the procedure indicated by P. W. Bridgman[4]; most of these latter had a diameter of approximately 1/16″. The advantage of the smaller diameter was the greater resistance giving a correspondingly greater change of resistance; the disadvantage, the greater difficulty in handling this brittle metal.

RESULTS

I. Without correcting for strain

Twenty-one separate individual single crystals of antimony have been studied and their tension coefficients measured. Because of the smallness of the effect it proved not to be sufficient to measure the coefficients once with the current flowing in but one direction. With most of the crystals the coefficient was determined with one tension and then under identical conditions with the current reversed; to check this result this entire process was then repeated with either the magnitude of the current or of the tension changed. The two determinations were likely not to agree if the crystal were slightly cracked. Furthermore the accuracy with which the coeffi-

[4] P. W. Bridgman, Proc. Amer. Acad. 63, 351 (1929).

cient could be determined under given conditions without reversal of the current was found by taking two determinations with only the galvanometer leads reversed in the two cases. In only a few cases did the difference between these two readings differ by more than 0.3×10^{-6} in absolute value. On the other hand, the readings with the current reversed were likely to differ by a considerably larger amount, usually of the order of 1.0×10^{-6}. These differences were thus larger than the error to be expected as intimated with the galvanometer leads reversed. It seemed at one time that these discrepancies were proportional to the magnitude of the current used, and so were to be ascribed to a tension coefficient of the Peltier effect, but further work showed this explanation to be untenable, so that probably they arise from some irregular heating effect and are eliminated by taking the average of the readings with the direct and reversed currents.

The values of the tension coefficient were then to be studied on the basis of Professor Bridgman's theory[2] as functions of the primary orientation of the crystal θ and of the secondary orientation φ. The angle θ was defined as the angle between the trigonal axis of the crystal and the cylindrical axis. The angle φ was defined as the angle between the projection of the cylindrical axis on the principal cleavage plane (which is perpendicular to the trigonal axis) and the projection on the same plane of the normal to that secondary cleavage plane which makes an angle of about 71° with the principal cleavage plane. The relation derived by Professor Bridgman was the following:

$$\beta=(1/\rho_\theta)\{\rho_{11}\sin^4\theta+\rho_{33}\cos^4\theta+(2\rho_{13}+\rho_{44})\sin^2\theta\cos^2\theta-2\rho_{14}\sin^3\theta\cos\theta\cos3\varphi\}, \quad (1)$$

where β is the tension coefficient, which is the relative change in resistance $\Delta R/R$ produced by a tension T of 1 kg/cm², the ρ_{rs}'s are five of the six tension coefficients necessary completely to define the behavior of the resistance of a trigonal crystal under the action of deforming forces, and ρ_θ is the specific resistance at the orientation θ. The expression is the same as that used for bismuth, since bismuth and antimony crystals have the same type of symmetry. The term in φ shows the trigonal symmetry. Since none of the twenty-one readings of the coefficient probably were entirely consistent with any of the others and the tension coefficients were quite small, it seemed worth while to use least squares in evaluating them. The values of the four constants and their probable errors[5] as found in this way directly from the experimental values are

$$\begin{aligned}\rho_{11}&=(+\ 0.24\pm0.09)\times10^{-10},\\ \rho_{33}&=(-12.20\pm0.33)\times10^{-10},\\ 2\rho_{13}+\rho_{44}&=(+5.72\pm0.53)\times10^{-10},\\ \rho_{14}&=(+5.10\pm0.16)\times10^{-10}.\end{aligned} \quad (2)$$

In Fig. 2 the full lines give the curves computed from these values for $\varphi=60°$, $\varphi=30°$, and $\varphi=0°$.

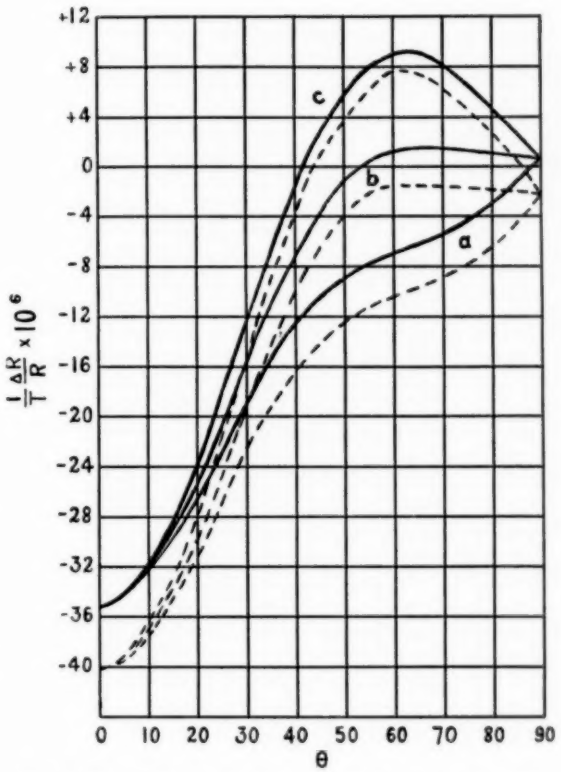

FIG. 2. Dependence of tension coefficients on orientation. *a*, $\varphi=0°$; *b*, $\varphi=30°$; *c*, $\varphi=60°$. Full curves, experimental curves. Dotted curves, corrected for strain.

[5] Since ρ_{11} and ρ_{33} determine the tension coefficients for $\theta=90°$ and $\theta=0°$, respectively, it appears from Eq. (2) that the tension coefficient for $\theta=90°$ is known with less error than for $\theta=0°$. The coefficient ρ_{14} gives the distance between the curves for $\varphi=0$ and for $\varphi=60°$ for a given primary orientation; this "spread" of the curves is very accurately known. The remaining constant $(2\rho_{13}+\rho_{44})$ determines the exact shape of the curve for $\varphi=30°$ and the error here is seen to be comparatively large.

This single set of curves is sufficient entirely to describe the behavior of the electrical resistance of antimony under tension, since from Eq. (1) it is known that the coefficient always varies between these indicated outside limits proportionately to cos 3φ. These curves are like the similar ones for bismuth in that the coefficient has a single constant value for $\theta=90°$ and for $\theta=0°$ (as it must according to the theory) and varies in sign according to the orientation; but they differ in that for bismuth the values of these constants have the same order of magnitude and the same sign, whereas for antimony the absolute magnitude at $\theta=0°$ is more than fifty times that for $\theta=90°$ and the signs of the two are different. A numerical comparison of the observed experimental values and the computed values of the tension coefficient with the constants of (2) is given in Table I and it is seen that the difference between the two only once exceeds 1.1×10^{-6}, which considering the smallness of the effect indicates satisfactory agreement. The one reading which differs by more than this amount lies on a very steep part of the curve where a small error in measuring φ necessarily produced a large error in β.

TABLE I.

θ	φ	Maker and size	$R\times10^{3}$	$\beta\times10^{6}$ expt. uncorrected	$\beta\times10^{6}$ theor. uncorrected	$\beta\times10^{6}$ expt. corrected for strain	$\beta\times10^{6}$ theor. corrected for strain
90°	16°	B L	2.09	+ 1.03	+ 0.54	− 1.92	− 2.40
83°	46°	B L	2.02	+ 3.04	+ 2.74	+ 0.39	+ 0.11
83°	24°	A s	1.98	+ 0.96	− 0.14	− 2.08	− 3.16
79°	17°	A s	2.48	− 2.03	− 1.70	− 5.25	− 4.92
77°	55°	B L	1.96	+ 5.05	+ 5.68	+ 2.83	+ 3.49
75°	40°	B L	2.18	+ 4.02	+ 3.87	+ 1.58	+ 1.44
75°	36°	A s	5.74	+ 1.79	+ 2.83	− 0.78	+ 0.26
73°	03°	B L	1.99	− 4.52	− 4.61	− 8.13	− 8.20
72°	06°	A L	5.51	− 4.43	− 4.57	− 8.00	− 8.16
67°	51°	B L	3.10	+ 6.76	+ 7.88	+ 4.97	+ 6.09
65°	38°	B L	5.96	+ 3.99	+ 3.24	+ 1.74	+ 0.83
64°	34°	A s	4.32	+ 2.64	+ 3.06	+ 0.21	+ 0.65
61°	17°	B L	1.50	− 3.46	− 3.75	− 6.75	− 7.07
62°	07°	B L	1.16	− 6.39	− 5.99	−10.02	− 9.64
62°	04°	B L	2.01	− 5.64	− 6.34	− 9.32	−10.03
68°	01°	A s	2.18	− 6.33	− 5.59	− 9.99	− 9.27
54°	53°	A s	1.93	+ 7.25	+ 7.06	+ 5.62	+ 5.45
50°	51°	A L	4.37	+ 5.04	+ 4.98	+ 3.29	+ 3.22
53°	36°	B L	1.41	+ 3.47	+ 1.92	+ 1.16	− 0.38
44°	06°	A s	1.64	−11.5	−10.46	−15.2	−14.1
22°	56°	A s	0.86	−21.7	−21.77	−25.6	−25.6

B indicates crystal was made by P. W. Bridgman.
A indicates crystal was made by the author.
L designates a large crystal of approximately 1/8″ diameter.
s designates a small crystal of approximately 1/16″ diameter.

Only two readings were made for θ less than 50°. This came about for two reasons: it is comparatively difficult to grow crystals with the principal cleavage plane nearly perpendicular to the cylindrical length, and, more important, crystals with such orientations are so exceedingly brittle that it is very nearly impossible to mount them in the apparatus without sufficient jarring to break them along a principal cleavage. The point for $\theta=22°$ fitted within experimental error on the curve computed from the points for θ between 44° and 90°, the value of β computed on this basis being -22.9×10^{-6} as compared with the experimental value of -21.7×10^{-6}. This furnishes a check on the correctness of the general trend of the curve which seems entirely satisfactory, although in the final calculation this lowest point was included and the values of the constants modified somewhat thereby.

Completely to determine the six coefficients which are necessary to describe the behavior of a trigonal crystal under the action of forces, the data derived from the effect of tension on antimony crystals must be supplemented by the values of the hydrostatic pressure coefficients when the current is flowing parallel to the trigonal axis and when it is perpendicular to it. Professor Bridgman's best values for these pressure coefficients at 30°C are:

$$\begin{aligned}\theta=90° \quad & [(1/p)(\Delta R/R)]_{90°}=+3.7\times10^{-6},\\ \theta=0° \quad & [(1/p)(\Delta R/R)]_{0°}=+19.4\times10^{-6}.\end{aligned} \tag{3}$$

These are taken from a recent paper[4] in which the pressure coefficients are carefully studied as a function of pressure; these values are extrapolated a short distance to zero pressure to be comparable with the very small forces used in the tension experiments. We have therefore the additional equations as given by Bridgman[2]

$$+3.7\times10^{-6}=-(\rho_{11}+\rho_{12}+\rho_{13})/(\rho_{\theta=90°}), \tag{4}$$

$$+19.4\times10^{-6}=-(2\rho_{13}+\rho_{33})/(\rho_{\theta=0}). \tag{5}$$

This gives finally for the six tension coefficients of resistance *uncorrected* for the changes of resistance arising from the change in dimensions caused by the application of the forces:

$$\begin{aligned} \rho_{11}&=+0.2\times10^{-10}, \quad \rho_{12}=-4.6\times10^{-10}, \\ \rho_{33}&=-12.2\times10^{-10}, \quad \rho_{13}=+2.7\times10^{-10}, \\ \rho_{14}&=+5.1\times10^{-10}, \quad \rho_{44}=+0.2\times10^{-10}. \end{aligned} \tag{6}$$

It is to be noted that these are of the order of magnitude of one tenth those found in the case of bismuth as was anticipated from the polycrystalline tension coefficients. This polycrystalline coefficient was found by Professor Bridgman to be approximately 5×10^{-6} and this lies within the limiting values found in this set of experiments. One would be inclined to explain his one reading of 20.0×10^{-6} as arising from a crack in the antimony which was not otherwise detectable, particularly as this metal is so very brittle.

II. Correcting for strain

In the case of bismuth the changes of resistance arising from the deformation of the crystals were so small compared with those actually produced by the tension that, being within experimental error, they could very properly be neglected.[6] In the case of antimony, however, with the increased precision of the method, the deformation of the crystals gives changes greater than the experimental error, sometimes of the order of magnitude of the tension coefficients themselves, and should be considered, although in practice the observed change of resistance will always include that arising from the change of dimension. As a matter of fact, since these corrections do not follow the same law of variation with the orientations as do the tension coefficients, Professor Bridgman's equation is rigorously only applicable when these corrections have been made.

Correcting for strain is not an entirely simple matter. As Professor Bridgman has pointed out in the case of hydrostatic pressure[7] the change of resistance due to the strain produced by the tension will consist of three parts: (1) that arising from change in length; (2) that from change in cross section; and (3) that from change in the orientation θ. These will be considered separately.

(*1*) *To find the relative change of resistance arising from the change in length produced by the application of a tension of 1 kg/cm² as a function of the primary orientation θ and of the secondary orientation φ.* The elastic behavior of antimony[7] is defined by the equations

$$\begin{aligned} e_{xx}&=s_{11}X_x+s_{12}Y_y+s_{13}Z_z+s_{14}Y_z+0Z_x \quad +0X_y, \\ e_{yy}&=s_{12}X_x+s_{11}Y_y+s_{13}Z_z-s_{14}Y_z+0 \quad +0, \\ e_{zz}&=s_{13}X_x+s_{13}Y_y+s_{33}Z_z+0 \quad +0 \quad +0, \\ e_{yz}&=s_{14}X_x-s_{14}Y_y+0 \quad +s_{44}Y_z+0 \quad +0, \\ e_{zx}&=0 \quad +0 \quad +0 \quad +0 \quad +s_{44}Z_x \quad +2s_{14}X_y, \\ e_{xy}&=0 \quad +0 \quad +0 \quad +0 \quad +2s_{14}Z_x+2(s_{11}-s_{12})X_y, \end{aligned} \tag{7}$$

[6] This has been shown quantitatively by applying the method of least squares to the *bismuth* data. The numerical values of the coefficients are, giving Professor Bridgman's values for comparison,

	Bridgman	Least Squares: Uncorrected	Least Squares: Corrected for strain
ρ_{11}	-7.7×10^{-9}	-7.2×10^{-9}	-7.7×10^{-9}
ρ_{33}	−6.6	−6.2	−6.7
ρ_{14}	+15.7	+13.5	+13.2
ρ_{12}	+5.6	+4.3	+4.2
ρ_{13}	+1.8	+1.6	+1.9
ρ_{44}	−12.3	−10.4	−13.1

The uncorrected values differ somewhat from those given by Professor Bridgman in his theoretical paper[2] since his values were computed from six graphically interpolated points and these are based on all forty-five directly observed points. The average difference between the experimental values of the tension coefficients of resistance and those computed from these uncorrected constants is 0.6×10^{-5}; in only four cases is this difference greater than 1.2×10^{-5}. Since the correction of β for strain for bismuth lies between 0.36×10^{-5} and 0.83×10^{-5}, depending on the crystal orientation, it is evident that the strain correction is of the same order of magnitude as the experimental error.

[7] P. W. Bridgman, Proc. Amer. Acad. **60**, 305 (1925).

in which Z represents the direction of the trigonal axis. The constants for this case have the values, T being expressed in dynes/cm²,

$$s_{11}=+17.7\times10^{-13},\quad s_{33}=+33.8\times10^{-13},$$
$$s_{12}=-\ 3.8\times10^{-13},\quad s_{44}=+41.0\times10^{-13},\quad (8)$$
$$s_{13}=-\ 8.5\times10^{-13},\quad s_{14}=-\ 8.0\times10^{-13}.$$

This immediately gives us, for $\theta=0°$, when T is given in the practical units of kg/cm²,

$$(1/T)(\Delta l/l)=s_{33}\times980\times1000=+3.31\times10^{-6},\quad (9)$$

which gives the order of magnitude of the correction to be expected from this source.

To find the most general dependence of $(1/T)(\Delta l/l)$ on θ and φ, it will be convenient to transform from the coordinates XYZ defined by the trigonal axis and the crystalline properties of the antimony to $X'Y'Z'$ axes defined by the characteristics of the cylinder in which the metal is cast. The relative elongation $e_{z'z'}$ will then give the change in length desired. We must first define these two sets of coordinates more precisely. The Z-axis, Fig. 3, is to be parallel to the

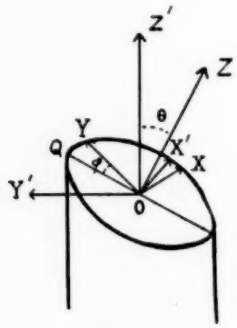

FIG. 3.

trigonal axis of the crystal, the Z'-axis to the cylindrical axis of the casting. The angle between them is then by definition θ. The Y-axis lies in the elliptical cross section of the principal cleavage plane and is the projection on this plane of the normal to the secondary cleavage plane making an angle of about 71° with the principal cleavage plane; thus the Y-axis makes an angle φ with the major axis OQ, by definition. The Y'-axis cannot of course lie in this plane, but it is to be in the plane QOZ', so that OQ is its projection on the principal cleavage plane. The nine direction cosines necessary completely to define the transformation are then known and are recorded in Table II. In the new set of coordi-

TABLE II.

	X'	Y'	Z'
X	$\cos\varphi$	$\sin\varphi\cos\theta$	$\sin\varphi\sin\theta$
Y	$-\sin\varphi$	$\cos\varphi\cos\theta$	$\cos\varphi\sin\theta$
Z	0	$-\sin\theta$	$\cos\theta$

nates the equations of elasticity have the form, since the tension is always along the Z'-axis,

$$e_{x'x'}=s'_{13}Z'_{z'},\quad e_{y'z'}=s'_{43}Z'_{z'},$$
$$e_{y'y'}=s'_{23}Z'_{z'},\quad e_{z'x'}=s'_{53}Z'_{z'},\quad (10)$$
$$e_{z'z'}=s'_{33}Z'_{z'},\quad e_{x'y'}=s'_{63}Z'_{z'},$$

where the six s''s define the behavior of the crystal in the primed set of axes and are known functions of the s's, the transformation of the s's being given by Voigt.[8] Carrying out the calculation for s'_{33}, we get for the relative change in length along the axis of the cylinder the equation

$$(1/T)(\Delta l/l)=s_{11}\sin^4\theta+s_{33}\cos^4\theta+(2s_{13}+s_{44})\sin^2\theta\cos^2\theta-2s_{14}\sin^3\theta\cos\theta\cos3\varphi.\quad (11)$$

The term in $\cos3\varphi$ is in agreement with the known trigonal symmetry.

(2) To find the relative change of resistance arising from the change in cross section produced by the application of a tension of 1 kg/cm². It is to be noted that OY' is the major axis of the *horizontal* elliptical cross section into which the tension deforms the circular cross section. This cross section originally had the area πr^2 and when strained has the area $\pi r^2(1+s'_{13})(1+s'_{23})$ so that

$$(1/T)(\Delta A/A)=s'_{13}+s'_{23},\quad (12)$$

where it is to be expected that one or both of these s''s will be negative. Evaluation of $\Delta A/A$ in terms of the s's gives for the correction due to change in cross section

$$(1/T)(\Delta A/A)=s_{13}(\cos^4\theta+\sin^4\theta+\cos^2\theta)+s_{12}\sin^2\theta+(s_{11}+s_{33}-s_{44})\sin^2\theta\cos^2\theta+2s_{14}\sin^3\theta\cos\theta\cos3\varphi.\quad (13)$$

[8] W. Voigt, *Lehrbuch der Kristallphysik* (pp. 589–592), 1910.

The values computed from this formula are negative as was to be expected.

(3) *To find the relative change of resistance arising from the change in the angle θ produced by the application of a tension of 1 kg/cm².* Since the specific resistance of a crystal is given by the relation

$$\rho_\theta = \rho_0 \cos^2\theta + \rho_{90} \sin^2\theta \tag{14}$$

we have

$$\frac{d\rho}{\rho} = \frac{2(\rho_{90}-\rho_0)}{\rho_\theta} \sin\theta\cos\theta d\theta. \tag{15}$$

It is immediately evident, as inspection shows to be true also in the case of the previous two corrections studied, that the change in resistance produced by the application of tension is independent of the secondary orientation at $\theta=0°$ and at $\theta=90°$. In the case of this third correction $d\rho$ vanishes at both these limiting points. It remains to find the value of $d\theta$ produced by the tension; $d\theta$ signifies a rotation about the X'-axis.

In determining $d\theta$, it must be borne in mind that the displacement of a point during the deformation of a body is compounded of a pure strain and of a rotation, the former being defined by the six elastic constants and the latter by three additional constants. Let us consider a small section in the middle of the cylindrical casting of the crystal, and let 0 be the very middle point which, since the tension consists of two equal and opposite forces, must remain unchanged in position. Let Q_2 be a point on the principal cleavage plane through 0 and in the plane $Y'OZ'$, Fig. 3. Q_1 is a point on the cylindrical axis having the same Z' coordinate as Q_2 relative to 0; this may be called ζ. The angle $Q_1 0 Q_2$ is by definition $(90-\theta)$. Similarly we may call η the relative Y' coordinate of Q_2.

According to Love, the most general displacement of a point Q after deformation when 0 is kept constant is given by the three expressions:

$$\begin{aligned} e_{xx}\xi + \tfrac{1}{2}e_{xy}\eta + \tfrac{1}{2}e_{xz}\zeta - \eta\omega_3 + \zeta\omega_2 &= dx', \\ \tfrac{1}{2}e_{xy}\xi + e_{yy}\eta + \tfrac{1}{2}e_{yz}\zeta - \zeta\omega_1 + \xi\omega_3 &= dy', \\ \tfrac{1}{2}e_{xz}\xi + \tfrac{1}{2}e_{yz}\eta + e_{zz}\zeta - \xi\omega_2 + \eta\omega_1 &= dz', \end{aligned} \tag{16}$$

where ξ, η, ζ are the coordinates of Q relative to 0 and the ω's are the three additional constants defining the rotation. Applying these equations to the point Q_1 when a tension is acting along OQ_1, i.e., along OZ', we have the conditions, since $\xi_1=\eta_1=0$,

$$\begin{aligned} dx_1' &= 0 \quad \text{or} \quad \tfrac{1}{2}e_{x'z'} + \omega_2 = 0, \\ dy_1' &= 0 \quad \text{or} \quad \tfrac{1}{2}e_{y'z'} - \omega_1 = 0, \\ dz_1' &= e_{z'z'}\zeta. \end{aligned} \tag{17}$$

Applying Eq. (16) to the point Q_2 gives the relations, ξ_2 being zero,

$$\begin{aligned} dx_2' &= \tfrac{1}{2}e_{x'y'}\zeta\cot\theta + \tfrac{1}{2}e_{x'z'}\zeta - \zeta\cot\theta\omega_3 + \zeta\omega_2, \\ dy_2' &= e_{y'y'}\zeta\cot\theta + \tfrac{1}{2}e_{y'z'}\zeta - \zeta\omega_1, \\ dz_2' &= \tfrac{1}{2}e_{y'z'}\zeta\cot\theta + e_{z'z'}\zeta + \zeta\cot\theta\omega_1. \end{aligned} \tag{18}$$

The assumption that there is no motion in the X' direction leads to a perfectly consistent result, i.e., $\frac{1}{2}e_{x'y'}=\omega_3$. From the last two conditions in Eq. (18) we can get the new angle between OQ_1 and OQ_2, since

$$\tan(\theta+d\theta) = \frac{\zeta+dz_2'}{\eta+dy_2'} \tag{19}$$

so that we have the relation

$$d\theta = \sin\theta\cos\theta\{e_{z'z'} - e_{y'y'} + e_{y'z'}\cot\theta\}. \tag{20}$$

This means that the final change in resistance due to change in angle is

$$\frac{1}{T}\frac{\Delta\rho}{\rho} = 2\sin^2\theta\cos^2\theta\frac{\rho_{90}-\rho_0}{\rho_\theta}\{s_{33}' - s_{23}' + s_{43}'\cot\theta\}, \tag{21}$$

and the problem again reduces to the determination of the s''s involved. On this basis, the final expression for the correction of the specific resistance of the crystals arising from the change in the angle θ is

$$\begin{aligned} \frac{1}{T}\frac{\Delta\rho}{\rho} = 2\sin^2\theta\cos^2\theta\frac{\rho_{90}-\rho_0}{\rho_\theta}\{&(s_{11}-s_{13})\sin^4\theta - (s_{33}-s_{13}-s_{44})\cos^4\theta + (s_{11}-s_{33}+s_{44})\sin^2\theta\cos^2\theta \\ &- 2s_{14}\sin\theta\cos\theta\cos 3\varphi\}. \end{aligned} \tag{22}$$

Thus the total effect on the resistance produced by the *strain* caused by the application of tension to trigonal crystals is given by the Eqs. (11), (13) and (22). Since $R=\rho l/A$, the relative change of resistance is

$$\Delta R/R=\Delta l/l-\Delta A/A+\Delta\rho/\rho, \qquad (23)$$

the correction for the change in cross section being subtracted. The numerical values of these corrections in the case of antimony are plotted in Fig. 4 in the same way as the tension coefficients were plotted in Fig. 2. These data are to be used to correct the four constants determined from the experiments with tension, the strain corrections being subtracted from the experimental values and least squares being applied again to these corrected observations. The resulting constants and their probable errors are

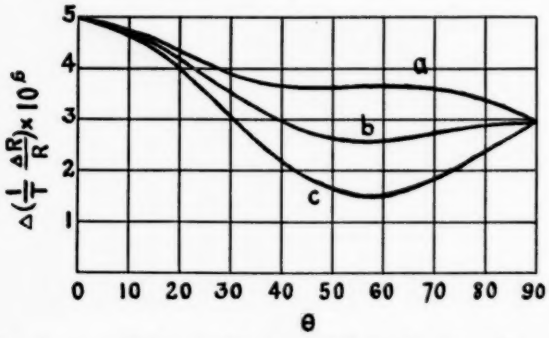

FIG. 4. a, $\varphi=0°$; b, $\varphi=30°$; c, $\varphi=60°$. Strain corrections of the tension coefficients.

$$\begin{aligned}
\rho_{11}&=(-\ 1.07\pm0.09)\times10^{-10},\\
\rho_{33}&=(-13.90\pm0.54)\times10^{-10},\\
2\rho_{13}+\rho_{14}&=(+\ 4.34\pm0.34)\times10^{-10},\\
\rho_{14}&=(+\ 5.81\pm0.16)\times10^{-10}.
\end{aligned} \qquad (24)$$

The curves in which these corrections have been made are indicated in the dotted lines of Fig. 2 and the corrected values of the tension coefficients in the last two columns of Table I.

The two constants derived from pressure measurements must also be corrected for strain. The analysis for this correction for pressure has already been carried out by Professor Bridgman.[7] The correction for angle is again zero for the limiting cases $\theta=0°$ and $\theta=90°$ and that arising from the combined changes in length and cross section is

$$\begin{aligned}((1/p)(\Delta R/R))&=2(s_{11}+s_{12})\cos^2\theta\\&\quad+2s_{13}\sin^2\theta+s_{33}(1-2\cos^2\theta).\end{aligned} \qquad (25)$$

Evaluating this correction in the two limiting cases which are needed, gives the values

$$\begin{aligned}
&\theta=90° \quad ((1/p)(\Delta R/R))_{90}=+5.4\times10^{-6},\\
&\theta=0° \quad\ \ ((1/p)(\Delta R/R))_{0}=+20.0\times10^{-6}.
\end{aligned} \qquad (26)$$

With all these *corrections for strain* the final values of the tension coefficients of resistance are

$$\begin{aligned}
\rho_{11}&=-\ 1.1\times10^{-10}, \quad \rho_{12}=-3.3\times10^{-10},\\
\rho_{33}&=-13.9\times10^{-10}, \quad \rho_{13}=+2.5\times10^{-10},\\
\rho_{14}&=+\ 5.8\times10^{-10}, \quad \rho_{44}=-0.6\times10^{-10}.
\end{aligned} \qquad (27)$$

These may be considered the tension coefficients of specific resistance.

CONCLUSION

In this work with antimony, a crystal of trigonal symmetry, Professor Bridgman's theory of the change of resistance has again been found to be in agreement with experimental results, as in the case of bismuth. The values of the six coefficients defining the change of resistance under the action of stresses have been found directly and have also been corrected for the change arising from strain. The latter procedure is the more defensible from a logical point of view, since the corrections for strain do not depend on the crystal orientations in exactly the same way as do the tension coefficients, so that the uncorrected readings can be expected to satisfy the Bridgman theory only approximately. However, in practice, since the corrections arising from change in cross section and from change in angle differ only slightly in their functional dependence on θ and φ from that of the tension coefficients and the correction for length not at all, both the uncorrected and the corrected observations can be represented within experimental error by Professor Bridgman's equation, the constants involved being of course different in the two cases. This view is upheld by the fact that the probable errors are very nearly equal in the two cases.

It is again a pleasure to thank the Director of the Laboratory, the authorities of Harvard University and particularly Professor Bridgman for the privilege of carrying on this work in the Research Laboratory of Physics.

New Phenomena in the Change of Resistance of Bi Single Crystals in Magnetic Fields

O. STIERSTADT, *Norman Bridge Laboratory of Physics, California Institute of Technology*

(Received August, 1932)

IT is well known that of all metals Bi shows the greatest change of resistance of electrical conductivity in a magnetic field. These changes in conductivity are strongly dependent upon the orientation of the crystal and upon the direction of the crystal axes with respect to the directions of the field and of the current. In the present investigation it has been possible for the first time by means of a specially constructed crystal-goniometer to investigate the conductivity of a metal-crystal in every desired configuration of current, field and crystal axes, which has not previously been done.

The Bi single crystal rods of 5 cm length and 2–3 mm diameter were rotated about an axis, which was always perpendicular to the long-axis of the rod and to the magnetic field. The crystallographic orientation of the single crystal rods gave the following three cases: (1) The principal axis (111) perpendicular to the axis of the rod and parallel to the rotation axis (P_1-crystals); (2) The principal axis (111) perpendicular to the axis of the rod and perpendicular to the rotation axis (P_2-crystals); (3) The principal axis (111) parallel to the axis of the rod and perpendicular to the rotation axis (P_3-crystals).

Besides in each of these three cases one had to discriminate, whether the traces of the imperfect cleavage planes ($11\bar{1}$) in the (111)-plane were perpendicular or parallel to the directions of the current or of the field and whether such extreme positions could be obtained by the rotation of the crystal in the field. This led to a subdivision of the three groups in the following three subgroups: $P_1^{\perp}$ and $P_1^{\parallel}$, $P_2^{\perp}$ and $P_2^{\parallel}$, $P_3^{\perp}$ and $P_3^{\parallel}$.

Fig. 1 shows the behavior of the conductivity of a $P_1^{\perp}$ crystal at a rotation in the constant magnetic field of $H=3000$ AW/cm; Fig. 2 shows the same for the $P_1^{\parallel}$-type. (φ = angle between current and magnetic field.)

It is evident that there is a fundamental difference between the resistance changes of a single crystal and of a polycrystal in a magnetic field. In polycrystalline materials it is well established except in the case of ferromagnetic metals that the change of resistance is greatest, when the direction of the current is at right angles to the magnetic field ($\varphi=90°$) and is least, when it is parallel or antiparallel to the field ($\varphi=0°$, 180°). These curves, however, show that this is not always the case for single crystals.

Measurements on *poly*crystals, therefore, are

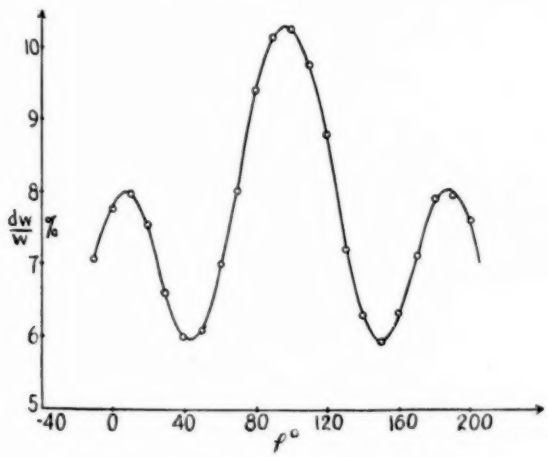

FIG. 1. $H=3000$ AW/cm.

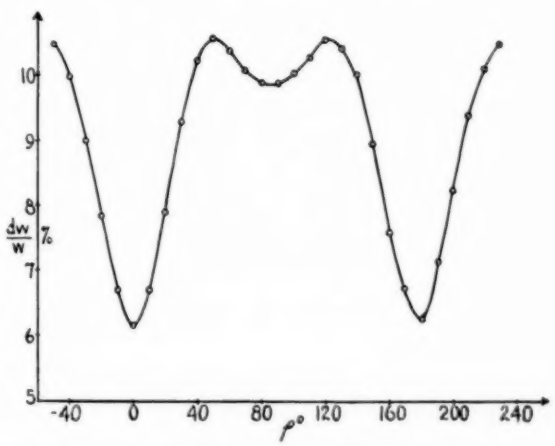

FIG. 2. $H=3000$ tW/cm.

not in general capable of elucidating the real laws of magnetic resistance changes of metals.

The shapes of the curves Figs. 1 and 2 which repeat themselves with a period of 180° [1] suggested the calculation of the Fourier coefficients of these periodic functions. The analysis gave the following results:

$P_1^{\perp}$ (Fig. 1) $A_0=7.7$, $A_1=-1.35$, $A_2=1.5$, $A_3=0.12$.

$P_1^{\parallel}$ (Fig. 2) $A_0=9.2$, $A_1=-1.7$, $A_2=-1.16$, $A_3=-0.15$.

The coefficient A_0 is of little interest as it is independent of the rotation of the crystal in the field.

The frequency A_1 is determined by the variation of the angle between the current and the field and is in no way connected with the symmetry of the crystal. It characterizes only the *poly*crystalline behavior.

The crystallographic significance of the third Fourier coefficient, A_3, is very simple. It is due to the sixfold symmetry of the Bi lattice (six imperfect cleavage planes of the type $11\bar{1}$).[2]

Both frequencies A_1 and A_3 with reference to their respective symmetry elements obey a $\cos^2$ law. Further investigation showed that all the observed phenomena of the magnetic resistance variation of Bi can be expressed as a sum of a series of $\cos^2$ terms.

The last period, A_2, is very difficult to attribute to the primary structure of the Bi lattice, since it goes through not one or three but two cycles upon rotating the crystal through 180°. We shall see from the measurements upon crystals into which small amounts of impurities have been introduced that the Fourier analysis of the curves shows that the *secondary* structure of the Bi lattice is responsible for the frequency A_2.

The P_2 series shows a much simpler behavior of the conductivity in a magnetic field than the P_1 series. Fig. 3a shows the $P_2^{\parallel}$-type. None of the $(11\bar{1})$-planes are brought by rotation into an extreme position with respect to the field, and therefore make no contribution to the change of

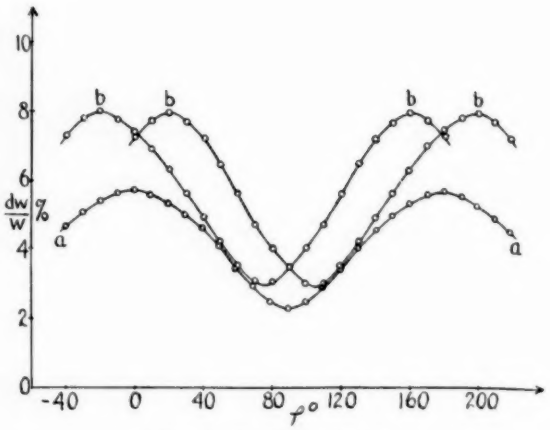

FIG. 3. $H=3000$ tW/cm.

resistance. In the $P_2^{\perp}$-case (Fig. 3b), however, one of the $(11\bar{1})$-planes reaches a perpendicular position with respect to the field at $\varphi=18°\ 25'$ (or at $\varphi=-18°\ 25'$, depending on the starting position of the crystal in the field), and after a further rotation of 90° a parallel position. Therefore the maxima and minima of the curves 3b are shifted from their 0° and 90° positions.

The P_3 crystal shows a very similar behavior.

The P_2 crystal is the first case observed for a nonferromagnetic material in which the magnetic change of resistance is greater when the current is parallel to the field than when it is perpendicular. Such a phenomenon previously has neither been observed nor suspected but follows simply from the fact that the influence of one of the crystal planes is far stronger than that of the direction of the current.

Finally, single crystals of the P_1-type with impurities have been investigated. These crystals show qualitatively the same picture as the pure Bi crystals, especially the appearance of the frequency A_2. Besides the *general* decrease of the resistance change with all kinds of impurities the frequency A_2 is affected in a *characteristic* way by the foreign metal atoms. This is another reason for the supposition that the frequency A_2 is due to a secondary structure. The frequency A_2 is diminished or increased with respect to the other frequencies A_n according to whether the impurities are to the left or to the right of the Bi column of the periodic system.

It is shown in all the above measurements that most of the important crystal planes influence the resistance change in some characteristic fashion.

[1] Complete polar-diagrams from 0° to 360° have been taken.

[2] Cf. Schubuikow and de Haas, Comm. Leid. 207.

This is true of all the planes which are necessary for the description of the elementary cell of Bi lattice. *Direct* electric or magnetic measurements do not discriminate these planes. The magnetic change of resistance may therefore be regarded as a means of crystal analysis. This type of crystal structure analysis is not as generally useful as the optical methods but is a very sensitive one for detecting structure elements which have not yet been found optically.

LETTERS TO THE EDITOR

Prompt publication of brief reports of important discoveries in physics may be secured by addressing them to this department. Closing dates for this department are, for the first issue of the month, the twentieth of the preceding month; for the second issue, the fifth of the month. The Board of Editors does not hold itself responsible for the opinions expressed by the correspondents.

Identification of the (2, 2) Band of Neutral OH. Satellite Series of the (1, 1) Band. Extensions of the (0, 0) Band

Analysis of some plates which we have obtained with very intense exposures of the ultraviolet "water vapor" bands, due to neutral OH, permit us to make approximately 150 new assignments of lines in the band sequence in the neighborhood of λ3064. Among these are about 75 lines which form the six principal branches of the (2, 2) band with its principal head at about λ3185. This brings the number of bands which have been identified in the OH system to a total of eight. The assignments are confirmed by application of the combination principle, both with respect to the upper level, by comparison with the $(\Delta F')$'s of the (2′, 0″) and (2′, 1″) bands, and with respect to the lower level by comparison with the $(\Delta F'')$'s of the (1′, 2″) band, recently identified by Johnston, Dawson and Walker.[1] Rotational and vibrational constants derived for the new (2, 2) band are in good agreement with the values derived from the (1′, 2″) band.

The remaining lines (approximately 75 in number) include the ${}^{RR}R_{21}$ and the ${}^{PP}P_{12}$ satellite series of λ3122, which have, heretofore, been unobserved, as well as extensions of the principal R series of both λ3122 and λ3064 and of the satellite series of λ3064. We also confirm Shaw's recent measurements[2] of 63 new assignments in the principal Q and P branches of λλ3064 and 3122.

A more complete description of the work will be submitted to this journal.

HERRICK L. JOHNSTON
DAVID H. DAWSON

Department of Chemistry,
The Ohio State University,
March 7, 1933.

[1] Johnston, Dawson and Walter, Phys. Rev. **43**, 473 (1933).

[2] R. M. Shaw, Astrophys. J. **76**, 202 (1932).

The Molecular Structure of Ozone

The author had independently reached Badger and Bonner's[1] conclusion that an obtuse-angled model for the ozone molecule is to be preferred to an acute-angled one in interpreting Gerhard's[2] careful results on the infrared absorption bands of that substance. It still seems of interest to submit the present interpretation, which differs from Badger and Bonner's in the frequency assumed for the missing fundamental ν_2, if only to emphasize the need for further measurements. Table I compares the various interpretations.

$\nu_2=440$ is thus seen to give somewhat worse agreement with the observed combination bands than does 760. Moreover, Wulf's[3] assignment of the 440 cm^{-1} interval between two progressions in the visible band system to ν_2 of the normal state does not seem secure, as it is unsupported by measurements of temperature coefficient of

[1] Badger and Bonner, Phys. Rev. **43**, 305 (1933).

[2] Gerhard, Phys. Rev. **42**, 622 (1932).

[3] Wulf, Proc. Nat. Acad. Sci. **16**, 407 (1930).

TABLE I. *Various interpretations.*

Observed Frequency (cm^{-1}) and type	*Calculated* Gerhard	Badger & Bonner	Benedict
—	$\nu_2=528$ (Z)	$\nu_2=440$ (D)	$\nu_2=760$ (D)
879 (N_2O_5 as impurity?)	—	$2\nu_2=879$ (D)	—
1030–1060 (irregular D)	$\nu_3=1033$ (D) $2\nu_2=1055$ (Z)	$\nu_1=1050$ (D)	$\nu_1=1046$ (D)
1355 (Z)	$\nu_1=1355$ (Z)	$\nu_3=1355$ (Z)	$\nu_3=1357$ (Z)
1515 (?)	$\nu_2+\nu_3=1561$ (D) $3\nu_2=1584$ (Z)	—	$2\nu_2=1520$ (D)
2108 (wide, irregular)	$2\nu_3=2066$ (Z) $2\nu_2+\nu_3=2088$ (D) $4\nu_2=2110$ (Z)	$2\nu_1=2100$ (D)	$2\nu_1=2085$ (D) $\nu_2+\nu_3=2117$ (Z)
2710 (?)	$2\nu_1=2710$ (Z)	$2\nu_3=2710$ (D)	$2\nu_3=2710$ (D)

absorption, and so may be a frequency difference of the upper state; and Wulf and Melvin[4] in other careful quantitative measurements on the ultraviolet absorption, found no indication of such a low frequency.

Further confirmation of the obtuse-angled structure, and a rough determination of the molecular dimensions, may be obtained from a consideration of the envelope of the irregular double absorption region 1030–1060 cm^{-1}. If ozone, with three atoms of like mass, has an apex half-angle $>45°$, the ratio of the least to the middle moment of inertia, $A/B=\rho<0.33$, and the molecule is of the class of "slightly asymmetric" molecules whose infrared bands are sketched by Nielsen.[5] Assignment of the absorption region to ν_1 means that the band is of Nielsen's type B, the electric moment vibrating along the middle axis of inertia. The general resemblance, particularly in the occurrence of a gap at the center of the band, is apparent; it must be remembered that many more lines will appear in the actual spectrum than on Nielsen's charts, transitions from levels as high as $J=30$ occurring with intensities of the same order of magnitude as lines near the center. The outstanding difference between the observed envelope and Nielsen's sketch—the unsymmetrical appearance that led Gerhard to ascribe the absorption to two distinct vibrations—may be accounted for by interaction of vibration with the rotation. The magnitude of such distortion is not so remarkable as it may seem on first sight: for in ν_1 the apex oxygen atom moves along the B axis with an amplitude twice the component of the amplitude of the end atoms along that axis. Thus on the crude mechanical picture of the vibration, a stretching of the bond between adjacent O's sufficient to increase the effective moment of inertia around the B axis by $\Delta B/B=x$, will increase the moment around the A axis by $\Delta A/A=3x$. And since A is the most powerful constant in fixing the position of the modified Q-branches that contribute most to the absorption envelope, a small x, of the order of magnitude of the diatomic-molecule convergence factor α, will cause a very considerable distortion of a type B band. This mechanical picture of the convergence is of course not exact, and further distortions are to be expected due to rotational centrifugal effects at the higher J values; however, envelopes were constructed, using the above model and energy levels of the asymmetric rotator derived by an approximative method similar to that of Ray,[6] and a fairly good duplication of the observed envelope was obtained with $A=6.4\times10^{-40}$, $B=71\times10^{-40}$ g cm^2, and $x=0.015$. These correspond to an apex half-angle of 61° and an 0–0 distance of 1.29A. These dimensions are very rough, for the reasons given above and because the envelope of an incompletely resolved band may present misleading features, as Professor Dennison has kindly pointed out, but they are quite reasonable and possibly accurate to ±10 percent.

The other bands whose envelopes are known are in agreement with this model. ν_3 at 1357 cm^{-1} shows the characteristic zero branch, shifted slightly to lower frequencies by convergence, and widened by asymmetry so that the maxima of the P and R branches are no longer resolvable. In the region of 200 cm^{-1} two bands, both presumably greatly distorted by vibrational convergence, overlap to give the observed irregular envelope.

Substitution of the three fundamental frequencies $\nu_x=1046$, $\nu_\sigma=1357$, $\delta=760$ into Mecke's[7] formulas (modified valence force system), gives real and reasonable values for the force constants only for apex half-angles ranging from 56 to 60 degrees, in satisfactory agreement with the angle obtained above.

WILLIAM S. BENEDICT

Contribution No. 303 from the Research Laboratory of Physical Chemistry, Massachusetts Institute of Technology, Cambridge, Mass., March 1, 1933.

[4] Wulf and Melvin, Phys. Rev. **38**, 330 (1931).
[5] Nielsen, Phys. Rev. **38**, 1432 (1931).
[6] Ray, Zeits. f. Physik **78**, 74 (1932).
[7] Mecke, Zeits. f. physik. Chemie **B16**, 421 (1932).

Vibrational Isotope Effects in Polyatomic Molecules. II

From considerations of symmetry, Langseth[1] has obtained expressions for the effects of isotopes of X atoms on the normal vibrations of pentatomic molecules YX_4. Following the method already used for symmetrical triatomic and tetratomic molecules,[2] we have developed the Dennison equations for the normal vibrations of molecules YX_4, obtaining relations for isotope effects due to isotopes of Y atoms and of X atoms. In the case of X atom isotopy, our results agree with those of Langseth for the inactive frequencies, but differ, for reasons to be pointed out in our complete paper, for the isotope shifts of the active frequencies. We shall merely state some of our results here, in particular those independent of the force constants.

Dennison[3] has shown that the frequencies of the symmetrical molecule YX_4 are: frequency ω_1 (single and inactive), ω_2(double and inactive), ω_3 and ω_4 (both triple and inactive). We shall refer to the frequency ω_i of the molecule with isotopes of either Y or X atoms as ω_i'.

Let M be the mass of Y atom, m the mass of X atom, $M+\Delta M$ the mass of isotope of Y, $m+\Delta m$ the mass of isotope of X, and $\mu=M(4m+M)^{-1}$.

Consider, first, molecules

$$Y^{(M)}X_4^{(m)} \quad \text{and} \quad Y^{(M+\Delta M)}X_4^{(m)}.$$

Then there will be no isotope shifts of the inactive frequencies, since the motion does not involve the Y atoms. The isotope shift of each active frequency depends upon the force constants, but the following relation is independent of the constants:

$$\omega_2'\omega_4'/\omega_3\omega_4=\mu^{\frac{1}{2}}(1+4m/M+\Delta M)^{\frac{1}{2}}. \qquad (1)$$

[1] A. Langseth, Zeits. f. Physik **72**, 350 (1931).
[2] E. O. Salant and J. E. Rosenthal, Phys. Rev. **42**, 812 (1932).
[3] D. M. Dennison, Rev. Mod. Phys. **3**, 303 (1931).

For molecules $Y^{(M)}X_4^{(M)}$ and $Y^{(M)}X_3^{(m)}X^{(m+\Delta m)}$, we have different relationships, naturally. For the inactive frequencies:

$$\omega_1'/\omega_1=\omega_2'/\omega_2=(1+\Delta m/4m)^{-\frac{1}{2}}. \quad (2)$$

The triple frequencies ω_3 and ω_4 of $YX_4^{(m)}$ are now replaced by two double frequencies, say ω_3' and ω_4' and two single frequencies, say ω_5' and ω_6', each depending on the force constants (this is the result essentially different from Langseth's), but related by

$$\omega_3'\omega_4'/\omega_3\omega_4=1-(\Delta m/8m)(\mu+\tfrac{1}{2}) \quad (3)$$

and

$$\omega_5'\omega_6'/\omega_3\omega_4=1-(\Delta m/8m)(\mu+2). \quad (4)$$

The degeneracy of the active vibrations is, as Langseth pointed out, completely destroyed in the molecule $Y^{(M)}X_2^{(m)}X_2^{(m+\Delta m)}$, but again we find that the frequency shift of each active vibration is not calculable from the masses alone, only shifts of certain pairs of frequencies being thus simply determined. This different result is, of course important in the use of the isotope effects for the assignment of the spectroscopic frequencies to the proper normal vibrations.

We are greatly indebted to Dr. Louis S. Kassel of the United States Bureau of Mines for pointing out to us that the relative concentrations of the different isotopic species, as stated on page 433,[2] are in error and should read

$$1 : 2a/b : (a/b)^2 \quad \text{and} \quad 1 : 3a/b : 3(a/b)^2 : (a/b)^3.$$

The relative abundances of the CCl_4 molecules with different proportions of isotopes of Cl were noted by Langseth. In general, if the relative concentration of $X^{(m)}$ to $X^{(m+\Delta m)}$ is b/a, then the molecules are present in the following proportions:

$$YX_4^{(m)} : YX_3^{(m)}X^{(m+\Delta m)} : YX_2^{(m)}X_2^{(m+\Delta m)} : YX^{(m)}X_3^{(m+\Delta m)} : YX_4^{(m+\Delta m)} = 1 : 4a/b : 6(a/b)^2 : 4(a/b)^3 : (a/b)^4.$$

Physics Department,
New York University,
March 8, 1933.

E. O. SALANT
JENNY E. ROSENTHAL

The Nuclear Spin of Sodium

We have made a direct measurement of the nuclear spin of sodium by means of the magnetic deflection of a beam of neutral sodium atoms.[1] Sufficient resolution is attained by the use of a magnetic velocity selector consisting essentially of an inhomogeneous magnetic field which spread the beam into a velocity spectrum, the field being of sufficient strength to cause a complete decoupling of the nuclear and electronic spins. By means of a movable selector slit we select a portion of this beam homogeneous in velocity to about 10 percent and corresponding to about half the velocity of the Maxwell distribution.[2]

This beam is then permitted to pass through a weak inhomogeneous field of the Stern-Gerlach type. This field is so chosen that there is still strong coupling between the nuclear and electron spins. Each magnetic level is thus under the influence of a different deflecting force and the beam splits up into a number of components. The beam is then further allowed to traverse a strong inhomogeneous field of the same type, supplied by a third magnet, so arranged as to bring the whole deflection pattern into the neighborhood of the original position of the undeflected beam. This serves as a focussing device to sharpen up the lines. The length of path of the beam is 61 cm. The method of detection is the Langmuir-Taylor surface ionization detector used ballistically.[2]

The beam splits up into four distinct components as shown in Fig. 1 which represents the experimental points of one particular run directly. We have checked this result under varied conditions. The peak marked A does not belong to the deflection pattern for the selected atoms. It is due to fast atoms from the small tails of the original beam. This we have proved abundantly.

The total number of magnetic levels of the atom is $(2I+1)(2J+1)$ where I is the nuclear spin, in units of $h/2\pi$ and J is the angular momentum of the external electron configuration. For sodium $J=\frac{1}{2}$, and the number

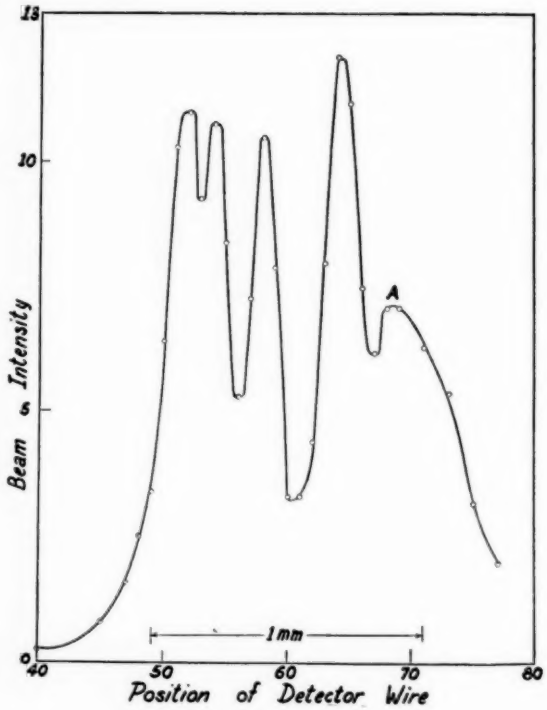

FIG. 1.

[1] Breit and Rabi, Phys. Rev. **38**, 2082 (1931).
[2] Rabi and Cohen, Phys. Rev. **43**, 377 (1933).

of levels is $4I+2$. Our method of velocity selection in a strong field involves the use of only one-half the total number of levels. We therefore obtain $2I+1$ components in the deflection pattern. Since we have four components we accordingly find the spin of the sodium nucleus to be $3h/4\pi$.

A complete description of the method and results will be published in this journal.

I. I. RABI
V. W. COHEN

Columbia University,
March 11, 1933.

Angular Distribution of Low Energy Cosmic Radiation and Interpretation of Angular Distribution Curves

One of us has made an experimental determination of the angular distribution of the cosmic radiation at two different elevations,[1] but an interpretation of the data on the assumption of straight line paths through the atmosphere was not advocated since it was uncertain to what extent the distribution might have been affected by divergences between the paths of primary and secondary rays and by scattering in their passage through the atmosphere. Since it is known that the soft rays suffer the greater deviations[2] we have measured the angular distribution of the radiation which is stopped by 3.8 cm of lead in order to determine the extent to which such scattering affects the angular distribution. At every 15 degree interval between the vertical and horizontal measurements of the coincidence counting rates of three G.M. counters[3] were made alternately with and without a block of lead inserted just above the lower counter.

Each counting rate was the average of fifteen or more independent data, an analysis of which showed that the fluctuations agreed with those to be expected statistically and for which the standard deviation is the quotient of the square root of the total number of counts by the total time. Two such complete runs taken several weeks apart were in good agreement. The differences in counting rates with their probable errors as calculated by combining both sets of data are shown by the experimental points in Fig. 1.

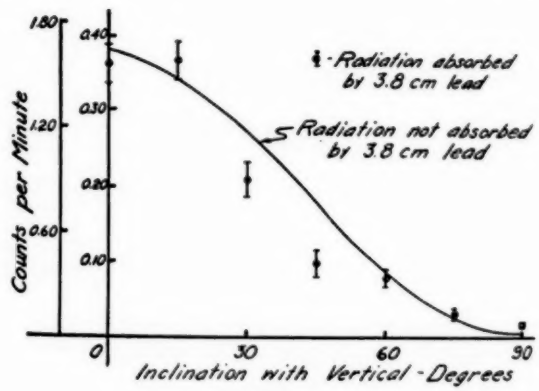

FIG. 1.

For comparison the continuous line represents the distribution of the rays which penetrated the lead plotted to a reduced scale. Although there is an indication that a small fraction of the soft rays, equal to about fifty percent of the horizontal rays, has been scattered through large angles, the majority are fully as concentrated about the vertical as are the penetrating rays, and we may conclude that the distribution of the total radiation is not appreciably broadened by scattering. We may, therefore, interpret the angular distribution of the total radiation on the basis of straight line paths through the atmosphere.

Assuming a simple exponential law the theoretical distribution is:

$$j(\theta)=j_0 e^{-\mu h \sec\theta}$$

In Fig. 2 are plotted three sets of experimental data showing the distributions on Mt. Washington, New Hampshire,

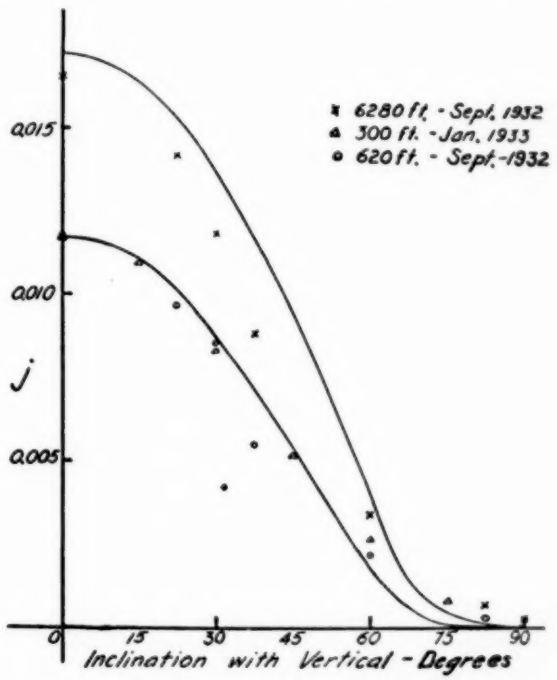

FIG. 2. Distribution of total radiation. Points are experimental; solid curves are computed for $\mu=0.18$ per meter of water for elevations sea level and 6280 ft.

at a base station near Mt. Washington, and on the roof of the Bartol Laboratory. The theoretical distributions for sea level and the top of Mt. Washington for $\mu=0.18$ per meter of water are represented by the continuous curves. The agreement between the observed and calculated dis-

[1] T. H. Johnson, Phys. Rev. **43**, 307 (1933).
[2] C. D. Anderson, Phys. Rev. **43**, 381 (1933).
[3] T. H. Johnson and J. C. Street, J. Frank. Inst. **215**, 239 (1933).

tributions at sea level is remarkably good and the absorption coefficient is in good agreement with the value 0.16 deduced by Millikan and Cameron[4] from the portion of their ionization-depth curve adjoining sea level. For the Mt. Washington elevation there would seem to be a discrepancy between the observed intensities and those calculated from $\mu=0.18$. There is, however, some uncertainty in the relative intensities as measured at the two different elevations arising from a change in the efficiency of the counters with counting rate. Although the change in efficiency was measured[1] the uncertainty of the measurement is sufficient to account for this apparent discrepancy. However, if the absorption coefficient increases with elevation as rapidly as indicated by the data of Millikan and Cameron, unaccountable differences appear between calculated and observed intensities both as regards angular distribution and relative values.

THOMAS H. JOHNSON
E. C. STEVENSON

Bartol Research Foundation of
The Franklin Institute, Swarthmore,
March 13, 1933.

[4] Millikan and Cameron, Phys. Rev. **37**, 235 (1931).

A Neutron of High Velocity, and Energy Relations for Nuclear Disintegration by Non-Capture

1. High velocity neutron

One of the photographs which we have obtained of the disintegration of N^{14}, by capture of a neutron from beryllium, into B^{11} and He^4 is remarkable with respect to the length of the track of the boron nucleus. The energy of the neutron which caused the disintegration is found by calculation to have been 16×10^6 electron-volts, which is about twice the value 7.8×10^6 usually[1] given for "fast" neutrons. The velocity of this neutron is found as 5.6×10^9 cm per sec. From the mass[2] 9.0155 of the beryllium atom, it is found that 6.9×10^6 electron-volts is the amount of energy given by the change of mass in the reaction with the incident α-particle, provided C^{12} is formed, or considerably less if the product is three α-particles. The α-particles used in the disintegration of the beryllium were those from Th *C'*, which for the ordinary higher velocity have an energy of 8.8×10^6 electron-volts. Thus, if no γ-rays are emitted in the process of emission of the neutron, the total energy available is 15.7×10^6 electron-volts, or, making allowance for the kinetic energy imparted to the C^{12} nucleus, the maximum energy of the neutron should be 14.7×10^6 electron-volts. The fact that the energy found experimentally is greater by 1.3×10^6 electron-volts might be due to the action on the beryllium of a particle of higher velocity than that assumed, but is much more probably due to the fact that present knowledge of the range-velocity relations of B^{11} is not sufficiently exact to give a better agreement. The high energy found seems to indicate that the amount of energy which is transformed into γ-rays when the neutron is emitted is zero or very small.

2. Disintegration by non-capture

If the neutron is not captured, then the reaction may be:

$$N^{14}\rightarrow B^{10}+He^4, \quad \Delta m=0.0077 \text{ mass units} \qquad (1)$$

$$N^{14}\rightarrow C^{13}+H^1, \quad \Delta m=0.0038 \qquad (2)$$

$$N^{14}\rightarrow C^{12}+H^2, \quad \Delta m=0.0091 \qquad (3)$$

However, (2) and (3) are excluded, at least in many of these events, by the fact that the track of the light atom has too great a line density of ions to be due to hydrogen.

The mass increase in (1) is 0.0077 as given by Aston's data. This corresponds to a gain of energy of 7.1×10^6 electron-volts. Thus the neutron must lose $(7.1\pm4.4)\times10^6$ electron-volts. The error of 4.4×10^6 electron-volts included here is the arithmetical sum of all of Aston's estimated errors, which are not likely to be all in one direction, so that the probable error is less than this.

The energy which must be supplied lies between 6 and

[1] I. Curie and F. Joliot, Nature **130**, 57 (1932).
[2] Bainbridge, Phys. Rev. **43**, 367 (1933).

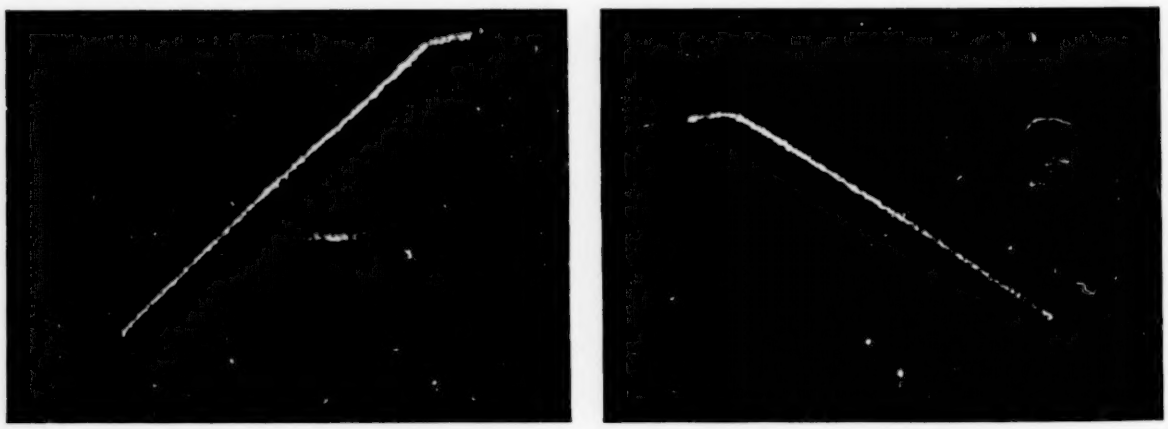

FIG. 1.

8×10^6 electron-volts if Aston's data are as accurate as is assumed by Chadwick.[3] In disintegrations of this type the kinetic energies of B^{10} and He^4 commonly amount to 1 to 3×10^6 electron-volts, so that in all about 9×10^6 electron-volts should be obtained from the loss of kinetic energy of the neutron. There is thus at present no good explanation from the energy standpoint as to how such disintegrations by non-capture are able to occur, particularly in the work of Feather, who used the comparatively slow α-particles from polonium, and thus obtained neutrons of energy 8×10^6 electron-volts.

Fig. 1 shows two views of a disintegration of a nitrogen nucleus, seemingly without capture of the neutron, since the plane of the event is such that the neutron could not have had a straight line path from the source if the event had occurred with capture.

WILLIAM D. HARKINS
DAVID M. GANS
HENRY W. NEWSON

G. H. Jones Laboratory,
University of Chicago,
March 13, 1933.

[3] Chadwick, Proc. Roy. Soc. **A136**, 692 (1932).

A New Kind of Radioactivity

The complexity of the process by which neutrons are produced and their energy measured invites a careful analysis of the data obtained. Such an analysis has bearing on several other problems but the present note will deal only with the application to the Be^9 nucleus. A more complete account will soon be published.

It appears that the experiments so far used to determine the upper limit to the range of protons produced by neutrons lead to an underestimate. The error may well be greater than twenty percent of the maximum range observed. It follows that Be^9 has more energy than two alpha-particles and a neutron.[1] From general considerations and especially on quantum theoretical grounds we are led to the conclusion that Be^9 should decompose spontaneously, giving off alpha-particles and possibly a neutron. If a He of mass five is temporarily stable no neutron would appear for awhile at least.

This matter has been investigated and the prediction verified. After a little trouble some radium-free Be was obtained. The activity was low enough to explain the failure of older workers to notice the effect. The contamination by the radium family as measured by radon content was less than enough to produce one percent of the activity. The thoron content showed, however, that the thorium family might have contributed twenty-five percent of the ionization measured. It can then be argued that the actinium family was also harmless. However, the question was decided definitely by range determinations with Al foils. The range proved to be about one centimeter in air and therefore quite easily distinguishable from the ordinary alpha-disintegrations.

The corresponding half-life turns out to be about 10^{14} years. This is in striking accord with the helium content of certain Beryls which has puzzled geologists since Rayleigh's[2] measurements. The explanation which has been offered for the abnormally high helium content of Beryls in terms of the radioactivity of Be^8 is now unnecessary and in fact certain strong objections can be offered against it. That is to say, we can estimate the mass of Be^8 from that of Be^9 or from the energy of the short range group of particles emitted in the bombardment of Li by protons. From these data it seems that the half-life of Be^8 would be extremely short and that this isotope could play absolutely no part in the chemistry of beryllium, it would have disappeared before any Beryl crystal could have been formed. The helium contained in Beryl may prove extremely interesting in connection with the existence of He^5. This isotope would exist in vanishing proportions in He from ordinary sources but might be a large fraction of the helium which results from the decomposition of Be^9.

Further investigations with counters and especially with the expansion chamber will, it is hoped, lead to results which will help to determine accurately the masses of the neutron and all the other light nuclei. Such information is essential to the development of the theory of the nucleus. In particular, alpha-disintegration can now be studied in an almost ideally simple case and defects in the present theory should be brought to light.

R. M. LANGER
R. W. RAITT

California Institute of Technology,
Pasadena, California,
March 14, 1933.

[1] In an article which has just come to hand, K. T. Bainbridge (Phys. Rev. **43**, 367 (1933)) announces a mass-spectroscopic determination of Be^9. His value is rather higher than we predicted but it is conceivable that our present determination of range is off enough to account for the discrepancy.

[2] Cf. Bulletin of the National Research Council, *Physics of the Earth* IV, p. 405.

The Equilibrium Theory of the Abundance of the Elements

It is possible to consider by statistical mechanics an assembly containing radiation, atomic nuclei, electrons, and neutrons; when all possible transmutations of the nuclei occur without the "annihilation" of any ultimate particles. One can calculate the abundances of the nuclei of the various sorts in such an assembly, when it is in equilibrium, in terms of the atomic masses and packing fractions. The simplest procedure is possible if the nuclei

(and neutrons) are made of electrons and protons; in this case three independent parameters, of which one is the temperature, suffice to determine all the equilibrium properties of the assembly. If the nuclei are made, on the other hand, of protons and neutrons as the ultimate particles, very nearly the same treatment will suffice. In the simpler of these two cases, a parameter ξ is associated with the extranuclear electrons in the assembly and a parameter η with the extranuclear protons. Corresponding to any nucleus of mass number M_s and atomic number N_s there exists a parameter μ_s given by

$$\mu_s = \xi^{M_s - N_s} \eta^{M_s} \exp(-Q_s/kT)$$

where Q_s is the energy required to build the nucleus s out of electrons and protons. The number of nuclei present (in the equilibrium state) of sort s is then

$$\overline{X}_s = \mu_s(\partial/\partial\mu_s)\Sigma \log f[\mu_s \exp(\epsilon/kT)]$$

and there are other familiar expressions for the other equilibrium properties.

It may happen that these equilibria are established nearly perfectly in the stars. The writer hopes to publish the theory shortly.

T. E. Sterne*

Harvard University,
March 15, 1933.

* National Research Fellow.

Conductivity of Rare Gases Irradiated by Their Own Resonance Radiations

At the Atlantic City meeting of the American Physical Society the writers[1] reported on an investigation of the conductivity of rare gases irradiated with their own resonance radiations and on the effect of the addition of small traces of impurities on this conductivity. The conductivity was determined by the volt-ampere characteristics of a pair of parallel plane disk collectors in the irradiated gas. The currents obtained do not reach a saturation value at any of the pressures or voltages used (1–12 mm; 0–150 v). This observation was also indicated by Penning[2] and has been recently confirmed by Kenty.[3] The writers have attributed this lack of saturation to the collection of those ions formed in the outer volume of the gas as well as those formed in the region between the collectors. To test this hypothesis volt-ampere characteristics were taken for a pair of parallel plane disk collectors fitted with guard rings. The collectors which were 5 mm in radius and had guard rings 5 mm wide were separated 5 mm. Collectors and leads were insulated with glass except on the adjacent faces of the collectors and rings. When they were mounted at right angles to the tube axis so that the space between them was shielded from the direct radiation, then, except at the lowest pressures, no measurable current ($<10^{-10}$ ampere) flowed between the guarded collectors. The total current (to collectors and guard-rings), however, was the same as that previously observed between unguarded collectors. When the collectors were turned so that the primary radiation illuminated the space between them, appreciable currents were obtained and the much larger total current was of the same order of magnitude as before. In no case were the collector surfaces exposed to the primary beam.

These results lead to two conclusions: first, that the ions which give rise to the observed conductivity must be formed in the space between the collectors; and second, that any metastable atoms which may produce these ions must also be formed in this space. It is difficult to reconcile these results with the propagation of resonance radiation through the gas by diffusion. In previously reported experiments, where collectors were found to receive measurable currents when shielded from the direct primary radiation, the collectors were unguarded and the observed currents probably were due to the collection of ions formed in the space surrounding the collectors. These ions could reach the collector edges. Hence the difference between the currents received by such an unguarded collector when turned parallel and then perpendicular to the primary beam is not to be attributed solely to the effects of the direct and scattered radiations. In Ne which contains a trace of A, with the collectors floating with respect to the discharge, the currents measured to the guard rings may be ten to fifty times those measured to the inner disks. Moreover, the currents measured between the guarded collectors exhibit decided maxima for small collector voltages (<10 v). These were first observed by Penning[2] who attributed them to ions diffusing in from the surrounding volume when the field between the collectors was so small that the ions were not trapped by the guard rings. This explanation the writers believe to be correct. Penning's use of guarded cylindrical collectors did not involve a change in their orientation with respect to the primary radiation.

If resonance radiation is not propagated to any considerable extent by scattering or absorption and reradiation in cases such as these where impurities are present which dissipate the energy of the scattered radiation, one must look for a new explanation for the conductivity observed in a side tube at right angles to the main discharge tube. It is possible that some of the primary radiation may be reflected into the side tube by the tube walls. In this case the degree of reflection by the tube walls must be greater than has generally been supposed so that less of the primary radiation is absorbed by the walls than has been supposed. Kenty[3] has already suspected that this may be true. If the observed conductivity is due to the action of the direct primary beam rather than to that of

[1] Duffendack and Smith, Phys. Rev. **43**, 374 (1933).
[2] Penning, Zeits. f. Physik **78**, 7 and 8, 454 (1932).
[3] Kenty, Phys. Rev. **43**, 181 (1933).

the scattered secondary radiation it is difficult to explain the relatively large conductivity observed in rigorously purified gas under conditions such that the photoelectric action of the primary beam is very small. However, if the scattered radiation plays any important rôle one would expect at least measurable currents for any orientation of the collectors. More complete and accurate data are necessary before any final conclusions can be drawn. The experiments are being continued.

O. S. DUFFENDACK
R. W. SMITH

Department of Physics,
University of Michigan,
March 15, 1933.

The Torque on Faraday's Magnet

Much of the recent discussion[1] of the torque on Faraday's revolving magnet concerns merely the choice between several simple ways of making the calculation, all of which yield correct results. On the other hand there is also a natural desire to understand this torque as arising from the same simple laws that are definitely known to hold for forces upon currents alone and upon magnetized matter alone; and in regard to this point divergent views have developed owing to the fact that here the torques upon current and magnetized matter cannot be separated in experiment and the distinction between them must of necessity rest in part upon speculative hypothesis.

By considering simple examples it can be seen that in the present state of knowledge no general answer to the question can be given. Two different possible distributions of the current among the molecules of the magnet will be described which would be indistinguishable to an observing physicist and yet which are of such a nature that in one case the torque certainly acts upon the magnetized matter while in the other it just as certainly acts upon the current. These two examples thus confirm the conclusion reached by various authors[2] on the basis of electron theory that in such cases the distribution of the true forces as between current and magnetic matter must depend upon the exact path of the conducting electrons through the material.

For simplicity let us as usual give to the magnet the form of a cylindrical bar uniformly magnetized longitudinally and mounted so as to revolve freely about its axis, and let the current enter with symmetrical distribution about the middle of the bar and leave at a point on the axis at one end. We shall also suppose the external circuit to be so arranged that the current exerts no torque upon that part of itself which lies within the magnet. The total torque on the bar is then known to be $i\Phi/2\pi$ where i is the total current and Φ the flux of induction through the cross section at which the current enters.

First distribution of the current

Let the magnetized matter consist of very thin wedges meeting by their edges along the axis of the bar, and let the current flow entirely through similar wedge-shaped spaces left between these wedges of magnetic matter (Fig. 1a).

In this case the observed torque arises entirely from forces exerted upon the magnetic matter by the partial field H_i due to the current. In the spaces through which the current flows we have, besides H_i, only the relatively weak "demagnetizing" field H_m due to the magnet, which at most points in the bar has a direction opposite to that of the principal flux; the effect of this field, acting upon the current, is only to produce a small back-torque in opposition to the principal one.

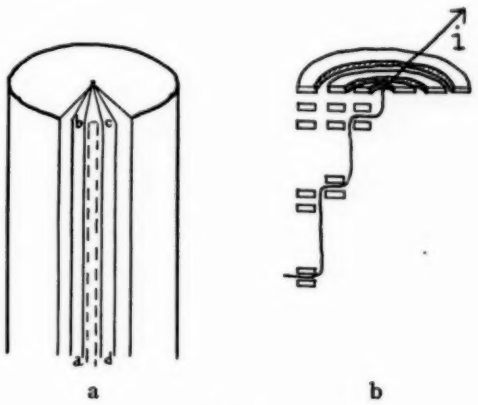

FIG. 1.

At first sight one is tempted to think that, on the contrary, the field of the current cannot possibly cause the magnet to revolve because of the symmetry, for if the magnet turns through an angle $d\theta$ the work done upon one of the Amperian circuits in it is measured by the change in the flux through that circuit, and there seems to be no such change. The displacement $d\theta$ must, however, be taken indefinitely small; and just as the Amperian circuit begins its displacement it approaches the wedges of current on one side and recedes from those on the other (the current being of course assumed to stand still). The flux through the circuit will therefore vary a little, and as a matter of fact a calculation of this variation leads at once to the actual torque. Displacing a wedge through $d\theta$ is equivalent to transferring a slice of thickness $d\theta$ from one side to the other, say from ab to cd. If now we integrate along a path $abcdefa$, where e and f lie at the other end of the bar, $\int \mathbf{H}_i \cdot d\mathbf{s} = 0$; but $\int_e^f = 0$, and, since bc forms part of a circle enclosing the entire current, $\int_b^c \mathbf{H}_i \cdot d\mathbf{s} = (d\theta/2\pi)4\pi i = 2id\theta$. Thus $\int \mathbf{H}_i \cdot d\mathbf{s}$ differs along the two sides of the wedge by $2id\theta$ and the work done upon the displaced slice, if its cross-sectional area is dA, will be $2iId\theta dA = id\theta d\Phi_m/2\pi$ (I = magnetization, $\Phi_m = 4\pi AI$). The torque on the magnetized matter is thus $(i/2\pi)\int d\Phi_m$, and subtracting the

[1] Zeleny and Page, Phys. Rev. **40**, 299 (1932); **24**, 544 (1926); Kimball, Phys. Rev. **28**, 1302 (1926).

[2] Cf., e.g., Kennard and Wang, Phys. Rev. **27**, 460 (1926).

small back torque on the current itself mentioned above we have, as usual, $i\Phi/2\pi$.

Second distribution of the current

Going now to the other extreme, let the magnetized matter have the form of very flat narrow cylindrical rings placed coaxial with the bar, and let the current flow alternately radially and longitudinally through similar cylindrical slots between the rings, as suggested schematically in Fig. 1b; let us suppose that the current otherwise ignores the molecular structure and distributes itself with exact symmetry about the axis. (The current must also be prevented from slipping sidewise by a suitable constraint.)

In this case the torque arises from the field of the magnet acting upon the current. For in this case H_i is strictly symmetrical and the argument just given shows correctly that the torque on the magnetic material vanishes; all of the lines of B are cut by the current and the usual calculation gives for the torque exerted on the current alone $\int riB\,dr = i\Phi/2\pi$ where $\Phi = \int B 2\pi r dr$.

The real case

Now so far as one can tell by inspection a magnet might actually be constructed according to either of the two models just described. If the conducting electrons were to move with entire disregard of the atoms, passing freely through them, then the mean force on the electrons would be determined by the mean value of the true magnetic intensity or B, and we should have an equivalent of our second distribution. It seems improbable, however, that the electrons do so move; they should tend to follow the spaces between the atoms (or to do something equivalent to this in quantum mechanics), and the result will then depend upon local conditions. If the interatomic space through which an electron slips resembles more nearly a longitudinal crack, we have an approach to the case of our first example (mean torque on magnet); if a transverse crack, an approach to the second (mean torque on the electron). It seems thus to the writer most probable that the torque in actual cases arises partly in one way and partly in the other, the amount arising from each cause being at present unknown.

If this be granted, then we cannot say that the force on a current is definitely either $j\times B$ or $j\times H$. We can only assert that either of these expressions, if paired off with the proper assumption as to forces on the magnetic material, will give correctly the total force-action upon a rigid body (or an incompressible liquid).

E. H. KENNARD

Cornell University,
March 20, 1933.

Improved Calculation of Ground State of H_2

The work of Hylleraas[1] on He shows that a great improvement in the treatment of a two-electron problem can be obtained by using wave functions in which the electronic separation enters explicitly. We have extended this method to the H_2 molecule, and wish to communicate our preliminary results.

The dissociation heat as measured experimentally is 4.46 ± 0.04 volts according to Richardson and Davidson,[2] 4.44 volts as given by Mulliken.[3] Adding the zero-point energy, 0.27 volt, gives -4.73 ± 0.04 as the energy of H_2 at the equilibrium nuclear separation, 1.4 Bohr radii (0.74A), referred to zero for separate atoms. Our computed values for three nuclear distances, R, are as follows, compared with the values read from a Morse curve constructed from spectroscopic data and passing through the minimum just described:

R	1.3	1.4	1.5
E(calc.)	−4.63	−4.69	−4.59
E(Morse)	−4.67	−4.73	−4.68

These results were obtained with a wave function in the form of a series:

$$\psi = \Sigma_{mnjkp} C_{mnjkp} e^{-\delta(\lambda_1+\lambda_2)}[\lambda_1^m\lambda_2^n\mu_1^j\mu_2^k\rho^p + \lambda_1^n\lambda_2^m\mu_1^k\mu_2^j\rho^p].$$

Here λ_1, μ_1 and λ_2, μ_2 are the ordinary elliptical coordinates of the two electrons respectively, and ρ is the ratio of their separation to $R/2$. The summation extends in principle over all not negative values of the indices such that $j+k$ is even, but we find such rapid convergence that no index need be carried higher than 2. The screening constant δ and the coefficients C are parameters to be varied in the usual way, in order to minimize the energy, and have different values for each R. So far, however, we have computed only with $\delta=0.75$. The terms used, and their coefficients for $R=1.4$, are as follows:

m	n	j	k	p	C	m	n	j	k	p	C
0	0	0	0	0	1	1	0	1	1	0	+0.0841
0	0	0	2	0	+0.5160	2	0	0	0	0	+0.0300
0	0	1	1	0	−0.2134	0	0	0	0	1	+0.1550
1	0	0	0	0	−0.3852	0	0	1	1	1	−0.0306
1	0	0	2	0	−0.0333	0	0	0	0	2	−0.0115
1	0	2	0	0	−0.0635						

A few other terms were tried and rejected, as they led to negligible decrease in the energy. In fact, the convergence is so rapid upon introducing the terms in succession, that we can state with some confidence that the inclusion of five or six more would bring the energy to within 0.01 volt of the convergence limit, and that this limit is -4.73 ± 0.02 volts, in complete agreement with experiment.

---

[1] E. A. Hylleraas, Zeits. f. Physik **65**, 209 (1930).

[2] O. W. Richardson and P. M. Davidson, Proc. Roy. Soc. **A123**, 466 (1929).

[3] R. S. Mulliken, Rev. Mod. Phys. **4**, 78 (1932).

Analysis of the problem indicates that the chosen value of δ is very nearly the optimum for $R=1.3$ and 1.4, but that for larger R a correspondingly larger δ would give slightly better results. We are now investigating this.

It may be of interest to give the best energy, -4.2 volts, obtainable from a combination of terms not including the electronic separation explicitly. This is the same value found by Hylleraas, by a long computation which he does not describe.

HUBERT M. JAMES
ALBERT SPRAGUE COOLIDGE

Harvard University,
Cambridge, Massachusetts,
March 17, 1933.

Influence of Inner Shells on Atomic Interactions

In applying wave mechanics to the study of the interaction of atoms more complex than He it has been customary to omit the inner shells from consideration. That the apparent success of computations of this sort does not justify this omission may be seen from a study of the normal state of Li_2.

The first attack on this problem was made by Delbrück.[1] In this work the inner electrons were included, but so many approximations were made in the numerical calculation that the results were seriously affected, as can be seen by comparing them with those of the writer, in obtaining which no such approximations were made. Bartlett and Furry[2] seem to misinterpret the work of Delbrück as showing the inner shells to be negligible and omit them entirely in a work which was otherwise more careful than Delbrück's, obtaining a result within 5 percent of the experimental value for the energy of dissociation. This close agreement must be viewed with some suspicion, however, for the corresponding computation in the case of hydrogen, that of Heitler and London, completed by Sigiura, gives a result in error by 34 percent.

There are three fundamental approximations made in work such as that of Bartlett and Furry: (1) an approximation in simplifying the operator used; (2) the omission of the inner shells; (3) the use of atomic wave functions to describe the outer electrons (the Heitler-London method). Such work does not seem to warrant a conclusion as to the importance of the inner shells in the interaction. The writer has, therefore, carried through without computational approximation a similar calculation including the inner shells and using the complete rigorous Hamiltonian operator. The wave functions for the outer electrons were the same as those used by Bartlett and Furry. The results of this computation are:

Internuclear distance (A)	2.78	2.98	3.18
Energy of interaction (volts)	−0.259	−0.294	−0.309

A Morse curve fitted to these points has its minimum very close to 3.18A, and the dissociation energy is thus computed as about 30 percent of the experimental value. By making the approximation of using an "interaction operator," as Bartlett and Furry do, the agreement with experiment was somewhat improved (dissociation energy 0.328 volt, equilibrium distance 3.07A). A comparison of these results with those of Bartlett and Furry indicates that the inner shells in Li_2 are responsible for a repulsion between the atoms which is decidedly important in comparison with the total energy of binding.

An attempt to better the results by adding functions of ionic type failed to give a perceptible improvement. By changing the shielding constant for the outer electrons the computed interaction energy can be increased by about 10 percent. It seems, however, that no rigorous computation designed along these lines can yield for the dissociation energy of Li_2 a value greater than 40 percent of that observed.

In view of these results it seems to be necessary to assume that the approximate agreement of the results of computations on the alkali metal molecules with experiment is due to a cancelling of errors, the neglect of the repulsion of the inner shells being counteracted by an underestimate of the attractive forces due to the outer shell. The interesting results of Rosen and Ikehara[3] must then be considered as of doubtful significance until some reason for expecting a systematic cancellation of these two types of error can be discovered.

The writer has for some time been of the opinion recently expressed by Furry,[4] that the best way to treat diatomic molecules is by using one-center functions for the electrons of inner shells, two-center functions for the others. A treatment of Li_2 by this method, using for the outer electrons the functions applied to the treatment of H_2 by Dr. A. S. Coolidge and the writer,[5] is now well under way. A more complete statement and analysis of the results of the research on which this note is a preliminary report, as well as a description of the methods used, will be published later in connection with a report on the more promising method mentioned above.

HUBERT M. JAMES

Harvard University,
Cambridge, Massachusetts,
March 17, 1933.

---

[1] M. Delbrück, Ann. d. Physik **5**, 36 (1930).

[2] J. H. Bartlett, Jr. and W. H. Furry, Phys. Rev. **38**, 1615 (1931).

[3] N. Rosen and S. Ikehara, Phys. Rev. **43**, 5 (1933).

[4] W. H. Furry, Phys. Rev. **43**, 361 (1933).

[5] Preceding letter.

Modified Scattering by Crystalline Hydrogen Halides

Using the Hilger constant deviation spectrograph we have measured the modified lines due to scattering of mercury lines λλ4047 and 4078 by crystals of HCl and HBr.

Detailed comparison with the infrared absorption band of crystalline HCl, reported by Hettner[1] at 3.66μ, and with the liquids of HCl and HBr[2] will be made in our complete report. We may remark here, however, that the Raman lines appear about 40 cm^{-1} broad, their centers being, for HCl 2760 cm^{-1}, for HBr 2465 cm^{-1}, showing a (0, 1) vibrational energy difference of about 10 cm^{-1} less than those of the liquids, and that these displacements are much too great to be attributed to Lorentz-Lorenz forces. As for the liquids,[2] HBr was the stronger scatter.

E. O. Salant
Dixon Callihan

Department of Physics,
Washington Square College,
New York University,
March 18, 1933.

---

[1] G. Hettner, Zeits. f. Physik **78**, 141 (1932).
[2] Salant and Sandow, Phys. Rev. **37**, 373 (1931).

THE AMERICAN INSTITUTE OF PHYSICS

INCORPORATED

GOVERNING BOARD

For The American Physical Society:

KARL T. COMPTON, *Chairman*
Massachusetts Institute of Technology

GEORGE B. PEGRAM, *Secretary*
Columbia University

JOHN T. TATE
University of Minnesota

For The Optical Society of America:

PAUL D. FOOTE
The Gulf Companies

LOYD A. JONES
Eastman Kodak Company

F. K. RICHTMYER
Cornell University

For The Acoustical Society of America:

H. D. ARNOLD
Bell Telephone Laboratories

HARVEY FLETCHER
Bell Telephone Laboratories

DAYTON C. MILLER
Case School of Applied Science

For The Society of Rheology:

E. C. BINGHAM
Lafayette College

WHEELER P. DAVEY
Pennsylvania State College

A. STUART HUNTER
du Pont Rayon Company

For The American Association of Physics Teachers:

HOMER L. DODGE
University of Oklahoma

PAUL E. KLOPSTEG
Central Scientific Company

FREDERIC PALMER
Haverford College

ADMINISTRATIVE STAFF

HENRY A. BARTON, *Director*
JOHN T. TATE, *Adviser on Publications*
MADELINE M. MITCHELL, *Editorial Secretary*
Office: 11 East 38th Street, New York, New York

JOURNALS

THE PHYSICAL REVIEW
REVIEWS OF MODERN PHYSICS
PHYSICS
JOHN T. TATE, *Editor*
J. W. BUCHTA, *Assistant Editor*
E. C. BINGHAM, *Rheology Editor*

THE JOURNAL OF THE OPTICAL SOCIETY OF AMERICA
THE REVIEW OF SCIENTIFIC INSTRUMENTS WITH PHYSICS NEWS AND VIEWS
F. K. RICHTMYER, *Editor*

THE JOURNAL OF THE ACOUSTICAL SOCIETY OF AMERICA
F. R. WATSON, *Chairman, Editorial Board*
WALLACE WATERFALL, *Managing Editor*

THE JOURNAL OF CHEMICAL PHYSICS
HAROLD C. UREY, *Editor*

THE AMERICAN PHYSICS TEACHER
DUANE ROLLER, *Editor*

The American Institute of Physics is a membership corporation of which five societies are the founding members. These five societies are the principal national societies devoted to pure and applied physics in America. Their names, and those of their representatives who form the Governing Board of the Institute, are given above. The principal work of the Institute is the publication of journals sponsored by the societies or by itself. The names and the editors of the journals are also listed above.

The broad purpose of the Institute is to represent, in all matters of wide or common interest, the five thousand or more members and subscribers associated with the Founder Societies and the journals. It aims to advance the science and profession of physics, and to promote cooperation between pure research, the applied sciences and the industries. To achieve these aims, it is greatly in need of an endowment and is empowered by law to administer grants and funds of any kind.

CONTENTS

APRIL 1, 1933

Scattering of X-Rays from Powdered Crystals . . . . . G. E. M. JAUNCEY AND FORD PENNELL 505

Diffraction of Low-Speed Electrons by a Tungsten Single Crystal . . . . . WAYNE T. SPROULL 516

Fluorescence Yield from the L_{III} Level of Uranium . . . . . REGINALD J. STEPHENSON 527

Attempts to Observe an Electron Affinity Spectrum . . . O. OLDENBERG 534

Continuous Electron Affinity Spectrum of Hydrogen . . . . C. K. JEN 540

Note on Kowalewski's Top in Quantum Mechanics . . . OTTO LAPORTE 548

Transport Phenomena in Einstein-Bose and Fermi-Dirac Gases. I . . . . . E. A. UEHLING AND G. E. UHLENBECK 552

Effect of Etching on the Relative Intensities of the Components of Double Laue Spots Obtained from a Quartz Crystal . . . . . M. Y. COLBY AND SIDON HARRIS 562

On the Interpretation of Heat in Relativistic Thermodynamics. . . . . R. C. TOLMAN AND H. P. ROBERTSON 564

Effect of Tension on the Electrical Resistance of Single Antimony Crystals . . . . . MILDRED ALLEN 569

New Phenomena in the Change of Resistance of Bi Single Crystals in Magnetic Fields . . . . . O. STIERSTADT 577

Letters to the Editor:

Identification of the (2, 2) Band of Neutral OH. Satellite Series of the (1, 1) Band. Extensions of the (0, 0) Band. . . . . HERRICK L. JOHNSTON AND DAVID H. DAWSON 580

The Molecular Structure of Ozone. . . . . WILLIAM S. BENEDICT 580

Vibrational Isotope Effects in Polyatomic Molecules. II . . . . . E. O. SALANT AND JENNY E. ROSENTHAL 581

The Nuclear Spin of Sodium . . . . . I. I. RABI AND V. W. COHEN 582

Angular Distribution of Low Energy Cosmic Radiation and Interpretation of Angular Distribution Curves. THOMAS H. JOHNSON AND E. C. STEVENSON 583

A Neutron of High Velocity, and Energy Relations for Nuclear Disintegration by Non-Capture. WILLIAM D. HARKINS, DAVID M. GANS AND HENRY W. NEWSON 584

A New Kind of Radioactivity . . . . R. M. LANGER AND R. W. RAITT 585

The Equilibrium Theory of the Abundance of the Elements. . . T. E. STERNE 585

Conductivity of Rare Gases Irradiated by Their Own Resonance Radiations. . . . . O. S. DUFFENDACK AND R. W. SMITH 586

The Torque on Faraday's Magnet . . . . . E. H. KENNARD 587

Improved Calculation of Ground State of H_2 . . . . . HUBERT M. JAMES AND ALBERT SPRAGUE COOLIDGE 588

Influence of Inner Shells on Atomic Interactions . . . . HUBERT M. JAMES 589

Modified Scattering by Crystalline Hydrogen Halides . . . . . E. O. SALANT AND DIXON CALLIHAN 590

LANCASTER PRESS, INC., LANCASTER, PA.